THE UNIVERSITY OF MICHIGAN

INDUSTRY PROGRAM OF THE COLLEGE OF ENGINEERING

COCURRENT FLOW OF IMMISCIBLE LIQUIDS IN PACKED BEDS

Robert G. Rigg

A dissertation submitted in partial fulfillment
of the requirements for the degree of
Doctor of Philosophy in the
University of Michigan
1963

May, 1963

IP-617

ACKNOWLEDGEMENTS

The author is indebted to many people who rendered assistance during the course of the doctoral program. Thanks are due particularly to:

Professor S. W. Churchill, chairman of the doctoral committee, for his guidance, assistance, and helpful suggestions during the course of this work.

Professors E. F. Brater, M. R. Tek, G. B. Williams, and J. L. York, committee members, for their suggestions and constructive criticism.

Dr. R. P. Larkins, who constructed much of the experimental apparatus used here.

Mr. James A. Craig for his generous assistance in various phases of the computer programming.

The shop personnel of the Chemical and Metallurgical Engineering Department for their assistance in equipment construction and the Computing Center at The University of Michigan for their donation of computing time.

The National Science Foundation for financial aid in the form of fellowships.

The Phillips Petroleum Company for their donation of isooctane.

The Union Carbide Chemicals Company for their donation of isobutanol.

The Industry Program of the College of Engineering for their cooperation and assistance in the preparation of the final form of this dissertation.

Last, but certainly not least, my wife, Veronica, for her help in preparation of the manuscript and for her patience and understanding during the course of my work.

TABLE OF CONTENTS

TABLE OF CONTENTS (CONT'D)

LIST OF TABLES

LIST OF TABLES (CONT'D)

LIST OF FIGURES

LIST OF FIGURES (CONT'D)

LIST OF FIGURES (CONT'D)

LIST OF APPENDICES

NOMENCLATURE

A	Cross sectional area of porous medium
A, A', A_1	Empirical constants
a	Empirical constant
B, B', B_1	Empirical constants
b	Empirical constant
C_1	Empirical constant
c, c', c_1	Empirical constants
D	Diameter of packed bed
D_1	Empirical constant
D_c	Diameter of capillary channel in packed bed
D_p	Diameter of packing particle
d	Diameter of a sphere
d_i	Diameter of individual drop
d_{32}	Sauter mean diameter
F	Friction factor defined by Equation (39)
g	Acceleration due to gravity
g_c	Gravitational conversion constant
H	Liquid holdup
i	Counting index
K	Permeability
K	Time constant
K, K'	Empirical constants
K'_o, K'_w	Relative permeabilities of oil and water phases, respectively
k_1, k_2	Empirical constants

ln	Logarithm to base e
L	Liquid flowrate
L	Length of capillary channel
L	Thickness of porous medium
m	Slope of holdup data line Equations (15) and (16)
N	Number of capillary channels
N	Number of droplets in a given photograph
P	Pressure
$\frac{dP}{dL}$	Pressure gradient
$\frac{\Delta P}{L}$	Pressure drop per length of bed, L
$(\frac{\Delta P}{\Delta L})_{TP}$	Two phase pressure drop, Equation (10)
$(\frac{\Delta P}{\Delta L})_{g}$	Pressure drop for gas flowing alone, Equation (10)
$(\frac{\Delta P}{\Delta L})_{\ell}$	Pressure drop for liquid flowing alone, Equation (10)
P_{RATIO}	Ratio of two phase pressure gradient due to friction to predicted frictional pressure gradient
p_I	Weight per cent isobutanol in water phase, Equation (B-2)
p_w	Weight per cent water in isobutanol phase, Equation (B-1)
Q	Volumetric flowrate
R	Fluid flowrate
R_1	Ratio of scale fluid density to metering fluid density
R_2	Ratio of float density to scale fluid density
R_{32}	Ratio of volume to surface area for Sauter mean sphere
R_T	Ratio of volume to surface area for total population of drops
r	Radius of sphere

r	Empirical constant
Re	Reynolds number
Rem	Modified Reynolds number defined by Equation (40)
RI	Phase holdup of non-wetting phase
RI_f	Value of RI as time $\rightarrow \infty$
S	Particle surface area per volume of packed space
S_v	Particle surface area per volume of packing particle
s	Empirical constant
T	Absolute temperature, °R
t	Temperature, °C
t	Time
U	Superficial liquid velocity
U_C, U_D	Superficial velocities of continuous and discontinuous phases, respectively
u	Velocity
V	Interstitial velocity
$\overline{V}_o$	Terminal drop velocity
V_s	Slip velocity
V_T	Volume of test section, see Equation (36)
V_w	Volume of overflow water from test section, see Equation (36)
v	Specific volume $= \frac{1}{\rho}$
W	Mass flowrate of fluid
w_f	Frictional work
w_s	Shaft work
We	Weber number
X	Discontinuous phase holdup

X	Ratio of $(\frac{\Delta P}{\Delta L})_\ell$ to $(\frac{\Delta P}{\Delta L})_g$
X_T	Total phase holdup
Z	Distance along test section

Greek Symbols

α	Empirical constant
β	Empirical constant
Δ	Denotes a difference
δ_f	Frictional pressure gradient
δ_{fp}	Predicted frictional pressure gradient
ϵ	Porosity
μ	Viscosity
ρ	Density
ρ_f	Continuous phase density
ρ_I	Isobutanol phase density, Equation (B-1)
ρ_w	Water phase density, Equation (B-2)
σ	Interfacial tension
ϕ_g	Functional relationship defined by Equation (10)

Subscripts

1	Upstream position
2	Downstream position
m	Mean
o	Organic phase
o	Oil phase
w	Water phase
I	Isobutanol phase
f	Refers to frictional contribution

ABSTRACT

The purpose of the research reported in this thesis was to investigate the upward cocurrent flow of immiscible liquids in packed beds.

Manometers were used to measure the pressure difference over segments of a vertical 4 inch ID by 82 inch long Lucite tube packed with one of three different sized glass spheres. Phase holdup measurements were obtained by trapping the contents of the test section. Flash photographs taken through the wall of the column allowed direct measurement of drop sizes near the wall. The three liquid pairs: isobutanol-water, isooctane-water, and isooctane-Alkaterge "C"-water were passed through beds of 0.501 inch, 0.340 inch, and 0.164 inch diameter glass spheres. Individual phase flowrates of approximately 0.65 gpm to 15 gpm were investigated over a complete range of flow ratios.

Experimental measurements indicate that steady state phase holdup can be approximated by assuming no slip velocity between phases. A more precise estimate of phase holdup can be obtained by an equation of the form:

$$RI = \left(\frac{U_O}{U_O + U_W}\right)^a$$

where RI represents phase holdup and U_O and U_W are the individual phase volumetric flowrates divided by the cross sectional area of the empty test section. The constant $\underline{a}$ has been evaluated for each system studied. In addition a limited amount of transient phase holdup data are presented.

The manometric data indicate that immiscible liquids flowing in a packed bed cannot be treated simply as if they comprised a single liquid phase with averaged physical properties. The data do however deviate from the "single-phase" prediction in a systematic manner. Measured two-phase pressure gradients are in all cases greater than the "single-phase" prediction. The measured values approach the "single-phase" curve asymptotically at both extremes of flow ratio and pass through a maximum at a flow ratio of approximately 75 volume per cent of the nonwetting phase.

These data were correlated in terms of a parameter, P_{RATIO}, which is the ratio of frictional pressure gradient (total pressure gradient less pressure gradient due to gravity) to that predicted by means of the "single-phase" assumption. P_{RATIO} is then a measure of the degree of phase interaction. Values of P_{RATIO} as great as 10 were observed. A correlation of P_{RATIO} with the independent experimental variables is presented. The pressure gradient in the entrance section was found in all cases to be less than that in the interior of the test section.

Phase interaction is attributable to surface energy effects. That is, during the formation of a dispersion by means of flow through a packed bed, energy is converted from pressure energy to surface energy. A sample calculation shows that surface energy effects are indeed an important contributor to pressure loss. The addition of a surfactant was found to have less effect on pressure drop than would be indicated by its effect on statically measured interfacial tension.

Sauter-mean drop diameters were computed and used to characterize interfacial area. Dispersed-phase drop diameters were found to be

directly proportional to packing diameter for the systems studied. In addition they were found to decrease exponentially with total mixture velocity. The effect of fluid properties on drop diameter was not fully ascertained, but an increase in interfacial tension causes an increase in drop diameter. In addition drop diameters were found to exhibit a Gaussian (normal) distribution in all cases.

I. INTRODUCTION

In recent years a great deal of interest has developed in the field of multi-phase flow. A large number of papers on this subject have been published but they have been concerned almost exclusively with the problems of gas-liquid flow in open pipes, fluidization of solids, and counter-current flow in packed beds.

A recent investigation of liquid-liquid extraction in a co-current flow system[45] performed at the University of Michigan has created a desire for information about the cocurrent flow of immiscible liquids in packed beds. The mass transfer investigation indicated a linear increase in mass transfer coefficients with velocity over the range of variables studied. As a result, any application of cocurrent liquid-liquid extraction would be limited only by fluid flow considerations. It is therefore desirable to be able to predict pressure gradient, phase holdup, and the amount of interfacial area produced in liquid-liquid flow in a packed bed. This information will not only provide design information for cocurrent extraction systems, but provides insight into the general problem of cocurrent two-phase flow.

It is the purpost of this study to investigate the cocurrent flow of immiscible liquids in packed beds, to determine the important physical variables and their effect on pressure gradient, phase holdup (the fraction of the void spaces occupied by the dispersed phase) and dispersed phase drop sizes, and if possible to present generalized correlations for predicting these functions. A search of the periodical literature has shown that no work of this type has been undertaken to date.

A preliminary investigation indicates that the following variables could all have some effect on the three dependent variables, i.e., pressure drop, phase holdup, and drop size:

(1) Flow rate of each liquid phase

(2) Ratio of flowrates of the two liquid phases

(3) Direction of flow (vertically upward, vertically downward, horizontal, inclined, etc.)

(4) Fluid properties of each phase (viscosity, density, interfacial tension)

(5) Entrance or mixing arrangement

(6) Packing shape (spheres, Raschig rings, Berl saddles, etc.)

(7) Packing size

(8) Packing material (determines wettability of packing)

(9) Column size

(10) Possibly others such as pH of solutions, packing orientation, etc.

Because of the large number of independent variables involved in such systems, it is necessary to limit the scope of the problem so that it can be adequately investigated in a reasonable length of time. As a result the present investigation was limited to one column size, one entrance arrangement, one flow direction, one packing shape, one packing material, three packing sizes, and three liquid-liquid systems. The liquid-liquid systems however, were chosen so as to give a relatively wide range of the physical properties, density, viscosity, and interfacial tension.

In attempting to correlate the data obtained from the above systems, it was decided to draw as much as possible from the single phase correlations for flow in packed beds and the correlations proposed for other two-phase flow systems. It is hoped that by this technique the results of this investigation can be made more general and can have a wider range of applicability.

II. LITERATURE REVIEW

An exhaustive search of the periodical literature has shown that to date no information on the cocurrent flow of immiscible liquids in packed beds has been published. There are, however, in the literature a large number of articles of value to the present problem. The more important of these articles are reviewed here. A supplementary bibliography is presented in Appendix H without comment. This supplementary bibliography contains articles which are not directly applicable to the present problem, but which are of interest to the worker in the general area of liquid-liquid or gas-liquid flow.

1. Single-Phase Flow in Packed Beds

The first significant contribution to the study of flow in packed beds, other than D'Arcy's law, was due to Blake,[4] who by dimensional analysis and analogy with flow in open pipes obtained the dimensionless correlating groups $\frac{\Delta P_f D_p}{LV^2\rho}$ and $\frac{D_p V\rho}{\mu}$ the latter of which is the Reynolds number. Substituting $\frac{U}{\epsilon}$ for V, where U is the superficial velocity and V is the actual interstitial velocity, and $\frac{\epsilon}{S}$ for D_p, where $S = \frac{\text{area of particle surface}}{\text{volume of packed space}}$, he proposed that the following unique relationship exists for turbulent flow:

$$\frac{\Delta P_f \epsilon^3}{LU^2\rho S} = F\left(\frac{V\rho}{S\mu}\right) \tag{1}$$

Furnas[27] presented the most comprehensive collection of data, but only proposed the simple correlation

$$\frac{-\Delta P_f}{L} = AR^B \tag{2}$$

where R = fluid flowrate, and A and B are constants for a given packing and fluid.

Following Blake's lead, several authors since have attempted to correlate packed bed flow data using some form of Reynolds number and friction factor.[8,9,11,13,18,46,47] Chilton and Colburn[18] proposed a two-range correlation with a different friction factor for the viscous and turbulent ranges. Carman[13] pointed out that for spheres the S in Blake's equation is given by

$$S = \frac{6(1-\epsilon)}{D_p} \tag{3}$$

Substituting this in Blake's equation, he showed that in the turbulent range the dependence of pressure drop on porosity is given by

$$\frac{-\Delta P_f}{L} \alpha \frac{1-\epsilon}{\epsilon^3} \tag{4}$$

Starting with the Kozeny equation and employing the above technique he found that in the viscous range the dependence of pressure drop on porosity would be given by

$$\frac{-\Delta P_f}{L} \alpha \frac{(1-\epsilon)^2}{\epsilon^3} \tag{5}$$

Leva[46,47] correlated a great deal of data from the literature by the friction factor-Reynolds number method with a separate equation for the viscous, transition, and turbulent flow regimes. He also included the effect of packing roughness. Brownell and Katz[8,9] assumed the Fanning friction factor relationship to be absolute and suggested a modified Reynolds number and modified friction factor to force their data to fit the Fanning relationship.

Morcom[56] proposed the following functional relationship based on dimensional analysis:

$$\frac{-\Delta P_f g \rho D_p^3}{L \mu^2} = F\left(\frac{D_p U \rho}{\mu}\right) = F(Re) \tag{6}$$

Assuming the function F to be of the form

$$F(Re) = \alpha\, Re + \beta\, Re^2, \tag{7}$$

he developed the two term correlating equation for all ranges of flow:

$$\frac{-\Delta P_f}{L} \frac{D_p^2}{\mu U} = \alpha + \beta\, Re \tag{8}$$

He found, however, that the constants α and β were functions of the bed

Ergun and Orning,[24,25] using an idealized physical model derived a two term equation very similar to that of Morcom but which includes the effect of porosity on pressure drop. Their final equation was

$$\frac{-\Delta P_f}{L} g_c = k_1 \frac{(1-\epsilon)^2}{\epsilon^3} \frac{\mu U}{D_p^2} + k_2 \frac{1-\epsilon}{\epsilon^3} \frac{U^2 \rho}{D_p} \tag{9}$$

The constants k_1 and k_2 have physical significance but were evaluated empirically. This equation is developed and discussed in detail in the section "Theory of Single Phase Flow in Packed Beds."

Fahien and Schriver[26] recently attempted to modify the Ergun equation to better account for wide variations in porosity and also to better fit data in the transition region.

Ranz[60] proposed that pressure drop in packed beds was merely an additive property of the pressure drop for flow past a single particle. A major problem, however, arises in deciding what velocity to use for the computation of drag coefficients. His results indicate order of magnitude agreement with packed bed data.

Most authors to date have assumed that packing size, packing shape, and porosity are sufficient to determine the permeability of a packed bed to a given fluid. Martin,[53] however, showed that particle orientation is also a factor in determining permeability. By packing beds of spheres in regular patterns he experimentally showed that beds with equal porosities but different packing arrangements produce different permeabilities.

Benenati and Brosilow[2] pointed out that even with a "random" packing of spheres point porosity varies considerably with distance from the wall of a circular container.

2. Two-Phase Flow in Open Pipes

Since most of the investigations of two-phase flow have been carried out in open pipes a brief review of the results and methods of attack of these investigations is presented here. (Since so little literature is available on cocurrent flow in packed beds it is extremely helpful to draw on the open pipe literature in analyzing results and drawing conclusions.)

2.1 Gas-Liquid Flow

A tremendous amount of data on gas-liquid flow in open pipes has been published but only four basic methods of analysis have been

used. The most satisfying but at the same time the most difficult approach is the analytical one. Due to the difficulty of application only two relatively simple flow regimes have been attacked by this method. Calvert and Williams[12] and Anderson and Mantzouranis[1] have presented theoretical analyses of annular flow in vertical pipes. Street[73] theoretically analyzed the "slug flow" regime.

The second basic approach to the problem of pressure drop and phase holdup in two-phase flow was first developed by Martinelli, Lockhart, et al.[51,54,55] By treating each phase of the two-phase system as if it were flowing by itself, and by drawing on single-phase pressure-drop correlations, they proposed a four regime empirical correlation of the following form:

$$\left(\frac{\Delta P_f}{\Delta L}\right)_{TP} \Big/ \left(\frac{\Delta P_f}{\Delta L}\right)_g = \phi_g^2 \ (X) \qquad (10)$$

where

$\left(\frac{\Delta P_f}{\Delta L}\right)_{TP}$ = Two-phase frictional pressure gradient

$\left(\frac{\Delta P_f}{\Delta L}\right)_g$ = frictional pressure gradient due to gas flowing alone

X = ratio of single-phase pressure gradients - $\left(\frac{\Delta P_f}{\Delta L}\right)_\ell \Big/ \left(\frac{\Delta P_f}{\Delta L}\right)_g$

Although the correlation left a great deal of scatter in the data, this approach has been widely used. Hoogendoorn[37] and Chenoweth and Martin[17] have pointed out limitations of the Martinelli-Lockhart approach and have presented improved correlations for high gas densities. Chisolm and Laird[19] added a correction for pipe roughness to the Martinelli-Lockhart approach. Recently Hughmark and Pressburg[38] pointed out that total mass

velocity appears to be an important variable in the interaction of two phases.

In a series of articles Govier and co-workers[6,7,30,31,32] treated a two-phase gas-liquid system as a single phase and presented plots of friction factor versus liquid Reynolds number with a parameter of gas-liquid ratio. Other authors who have applied the same general technique are Brigham and co-workers[5] and Bertuzzi and co-workers.[3]

Recently a general dimensional analysis was applied to two-phase flow by Ros.[63] He found, however, after correlating a tremendous amount of data, that only four of his original nine dimensionless groups had a significant effect on pressure drop.

2.2 Liquid-Liquid Flow

Recently some interest has developed in the flow of immiscible liquids in open pipe, with particular application to the reduction of pressure gradients by injection of water into crude oil pipelines. Gemmell and Epstein[29] and Charles and Redberger[16] have applied numerical analysis to the horizontal, stratified flow of oil-water mixtures but found only moderate agreement between theory and experiment. Experimental investigations of horizontal oil-water flow in pipes by Charles, Govier and Hodgson,[15] Russell and Charles,[64] and Russell, Hodgson and Govier[65] have not resulted in a satisfactory correlation but have indicated some interesting results. Reduction of pressure gradient by as much as a factor of 10 has been observed. Flow patterns similar to those for gas-liquid flow have been observed.

In the vertical flow of oil-water mixtures in open pipes, Govier, Sullivan and Wood[33] observed the following flow patterns for increasing oil rate at constant water rate: drops of oil in water, slugs of oil in water, froth, drops of water in oil. They also observed that frictional pressure drop is independent of the oil viscosity as long as water is the continuous phase. Brown and Govier[6] felt that frictional pressure drop was approximately equal to that of the continuous fluid flowing alone at the mixture velocity. They also found that at a constant superficial oil velocity the slip velocity is approximately constant.

Cengel, et al.[14] treated dispersions of organic solvents in water as single-phase fluids and calculated pseudo viscosities for the mixtures. They found that at low velocities the viscosities tended to increase.

3. Countercurrent Flow in Packed Beds

Since pressure drop in countercurrent flow is important only with respect to loading and flooding, no discussion of the literature on this subject will be presented here. It is interesting to note, however, that White[77] found that any wall effect on pressure drop was negligible when

$$\frac{D_{tower}}{d_{packing}} > 6$$

This section will, therefore, be devoted to a review of the literature on phase holdup in countercurrent flow in packed towers.

Jesser and Elgin[40] first postulated a simple expression for liquid holdup in a gas-liquid packed tower of the form

$$H = bL^s \qquad (11)$$

where

H = liquid holdup

L = liquid flowrate

b = constant dependent only on area of packing

s = constant dependent only on shape of packing.

Gayler and Pratt[28] first observed different types of holdup. Wicks and Beckman[78] noted three types of holdup: permanent, free and total. They also noted that channelling of the dispersed phase occurred for

$$\frac{D_{tower}}{d_{packing}} < 6 .$$

From dimensional analysis they derived the following expression for total holdup for a given system:

$$X_T = A_1(U_D)^r + B_1(U_D)(U_C)^s \qquad (12)$$

Markas and Beckman[52] noted a hysteresis effect on permanent holdup and modified Equation (12) to

$$X_T = A_1 + B_1(U_C) + C_1(U_D) + D_1(U_C)(U_D) \qquad (13)$$

More recently Johnson and Lavergne[41] applied Bernoulli's equation to each phase separately and obtained the following expression for dispersed phase holdup in packed towers:

$$\frac{X^3}{U_D^{1.5}} = A' \frac{U_C^r}{U_D^{1.5}} \left(\frac{X}{1-X}\right)^3 + B' \qquad (14)$$

where A', B' are r are empirical constants for a given system.

The most satisfying correlation from a theoretical view point is that of Sitaramayya and Laddha[71] which relates holdup to slip velocity or the relative velocity between the dispersed phase and the continuous phase. In a countercurrent packed tower the slip velocity V_s is given by

$$V_s = \frac{U_D}{\epsilon X} + \frac{U_C}{\epsilon(1-X)} \tag{15}$$

The authors assumed

$$V_s = \bar{V}_o\,(1-X) \tag{16}$$

where $\bar{V}_o$ is a limiting mean droplet velocity, rearranged Equation (15) and plotted $(U_D + \frac{X}{1-X}\,U_C)$ versus $X(1-X)$. Their data produced a straight line through the origin with a slope m, which was found to be a given function of the fluid properties and the packing properties.

4. Cocurrent Flow in Packed Beds

A search of the periodical literature revealed only two articles which dealt with cocurrent flow in packed beds and in both cases the systems studied were gas-liquid. Dodds, et al.[22] presented pressure-drop data on gas-liquid flow in packed beds but did not attempt a general correlation. Their data are limited to rather low pressure drops. Larkins[44] covered a much wider range of flowrates and was able to correlate his data plus some industrial data fairly well by the Martinelli-Lockhart approach.

Although no literature is available on cocurrent liquid-liquid flow in packed beds, several articles have been written on cocurrent flow of liquids in porous media. An excellent review of this work can be found in a book by Scheidegger.[66] Brownell and Katz[10] proposed a Reynolds

number-friction factor correlation with a different form of the two correlating groups for the wetting and non-wetting phases. The more widely accepted approach, however, is that presented by Leverett.[48] Beginning with D'Arcy's law which defines permeability of a medium as

$$K = \frac{Q\mu L}{A\Delta P_f} \tag{17}$$

he defined an effective permeability for each phase as

$$K_o = \frac{Q_o\mu_o L}{A\Delta P_f} = \text{oil permeability} \tag{18}$$

and

$$K_w = \frac{Q_w\mu_w L}{A\Delta P_f} = \text{water permeability} \tag{19}$$

where

Q = volumetric flowrate

μ = viscosity

A = cross sectional area

$\frac{\Delta P_f}{L}$ = frictional pressure gradient

The relative permeabilities $K_o' = \frac{K_o}{K}$ and $K_w' = \frac{K_w}{K}$ were found to be functions of water saturation or water holdup only. It was observed, however, that $K_o' + K_w'$ was sometimes less than unity. This was attributed to the Jamin effect or the situation where droplets of oil (non-wetting phase) are lodged in apertures in the medium through which they cannot pass until the pressure gradient is increased.

5. Drop Breakup and Interfacial Area

Almost all investigations of interfacial area to date have been performed in mixer-settler type equipment due to the ease of making measurements. The results of these studies, however, aid in understanding the drop sizes obtained in other types of equipment.

Hinze[35] describes several types of drop breakup and attempts to establish a theoretical basis for predicting stable drop sizes. He points out that viscous stresses and dynamic pressures cause deformation and, as a result, splitting in liquid-liquid systems. Surface tension forces tend to counteract deformation. He states that a critical Weber number exists above which breakup will occur. He defines the Weber number as

$$We = \frac{D\rho_C U^2}{\sigma} \tag{20}$$

where D = drop size. The value of the critical Weber number depends on the breakup mechanism. Mugele[57] used a force balance to determine the critical Weber number for a drop exposed to the drag of a continuous medium.

Several authors[20,23,42,62,69,70] have presented highly empirical correlations for stable drop sizes in agitated mixtures. The only consistency among their results is that the mean drop diameter is inversely proportional to the first power of the impeller speed. Shinnar[69] even found a variation in this exponent depending on whether the agitation is causing breakup of drops or merely preventing coalescence of existing drops. Levich[49] in a review of Russian work on the subject implied that very little is known about drop breakup due to turbulence and that only

the simpler cases of breakup due to laminar drag forces have been even reasonably well covered.

Another group of authors proposed dimensional analysis as a tool for attacking this problem.[61,74,75] Rodger, Trice, and Rushton[61] found the interfacial area produced in an agitated liquid-liquid mixture to be proportional to the 0.36 power of the Weber number. They also found the effect of the relative viscosity of the two liquids to be small, but observed an exponential increase of interfacial area with $\Delta\rho/\rho_f$, where ρ_f is the continuous phase density.

Only three investigations of drop sizes in flow equipment have been found in the literature. Sleicher[72] studied maximum drop sizes in cocurrent turbulent flow in a pipe and found the maximum drop size to be independent of the inlet drop size as long as inlet drops are not too small. Weaver, Lapidus, and Elgin[76] in an investigation of liquid spray towers photographically observed a Gaussian distribution of drop sizes. On the other hand Lewis, Jones, and Pratt[50] found a non-Gaussian distribution when fairly uniform droplets were allowed to flow countercurrently to the continuous phase in a packed bed. They, however, did agree with Sleicher that the inlet drop size has little effect on the outlet size.

III. THEORY OF SINGLE-PHASE FLOW IN PACKED BEDS

Before attempting to study two-phase flow in packed beds a sound understanding of the theory of single-phase flow in packed beds is necessary. From a theoretical view point the most satisfying approach to single-phase flow in packed beds is that of Ergun and Orning.[25] In this section a development of their flow equation will be presented along with a discussion of its strong and weak points.

To begin, assume that a packed bed is equivalent to a number of parallel, equal sized capillary tubes such that the internal surface area of the tubes is equal to the surface area of the packing and that the total internal volume of the tubes is equal to the void volume of the packed bed. The well known Poiseuille equation for flow in capillary tubes is then applicable:

$$-\frac{dP_f}{dL} g_c = 32\mu V/D_c^2 \qquad (21)$$

where D_c = diameter of the channel. In a capillary the kinetic energy losses due to entrance and exit effects occur only once. However in a packed bed the number of times these kinetic energy losses occur is statistically related to the number of particles per unit length. As a result a term accounting for these kinetic energy losses must be added to Equation (21). Equation (21) then becomes

$$-\frac{dP_f}{dL} g_c = 32\mu V/D_c^2 + \frac{\beta}{2} \rho V^2/D_c \qquad (22)$$

where the factor β accounts for the number of times the kinetic losses occur. In addition the stream lines frequently converge and diverge in

a packed bed so a correction factor must be included in the viscous term of Equation (22):

$$-\frac{dP_f}{dL} g_c = 32\,\alpha\mu V/D_c^2 + \left(\frac{\beta}{2}\right)\rho V^2/D_c \qquad (23)$$

Equation (23) is of limited value in its present form since the channel diameter D_c and the actual interstitial velocity V are unknown. The mean pore velocity given by $\frac{U}{\epsilon}$, where U is the mean superficial velocity (the velocity if no packing were present) may be substituted for V. In reality V varies from point to point along the bed as the area available for flow contracts and expands. The expression $\frac{U}{\epsilon}$ is, however, the best approximation available for V at the present time.

To eliminate D_c recall the original assumption that the internal surface area of the capillary tubes is equal to the surface area of the packing. If the capillaries are assumed to be cylindrical, the specific surface, S_V, of the packing (the surface area of the packing per unit volume of packing material) is given by the following equation:

$$S_V = NL\pi D_c/L\pi(D^2/4)(1-\epsilon) \qquad (24)$$

where N = the number of capillaries in the bed and D = the diameter of the packed bed. The second original assumption (that the internal volume of the capillary tubes is equal to the void volume of the packed bed) yields the following relationship:

$$N\pi D_c^2/4 = \pi D^2\epsilon/4 \qquad (25)$$

Elimination of N between Equation (24) and (25) gives the following expression for D_c in terms of measureable bed parameters:

$$D_c = \frac{4\epsilon}{1-\epsilon} \frac{1}{S_v} \tag{26}$$

Substitution of Equation (26) and the expression

$$V = \frac{U}{\epsilon} \tag{27}$$

into Equation (23) yields

$$-\frac{dP_f}{dL} g_c = 2\alpha \frac{(1-\epsilon)^2}{\epsilon^3} \mu S_v^2 U + \frac{\beta}{8} \frac{1-\epsilon}{\epsilon^3} \rho S_v U^2 \tag{28}$$

It is interesting to note here that the dependence of pressure gradient on porosity given by Equation (28) is the same as that proposed by Carman and observed by several experimental workers.

It has been common practice in recent years to replace S_v, the specific surface area, in Equation (28) with an equivalent diameter for any shape particle. This diameter D_p is derived from the relations for spheres. For a sphere S_v is given by

$$S_v = \frac{4\ \pi r^2}{\frac{4}{3}\pi r^3} = \frac{3}{r} = \frac{6}{d} \tag{29}$$

The equivalent diameter for any particle is, therefore, defined as

$$D_p = \frac{6}{S_v} \tag{30}$$

Substitution of Equation (30) into Equation (28) gives

$$-\frac{dP_f}{dL} g_c = 72\ \alpha \frac{(1-\epsilon)^2}{\epsilon^3} \frac{\mu U}{D_p^2} + \frac{6\beta}{8} \frac{1-\epsilon}{\epsilon^3} \frac{\rho U^2}{D_p} \tag{31}$$

In its present form the flow equation is completely general. If now, however, only constant density fluids are considered, Equation (31) can be integrated to give

$$-\frac{\Delta P_f}{L} g_c = 72\,\alpha\,\frac{(1-\epsilon)^2}{\epsilon^3}\,\frac{\mu U}{D_p^2} + \frac{6\beta}{8}\,\frac{1-\epsilon}{\epsilon^3}\,\frac{\rho U^2}{D_p} \qquad (32)$$

In order to apply Equation (32) to an actual calculation the so-called constants α and β must be evaluated. This can be accomplished by fitting experimental data to the above equation but it would be preferable to obtain at least an approximate value for these numbers from theoretical considerations. The correction factor α in the viscous energy term represents the ratio of actual viscous energy losses to that predicted for a fluid flowing at velocity V through a capillary of length L. However the method by which V has been evaluated causes it to be a numerical measure of only the component of velocity parallel to the axis of the bed. The velocity which should be used to measure viscous losses is that parallel to the walls of the channel.

If the bed is assumed to be composed of spherical particles, the ratio of actual path length to bed length would be given by the ratio of one half the circumference of a particle to its diameter or $\frac{\pi}{2}$. At the same time, however, the ratio of the velocity parallel to the surface of the particle to the component of velocity parallel to the axis of the bed is given by the same number. The value derived for α is, therefore, $(\frac{\pi}{2})^2$ or approximately 2.47.

Since the kinetic energy term of Equation (32) is not dependent on the length of the bed but merely the number of contractions in the flow

path per unit of channel diameter, the same reasoning cannot be applied there. It does, however, follow that the velocity to be used in this term is the same as that used in the viscous energy term. Since velocity appears to the second power the correction factor $\frac{\pi}{2}$ must be squared before putting it in the equation. The simplest assumption concerning the number of times the flow path contracts is that it contracts once for each channel diameter of length along the bed. Making the proposed substitutions in Equation (32) yields

$$\frac{-\Delta P_f}{L} g_c = 72\left(\frac{\pi}{2}\right)^2 \frac{(1-\epsilon)^2}{\epsilon^3} \frac{\mu U}{D_p^2} + \frac{6}{8}\left(\frac{\pi}{2}\right)^2 \frac{1-\epsilon}{\epsilon^3} \frac{\rho U^2}{D_p} \tag{33}$$

or

$$\frac{-\Delta P_f}{L} g_c = 177 \frac{(1-\epsilon)^2}{\epsilon^3} \frac{\mu U}{D_p^2} + 1.85 \frac{1-\epsilon}{\epsilon^3} \frac{\rho U^2}{D_p} \tag{34}$$

In actual practice the two constants are replaced by experimentally evaluated constants k_1 and k_2, respectively. Ergun[24] evaluated the constants k_1 and k_2 for a great deal of data and obtained the following results:

$$k_1 = 150$$

$$k_2 = 1.75$$

It is very satisfying to note how closely the experimental numbers agree with the predicted ones.

The form of Ergun's equation which is most widely used and which will be used here is

$$\frac{-\Delta P_f}{L} g_c = k_1 \frac{(1-\epsilon)^2}{\epsilon^3} \frac{\mu U}{D_p^2} + k_2 \frac{(1-\epsilon)}{\epsilon^3} \frac{\rho U^2}{D_p} \quad . \tag{35}$$

IV. EXPERIMENTAL PROGRAM

1. Introduction

Due to the lack of knowledge in the area of two-phase flow, any investigation of this subject must be based on a sound experimental program. In addition, due to the complete lack of data on cocurrent flow of immiscible liquids in packed beds, an experimental investigation of this subject must be largely exploratory in nature. As a result even the most carefully designed experimental program would probably not solve all the problems associated with this subject. Therefore the experimental program must be explained in detail so that workers with further interest in this area need not repeat work unnecessarily.

As pointed out in the introduction, a large number of independent variables may possibly effect the flow characteristics of immiscible liquids in packed beds. The number of these variables actually studied must of necessity be limited. This section describes in detail the experimental equipment and operating procedures used to study these variables and also describes the manner of selection and ranges of variables studied.

2. Experimental Apparatus

The main piece of experimental apparatus used in the present study was the test section which consisted of an 82-inch long 4-inch ID transparent Lucite tube with Lucite flanges attached at each end. The tube actually consisted of two sections of tube joined at the center by a 1-1/2 inch lap joint supported by a two-section 4-inch Lucite collar held in place by steel wire. The flanges enabled the test section to be

mounted vertically between two 4-inch, flanged quick-closing valves. Since the purpose of the valves was to trap the contents of the test section during a run, a system of weights and pulleys was provided to close the valves simultaneously and as rapidly as possible. The valve handles were connected by steel cables through a system of pulleys to a single weight which could be dropped thus actuating the valves simultaneously.

In order to obtain accurate holdup measurements the packed portion of the column had to extend as close as possible to the valve disks. Therefore retaining screens were placed inside the valves and the valves themselves were filled with packing. A detailed drawing of the lower valve connection is shown in Figure 1.

In order to measure pressure drop in the test section, four holes were drilled and tapped along the length of the tube. In these were placed 1/8 inch pipe to 3/16 inch copper tubing connectors which were in turn connected to a manometer manifold system by means of 3/16 inch copper tubing. The 3/16 inch size was used to minimize errors caused by the two-phase mixture being drawn into the manometer lead lines. An additional pressure tap was placed just below the valve disk in the lower quick-closing valve to measure pressure drop in the entrance section. To prevent the packing particles from plugging the pressure taps, four small holes were drilled in the end of each 1/8 inch pipe connector. Two copper wires, crossed at right angles, were then inserted in the holes. This kept packing particles out of the pressure tap without introducing a capillary pressure error sometimes caused by placing fine wire screens over the openings.

Inside diameter of column	=	3.96 in.
Cross sectional area	=	0.08553 ft.^{2}
Total volume between valve disks	=	0.629 ft.^{3}
Packed volume	=	0.615 ft.^{3}
Length of packed section	=	86.25 in.
Distance between taps 1 and 2	=	11.09 in.
Distance from entrance to packed section to tap 2	=	7.09 in.
Distance between taps 2 and 3	=	24.00 in.
Distance between taps 3 and 4	=	24.06 in.
Distance between taps 4 and 5	=	24.00 in.

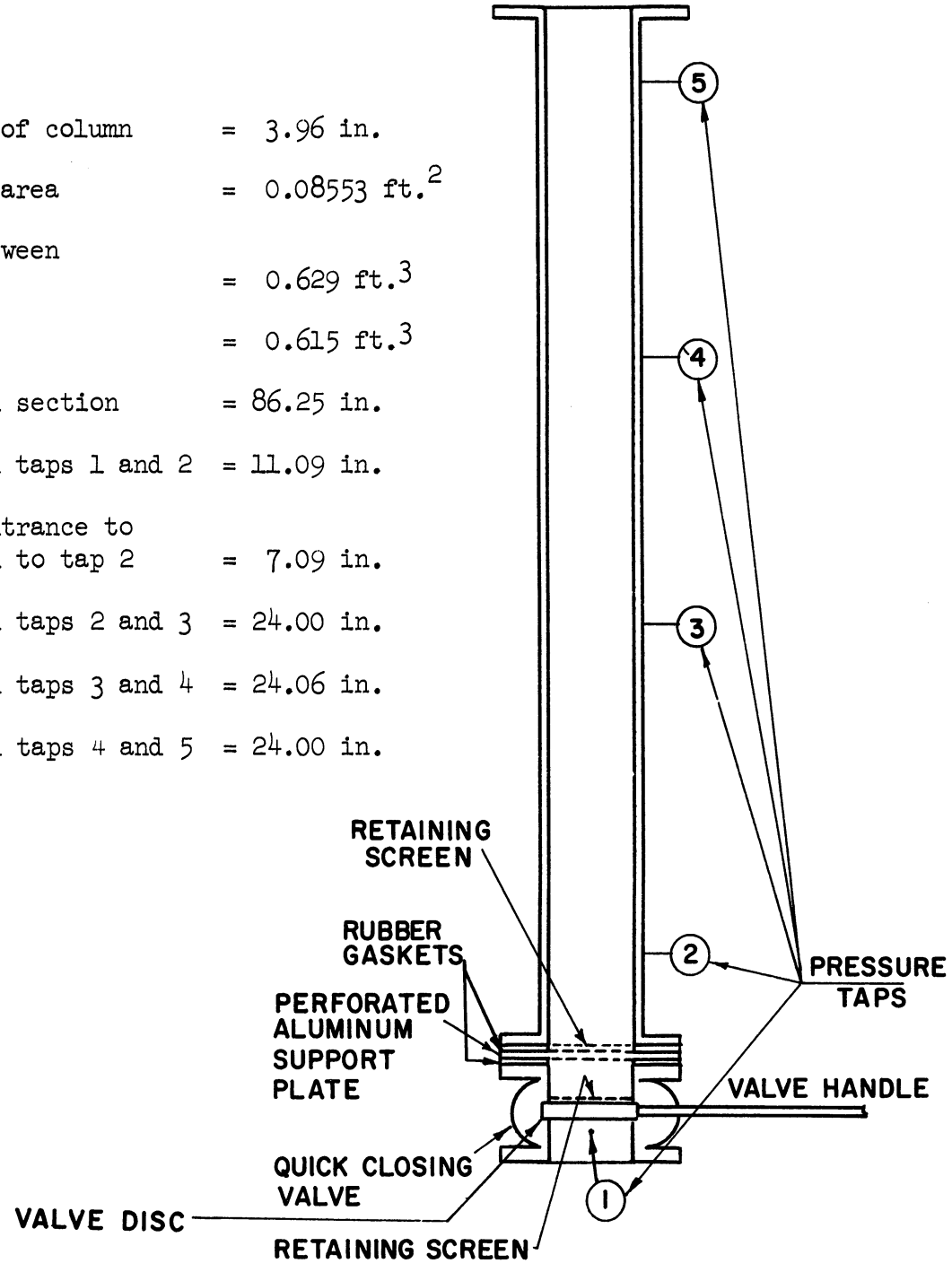

Figure 1. Test Section Dimensions (Not to Scale).

Complete test section dimensions and pressure tap locations are given in Figure 1.

To facilitate the description of the flow system associated with the test section, consider the system in operation. A schematic flow diagram is shown in Figure 2. All lines unless otherwise stipulated were 1-1/2 inch galvanized pipe. The two liquids were picked up from their respective 200 gallon storage tanks and pumped to separate rotameter systems. A recycle line to the storage tank with a manual control valve was provided for each liquid system. The water pump was a 5 hp. turbine pump while the organic liquid pump was a 3 hp. centrifugal pump. Water inlets were provided in both systems for flushing and filling purposes.

Two Fischer & Porter rotameters were used in each liquid system to measure flowrates. A large rotameter of approximately 20 gpm maximum capacity and a smaller rotameter of approximately 8 gpm maximum capacity were used in series in each system. The large meter in the water system was a Fischer & Porter Model 10A1735 rotameter with a size 8 tube and an SVP-87 float, while the small meter was a Fischer & Porter Model 10A1735 rotameter with a size 6 tube and an SVP-67 float. The large meter in the organic liquid system was a Fischer & Porter Model 10A1735 rotameter with a size B8 tube and a BNSVT-83 float, while the smaller meter was a Fischer & Porter Model 10A1735 rotameter with a size B6 tube and a BSVT-64 float. The piping was arranged so that the liquids could flow through both rotameters in series, the large rotameter only, or neither rotameter. Line pressures could be monitored by the gauges shown in Figure 2.

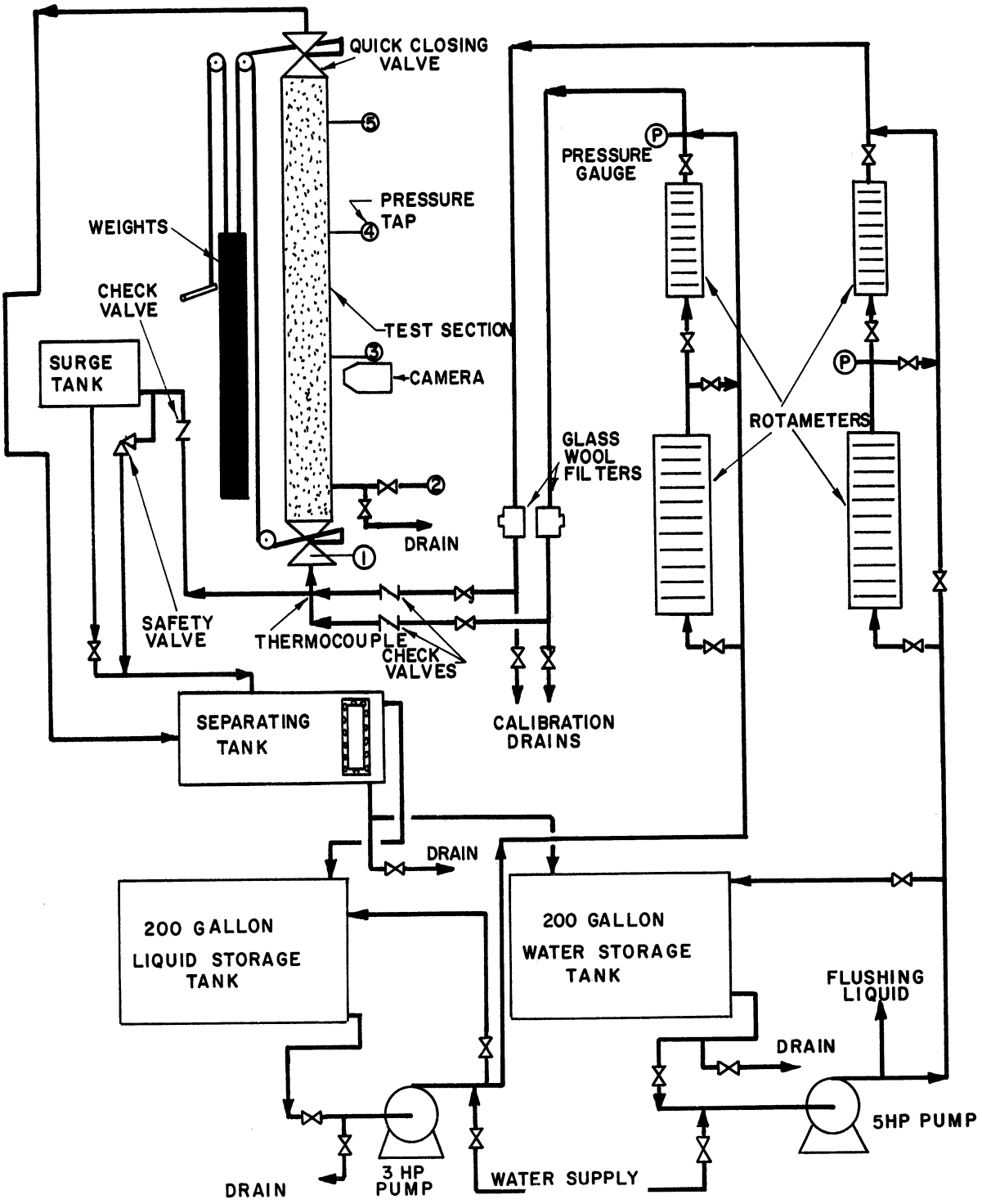

Figure 2. Schematic Diagram of Experimental Apparatus.

After leaving the rotameter systems the liquids flowed through filters, past calibration drains, through check valves and came together in a 2 inch cross. The filters consisted merely of a copper wire screen placed in a tee in the line with a small amount of glass wool over the screen. The sidearm in the tee enabled the glass wool to be changed periodically.

An immersion type copper-constantan thermocouple was used to measure the temperature at the inlet to the test section. It was mounted in a 1-1/2 inch length of 1/4 inch stainless steel tubing and mounted directly through the wall of the 2 inch cross. A commercial temperature indicator was used to obtain temperature readings.

During normal operation the liquid mixture flowed out through one arm of the 2 inch cross, through the lower 4 inch quick-closing valve and into the test section. The effluent mixture from the test section flowed through a 1-1/2 inch line and entered an opening half way up the wall of a 140 gallon separating tank. A glass window in the front of the separating tank allowed visual observation of the position of the interface between the two liquids. The separated liquids then flowed by gravity, through 2 inch lines, back to their respective storage tanks. The position of the liquid interface was maintained approximately midway in the tank by adjusting the flowrate of the heavier liquid.

In order to eliminate the possibility of a water hammer when the quick-closing valves were actuated, a by-pass for the flowing liquids was provided through the fourth arm of the 2 inch cross located at the entrance to the test section. A 2 inch line led from the cross, through

a check valve and into a surge drum. Before each run the surge drum was pressurized with air to a pressure at least 10 psi greater than that expected at the entrance to the test section. This kept the check valve in the by-pass line closed. When the quick-closing valves were actuated the check valve in the by-pass line was forced open and the liquid mixture began to fill the surge tank. The drain valve on the surge tank was then opened and the liquid mixture drained into the separating tank. If for some reason the drain valve were not opened and the pressure in the surge tank continued to build up, a relief valve set for 100 psig was provided to dump the system into the separating tank.

As mentioned previously, all piping was galvanized but the storage and separating tanks were constructed of ordinary carbon steel sheet. To prevent corrosion and thereby contamination of the liquids these tanks were painted inside and out with DuPont Imlar Vinyl Chemical Resistant Paint.

Pressure drop measurements were obtained by means of a dual, well-type manometer manufactured by the Meriam Instrument Company with a 40 inch range and a maximum operating pressure of 350 psig. One manometer tube was filled with mercury while the other was filled with a manometer fluid provided by the King Engineering Company; this fluid had a specific gravity of 1.750 at 20°C relative to water at 4°C.

The manifold system shown schematically in Figure 3 enabled either the high or low range manometer to be connected across any two pressure taps in the system. The numbered circles in Figure 3 correspond to the numbered pressure taps in Figure 2. An Ashcroft laboratory test

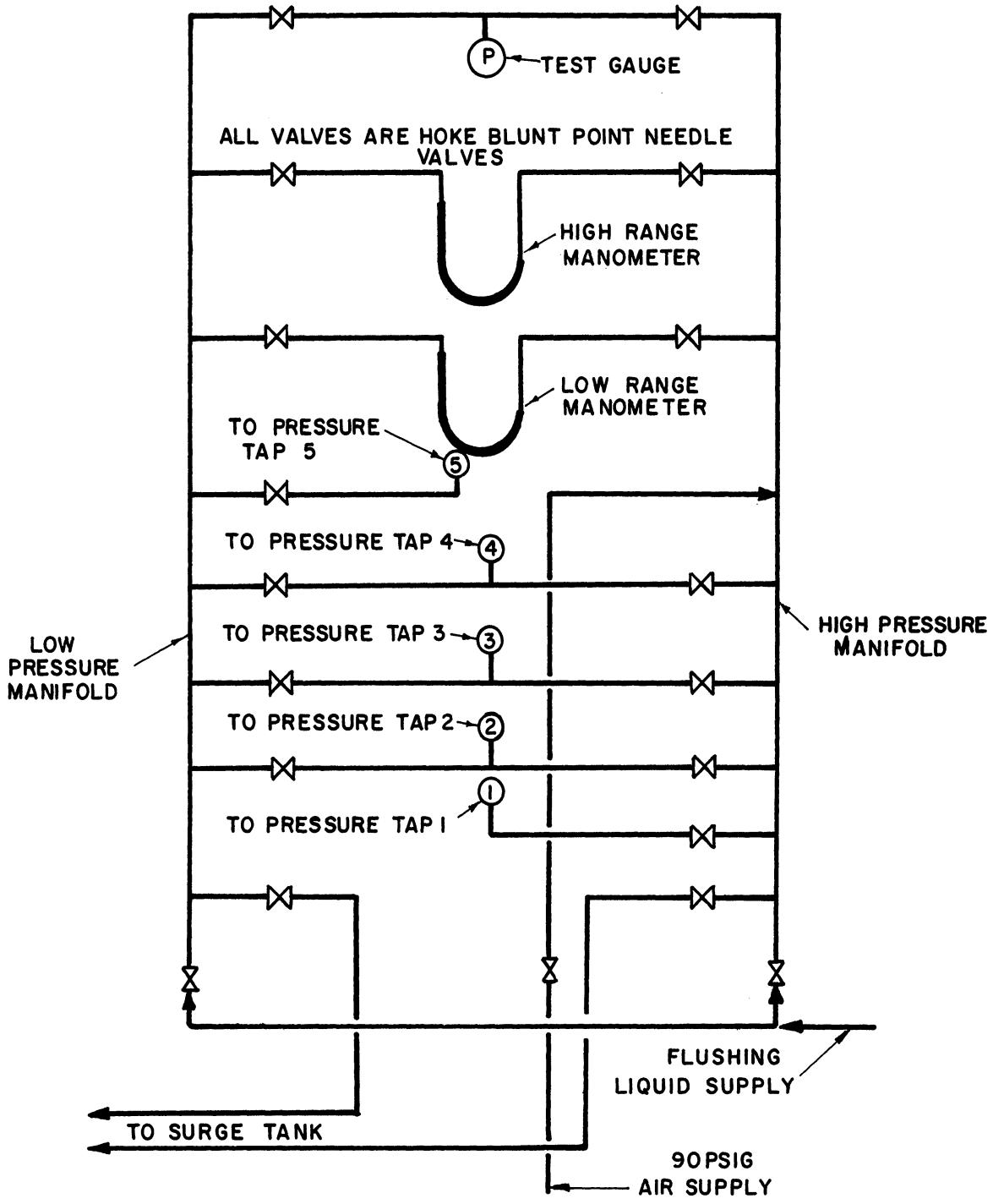

Figure 3. Schematic Diagram of Pressure Manifold System.

gauge with a range of 0 to 100 psig was connected to the manifold system so that static pressure at any point in the test section could be obtained. A supply of flushing liquid taken directly from the water pump discharge, the highest pressure location in the system, was provided. As a result during operation the manometer lines were always filled with the water phase. In addition the building air supply at a supply pressure of approximately 90 psig was connected to the manifold system. The manifold system could, therefore, be used to fill and meter the pressure in the surge tank. Connections for this purpose are shown in Figure 3. The system was constructed entirely of 1/8 inch brass pipe and 3/16 inch copper tubing. All valves were Hoke blunt point needle valves.

3. Photographic Equipment

To measure the dispersed phase drop sizes during a run, flash photographs of the flowing system were taken through the wall of the test section. The camera used for this purpose used a 50 mm Argus lens with an adjustable focus and having f/2.8 to f/22 stops. The resulting magnification was approximately 2.9X. A ground glass focusing plate mounted in the film holder allowed the droplet images to be focused on the film without a trial and error procedure. The film used was Kodak Contrast Process Ortho 4" x 5" cut film. This is a fine grained orthochromatic film used for high contrast applications. The film was exposed by means of a high intensity light flash from a General Electric FT 220 flashtube powered by the discharge of a 76 microfarad capacitor initially charged to 2250 volts.

The camera was positioned approximately 24 inches from the bed entrance as shown in Figure 2. The relative positions of camera, flash-tube, and test section are shown in Figure 4. Arrangement a, using transmitted light, is the preferred arrangement since it eliminates distortion due to reflection. This arrangement was used with the largest packing size. For smaller sizes, however, the light produced by this arrangement was too diffuse to adequately expose the film, so arrangement b was used.

4. Operating Procedures

Before starting actual operation the four rotameters were calibrated by passing water through them and weighing the water collected in a given time. The calibration curves agreed substantially with those provided by the manufacturer. For use with liquids of density different from that of water, rotameter correction factor curves supplied by the manufacturer were used. These correction factors were checked by the direct weighing method for at least three points for each liquid and were found to be quite accurate. A plot of this correction factor for meters calibrated with water and using a stainless steel float is given in Appendix A.

As was mentioned earlier the porosity of the packed bed is an important variable in the present investigation. In order to accurately measure porosity and to assure a reproducible packing arrangement the following procedure was used in packing the test section:

(1) The bottom of the test section was sealed by means of a rubber gasket and an aluminum plate bolted to the bottom plastic flange. The test section was then placed in an

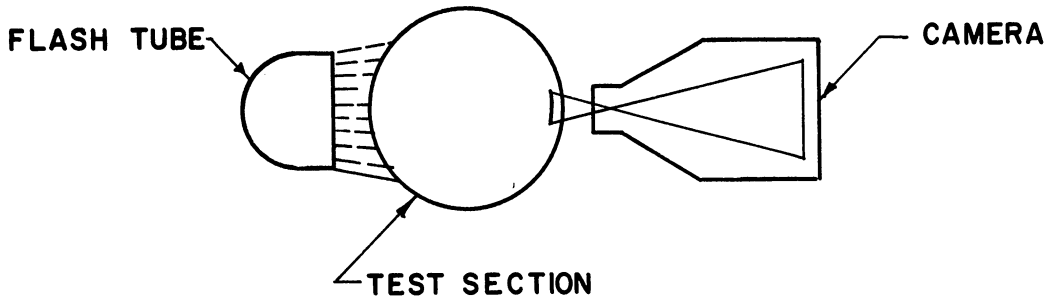

(a) Transmitted Light

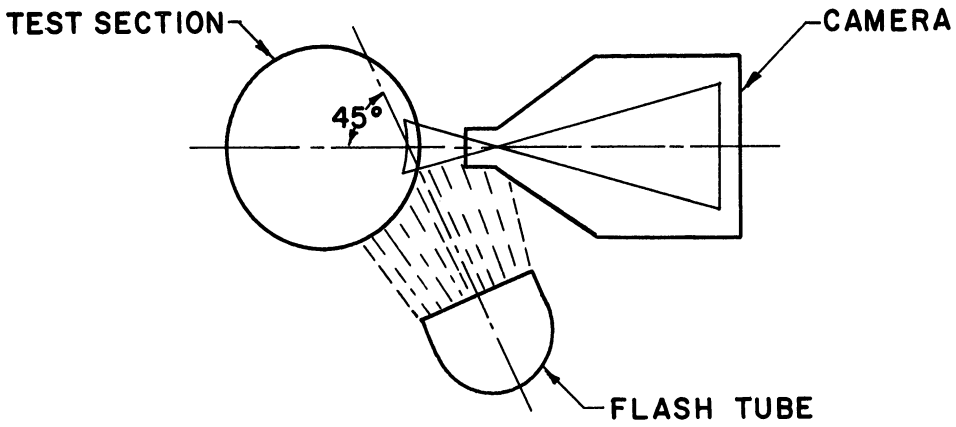

(b) Reflected Light

Figure 4. Arrangement of Photographic Equipment (Top View)

upright position on the floor, the pressure taps were sealed off, and the test section filled with water to the uppermost pressure tap. An overflow line from this tap led to a graduated cylinder.

(2) Packing was slowly poured into the test section and the overflow water collected. The column was intermittently tapped with a rubber hammer to ensure adequate settling of the particles. This method of packing eliminated further settling during operation.

(3) The following expression was then used to compute porosity:

$$\epsilon = 1 - \frac{V_W}{V_T} \qquad (36)$$

where

V_W = volume of overflow water collected

V_T = total volume of test section between the lower flange and the uppermost pressure tap.

(4) The porosity was independently measured by weighing the amount of packing introduced into the test section. By using the density of the packing material an equation similar to Equation (35) could be used to compute porosity. The two values for porosity agreed within 2% in all cases.

(5) Since it was originally assumed that capillary pressure may have some effect on pressure drop, the test section was next allowed to drain slowly ($\sim$1/2 hour) through the lowest pressure tap to determine permanent holdup. The

permanent holdup was in all cases less than 2.65% of the total void volume indicating that capillary pressure is not an important variable.

(6) The quick-closing valves were then filled with packing to the retaining screen, the plate removed from the bottom of the test section, and the test section bolted in place. The pressure taps were connected and the equipment was ready for operation.

In order to eliminate possible errors in the constants of the Ergun equation from influencing the results of the present study, single-phase pressure-drop measurements were made for each packing. The procedure used in these runs was essentially the same as that used in the two-phase runs which is described below.

The procedure used in a typical two-phase run was approximately as follows. The drain valve from the surge tank was closed and the surge tank pressurized with air. The quick-closing valves were opened and the two liquid pumps started. The flows were adjusted to the desired levels by means of the recycle valves and the valves adjacent to the rotameters. The manometer lead lines were then flushed by introducing flushing liquid into the pressure manifolds and then opening the valves to the pressure taps one at a time. The flushing liquid supply was then turned off and pressure taps 2 and 3 connected across the appropriate manometer. When a constant reading was obtained, the valves leading to the manometer were closed and the pressure tap lead lines reflushed. This ensured that the lead lines were filled with the aqueous phase. Pressure taps 2 and 3 were

again opened and a reading taken. Taps 4 and 5 were then connected to the manometer and a reading was taken. A second reading was then taken between taps 2 and 3 and this process continued until both readings were constant. Readings were then taken for the pressure difference between taps 3 and 4 and taps 1 and 2. All valves leading to pressure taps and manometers were then closed and the inlet temperature was recorded. Comments regarding the flow pattern were noted at that time.

The procedure for measuring phase holdup was then started by dropping the weight which actuated the quick-closing valves. As soon as the valves were closed the drain valve from the surge tank was opened and the pumps were turned off. The two liquid phases were then allowed to separate in the test section. One of two methods was then used to measure phase holdup. If a readily discernible interface formed between the two phases the distance from the interface to the lower flange was measured. Since the total volume contained between the two valve disks and the porosity in the packed section are known, the fraction of the void spaces occupied by the discontinuous phase could be computed. If no clear interface formed (e.g., in the case of very small packing) a more time consuming method of obtaining holdup data was required. The test section was allowed to drain slowly through the sample tap located at pressure tap 2 as shown in Figure 2. The volume of the more dense phase contained in the column was measured and used to compute the phase holdup.

A few runs were made to measure the time dependence of phase holdup. In these runs no pressure drop measurements were made. The flow of one

phase was established and allowed to completely fill the test section. The flow of the second phase was then established. After a short time the quick-closing valves were closed and the holdup measured. A series of such runs over varying lengths of time provided data on the time dependence of holdup.

5. Photographic Techniques

Following completion of the pressure drop and phase holdup runs for a given system a series of photographs at various velocities and flow ratios was taken. Photographs could not be taken during the runs themselves because of a lack of space. The desired flowrates were established and a film holder placed in the camera. Since the open lens technique of flash photography was used (the camera lens was open at all times) the protecting shield was not removed from the film holder until just a few seconds prior to triggering the flashtube. Normal room light intensity was not great enough to expose the film. The intense light emitted by the flashtube was required to expose the film. At least two photographs were taken at each set of flow rates.

The film was then developed for 5 minutes at 68°F in Kodak D-11 developer, rinsed for 30 seconds, placed in Kodak Acid Fix for 10 minutes, rinsed for 30 seconds, placed in Kodak Hypo Clearing Agent for 2 minutes, rinsed for 10 minutes and dried.

Drop sizes were then measured directly from the negatives with the help of a comparator which produced a 10X enlarged image on a ground glass screen. This resulted in an overall magnification of approximately 30X. Drop diameters parallel to the axis of the test section were measured

using one of two triangular templates; one graduated in tenths of an inch to a maximum of 1.5 inches, the other graduated in hundredths of an inch to a maximum of 0.5 inches. Only diameters parallel to the axis of the cylindrical test section were measured, because the curvature of the walls of the test section produced a slight distortion perpendicular to the axis. All drops in reasonable focus were measured. The number of drops counted per photograph ranged from as few as 11 to as many as 283.

In order to obtain actual drop sizes it was necessary to calibrate both the camera and the comparator. This was accomplished by photographing a sphere of known diameter and measuring its diameter on the negative and on the comparator image of the negative. The camera magnification was 2.94X while the comparator magnification was 10.0X.

6. Properties of Systems Studied

A single packing shape was used in this study in order to isolate the effect of packing size on pressure drop, phase holdup, and drop size. Spheres were chosen because of their simple geometry and their lack of any particle orientation effect. For the same reason as mentioned above a single packing material was selected. Glass was used with the hope of being able to observe flow patterns in the bed more closely than with opaque materials. Spheres were selected from commercially available sizes to give a wide range without introducing a wall effect.

Fluid pairs were also selected to give a wide range of physical properties. In all cases water was one of the fluids; isobutanol, isooctane, and isooctane with a surfactant added were used as the second phase.

The systems used in this investigation were:

(1) Saturated solutions of water and isobutanol on 0.501 inch spheres.

(2) Saturated solutions of water and isobutanol on 0.340 inch spheres.

(3) Saturated solutions of water and isobutanol on 0.164 inch spheres.

(4) Water and isooctane on 0.164 inch spheres.

(5) Water and isooctane on 0.340 inch spheres.

(6) Water and isooctane with Alkaterge "C" (a surfactant) added on 0.340 inch spheres.

6.1 Packing Properties

The two larger sizes of glass spheres were made of flint crystal glass and were obtained from the Peltier Glass Company of Ottawa, Illinois. The small glass spheres are called 3M Brand Spherical Impact Media IM0406(S) and were obtained from the Minnesota Mining & Manufacturing Company.

The characteristic diameter of each size of spheres was obtained by two different methods. Fifty spheres of each size were selected at random and the diameter of each sphere was measured five times in random directions by means of a micrometer. An arithmetic mean diameter was computed from these measurements. The total volume of the fifty spheres was next determined by water displacement. The mean particle diameter was computed from this volumetric measurement based on the assumption of a perfectly spherical shape. The glass density, which was required to compute porosity by the direct weighing method, was computed by dividing the

weight of the fifty spheres by the volume determined by the water displacement method. The two values of diameter and the value of density are presented in Table I along with the two values determined for porosity. Since the column had to be repacked with the medium sized packing in order to make the isooctane-water runs, two values of porosity are presented in Table I. The first was that used for the water-isobutanol runs and the second for the water-isooctane and water-isooctane-Alkaterge "C" runs. Figure 5 shows samples of the three packings used.

6.2 Fluid Properties

The solutions used in the runs involving water and isobutanol were prepared by circulating tap water and commercial grade isobutanol through the experimental equipment for a period of about 4 hours. The isobutanol was used as received from the Union Carbide Chemicals Company. To prevent the formation of a stable emulsion, the water phase was acidified to 0.0001 N HCl. This small concentration of acid was found not to affect the physical properties of either phase.

The isooctane used in this investigation was Pure Grade Isooctane and was obtained from the Phillips Petroleum Company. It contained a minimum of 99 mole per cent 2, 2, 4-Trimethyl Pentane. The interfacial tension of the isooctane-water system was reduced for the final set of runs by preparing a 0.009 volume per cent solution of Alkaterge "C" in isooctane. Alkaterge "C" is an organic-soluble surfactant supplied by the Commercial Solvents Company of Terre Haute, Indiana.

The physical properties of all fluids used in this investigation are presented in Table II. Literature values were used when available.

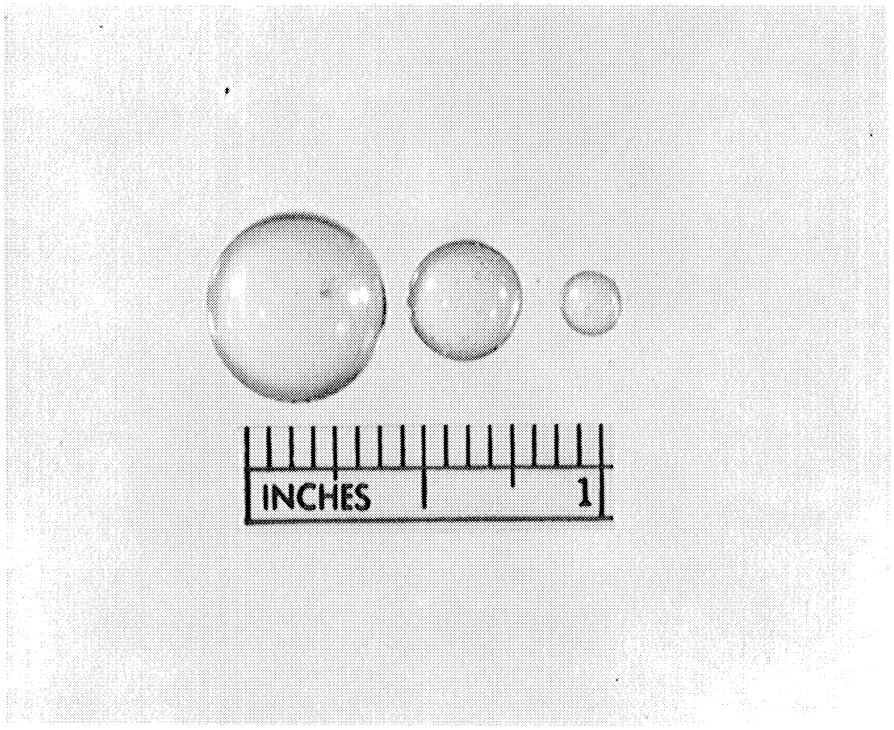

Figure 5. Photograph of Typical Packing Particles.

Those values which were not available in the literature were measured in the Sohma Precision Laboratory. In addition the literature values of physical properties were checked experimentally and found to be in good agreement in all cases. Viscosity was measured by means of an Ostwald viscometer, density by means of a precision hydrometer, and interfacial tension by means of a ring type tensiometer.

Since viscosity is a strong function of temperature, all viscosity data were fitted with curves of the form

$$\log_{10} \mu = A + \frac{B}{T} \qquad (37)$$

where T = absolute temperature. These equations could then be used to compute the liquid viscosities for any run.

Plots of viscosities as functions of temperature plus all equations used to compute the data in Table II are presented in Appendix B.

TABLE I

PROPERTIES OF PACKING MATERIALS

Diameter by direct measurement (in.)	Diameter by water displacement (in.)	Glass density (gms/in^3)	Packed porosity by direct weighing	Packed porosity by water displacement
0.501	0.502	40.57	0.400	-
0.339	0.340	40.89	0.383	0.379
			0.382(a)	0.377(a)
0.165	0.163	47.98	0.337	0.345

(a) These values were obtained when the test section was repacked for isooctane-water runs.

TABLE II

PHYSICAL PROPERTIES OF FLUIDS

Fluid	Composition	Density @75°F (gms/cc)	Viscosity at 75°F (cp.)	Interfacial Tension against saturated water solution at 75°F (dynes/cm.)
Water	-	0.998[36]	0.915[43]	-
Water saturated with isobutanol	8.4 wt.% isobutanol[68]	0.987[59]	1.30(L)	-
Isobutanol saturated with water	83.5 wt.% isobutanol[68]	0.832[59]	3.10(L)	2.1[39]
Isooctane	99 mole % min. 2, 2, 4-Trimethyl Pentane	0.692[36]	0.478(L)	49.5[34]
Isooctane with Alkaterge "C"	0.009 vol. %(L) Alkaterge "C"	0.692[36]	0.478(L)	16.0(L)

Superscripts indicate number of reference which is source of data. (L) numbers indicated thus were measured in the laboratory.

V. EXPERIMENTAL RESULTS

1. General

This section of the thesis presents the experimental results obtained from the preceding experimental program. Observations and a discussion of the results are presented but no attempt at correlation is included. That subject is treated in the following section.

Use of the experimental apparatus and systems presented in the previous section limits further selection of independent variables to the flowrates of the individual phases. Since the research was largely exploratory, an attempt was made to cover as wide a range of these variables as possible. An upper limit was imposed by the capacity and developable head of the pumps. A lower limit was imposed by the range of the rotameters and the sensitivity of the manometers. This lower limit, however, was not a serious limitation because in this flow range frictional pressure drop becomes very small relative to static pressure drop. Approximately 40 runs were performed on each system in an attempt to blanket the ranges of available flowrates. In addition, approximately 10 of these runs were repeated to see if the results were reproducible. No attempt was made to evaluate reproducibility numerically but these additional points are included in the data plots for examination. In examining the data for internal consistency it should be remembered that each data point stands alone, i.e. it does not depend on the data points preceding it. Recall that following each run the quick-closing valves are closed and the flows shut off. For each succeeding run the flows of the two phases must be reestablished.

In addition to the numerical data presented later in this section, visual observations of flow patterns were recorded. Although no correlateable effect of flow pattern on pressure drop, phase holdup, or drop size, was observed, descriptions of these flow patterns are included for comparison purposes.

Three flow patterns or "modes" of flow were observed during this investigation. In the "bubble flow" regime small droplets of the dispersed phase were distinctly observable in the continuous phase. A second flow pattern "homogeneous flow" occurred only at high flow rates. In this pattern no distinct droplets could be observed, but the liquid mixture in the test section had a "milky" appearance. However, when the quick-closing valves were actuated, the "milky" appearance quickly disappeared and small droplets could be observed in the test section. In addition analysis of enlarged photographs of "homogeneous flow" showed very small droplets to be present. In light of these two observations "homogeneous flow" can be considered merely an extension of "bubble flow" to very small drop sizes. Although no distinct boundaries of the "homogeneous flow" regime were obtained, it seems to occur at high total flowrate, small packing diameter, and low interfacial tension. These are precisely the conditions expected to produce very small droplets.

The third flow pattern is by far the most difficult to describe. "Slug flow" has been observed and described a number of times in the literature, but only Larkins[44] has used the term to describe the flow pattern observed here. "Slug flow" as observed here is best described by considering the test section to be initially in "bubble flow" (see

Figure 6a). A "slug" or volume of fluid in "homogeneous flow" approximately 4 to 6 inches thick next appears at the entrance to the test section (Figure 6b). As the "slug" moves up through the bed, its shape becomes very irregular and very elongated (Figure 6c). In most cases the "slug" seemed to disappear approximately 3 to 5 feet from the entrance to the bed, but in some cases it continued the full length of the column. The separation of the "slugs" varied but on the average was approximately one foot. Although again no definite boundaries for the "slug flow" regime could be obtained, it seemed to occur most often at high flow rates and at flow ratios in the vicinity of 75% organic phase.

During the course of the experiments it was extremely difficult to determine which of the phases was continuous. Since in all cases the water phase preferentially wetted the glass packing, it was to be expected that the water phase would be continuous. This was indeed observed at low ratios of organic phase to water phase. However as the flowrate of organic phase was increased, the "slug flow" and "homogeneous flow" regimes developed and visual observation was of little value. Observation of the settling process following the closing of the quick-closing valves, however, did give an indication as to which phase was continuous. At low flow ratios of organic phase to water phase, droplets of the discontinuous phase could be seen rising in the continuous phase. The organic phase (in all cases the lighter phase) was therefore discontinuous. However for very high flow ratios of organic phase to water phase, droplets of the discontinuous phase were seen to fall in the continuous phase, indicating that the water phase was discontinuous. The flow ratios for runs in which

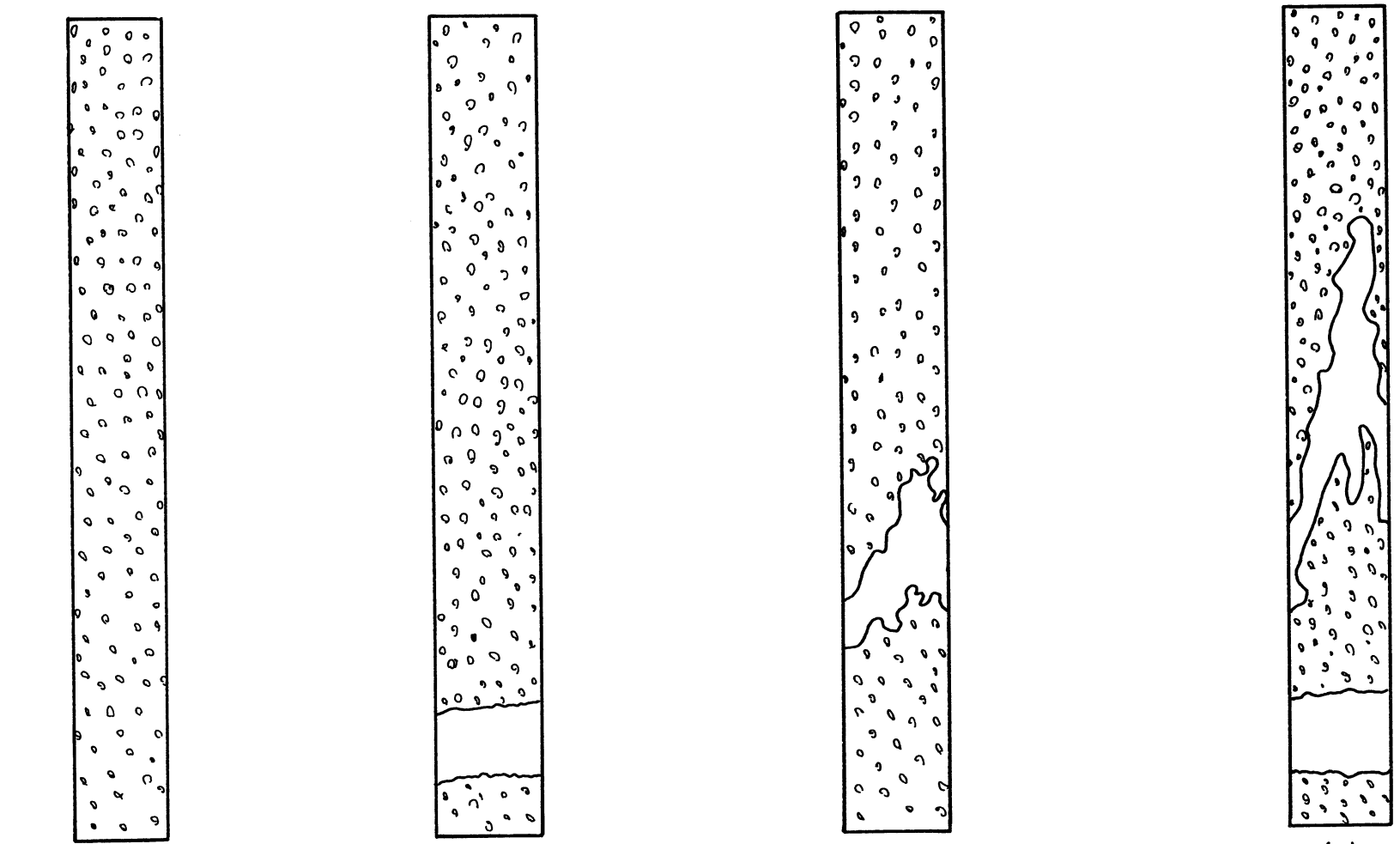

Figure 6. Appearance of "Slug Flow" Pattern.

this was observed were in all cases greater than approximately 75% organic phase.

2. Data Processing

In order to save a great deal of work the raw data were processed on an IBM 7090 digital computer at The University of Michigan Computing Center. For the single-phase runs the following items of data were punched on IBM cards. One card was used for each run.

(1) a five digit code number

(2) the uncorrected flowrate taken from the rotameter, gpm

(3) temperature, °F

(4-11) four manometer readings for the pressure differences between successive pressure taps and four code numbers (0 or 1) indicating which manometer (low range or high range) was used; the manometer readings were punched directly as inches of manometer fluid.

A card preceding each set of single-phase data gave all information which applied to the entire set, such as physical properties, packing diameter, etc. The digital computer then computed and applied the rotameter correction factor, computed the liquid viscosity, computed actual pressure drops, averaged the latter three pressure drops, corrected this for static pressure drop, and computed the parameters necessary for evaluation of the constants in the Ergun equation. It then evaluated these constants for each data set by a least squares technique. The computer then printed the results in tabular form as shown in Appendix C. The number

of digits reported in the data tables does not indicate the significance of the data. The tables were automatically printed by the computer and the numbers have not been rounded off.

For each two-phase run the following items of data were punched on an IBM card:

(1) a five digit code number

(2-3) the uncorrected flowrates of each phase taken from the rotameters, gpm

(4) temperature, °F

(5-12) four manometer readings in inches of manometer fluid and four code numbers (0 or 1) indicating which manometer was used

(13) either the height of the liquid interface above the lower plastic flange in inches or the volume of the water phase drained from the column in cc.

Two cards preceding each data set contained all information which applied to the entire set. The following information was automatically computed: corrected flow rates; total pressure gradients (The pressure due to the fluid in the manometer lead lines was added to the manometer reading to obtain the difference in total pressures between the two pressure taps. The pressure gradient was then computed.); the average of the three pressure gradients inside the column; and the discontinuous phase holdup. (See Appendix D)

The five digit code number mentioned previously, which identifies each run, consists of three parts. The first three digits are the number of the run itself. All runs, both single-phase and two-phase, were numbered consecutively. The fourth digit is an alphabetic character

indicating the fluid used in addition to water (I = isobutanol, O = iso-octane, W = water - used only for single-phase water runs). The fifth digit is also an alphabetic character indicating the flow pattern (B = bubble flow, H = homogeneous flow, S = slug flow, O = single-phase run).

Table III serves as a guide to the extensive data tables found in the appendices.

3. Pressure Gradient

3.1 Single-Phase Pressure Gradient

Single-phase pressure gradient data were obtained for two reasons: (1) to check the reliability and accuracy of the experimental techniques used; (2) to evaluate k_1 and k_2 in Ergun's equation precisely.

To evaluate k_1 and k_2 Equation (35) was rearranged to give

$$-\frac{\Delta P_f}{L}\frac{g_c D_p^2}{\mu U}\frac{\epsilon^3}{(1-\epsilon)^2} = k_1 + k_2\frac{D_p\rho U}{\mu(1-\epsilon)} \tag{38}$$

If k_1 and k_2 are indeed constants, a plot of

$$\left(-\frac{\Delta P_f}{L}\frac{g_c D_p^2}{\mu U}\frac{\epsilon^3}{(1-\epsilon)^2}\right) \text{ versus } \frac{D_p\rho U}{\mu(1-\epsilon)} \text{ will give a straight}$$

line with intercept k_1 and slope k_2. The $\frac{\Delta P_f}{L}$ here is the frictional pressure gradient only. The static pressure gradient due to the vertical position of the column must be subtracted from the total pressure gradient before it is used in this equation. To save space define

$$F = \left(\frac{\Delta P_f}{L}\frac{g_c D_p^2}{\mu U}\frac{\epsilon^3}{(1-\epsilon)^2}\right) \tag{39}$$

and

$$\text{Rem} = \frac{D_p\rho U}{\mu(1-\epsilon)} \tag{40}$$

TABLE III

CODING OF DATA RUNS

Inclusive Run Numbers	Systems Involved
1-20, 45-51	Single-phase runs on 0.501-in. spheres
21-44, 52-87	Water-isobutanol on 0.501-in. spheres
88-113	Single-phase runs on 0.340-in. spheres
114-195	Water-isobutanol on 0.340-in. spheres
196-217, 286-305	Single-phase runs on 0.164-in. spheres
218-285	Water-isobutanol on 0.164-in. spheres
306-350	Water-isooctane on 0.164-in. spheres
351-371	Single-phase runs on 0.340-in. spheres
372-430	Water-isooctane on 0.340-in. spheres
431-470	Water-isooctane-Alkaterge "C" on 0.340-in. spheres

The data for all single-phase runs were processed as described earlier and the results are presented in Tables I - X, Appendix C. All the data for a given packing size were used to evaluate k_1 and k_2 by a least squares technique, i.e. the sum of squares of $(F-k_1-k_2 \cdot Rem)$ was minimized by differentiating with respect to k_1 and k_2 and equating the resulting derivatives to 0. These two equations were then solved for k_1 and k_2. Since a significant effect of column length on pressure drop was not noted, the average of the three pressure drops measured inside the test section was used in this correlation. The values of these constants are presented in Table IV.

TABLE IV

VALUES OF ERGUN EQUATION CONSTANTS

Packing	k_1	k_2
0.501-in. spheres	315	1.16
0.340-in. spheres	254, 349[a]	1.52, 1.19[a]
0.164-in. spheres	210	1.28
Ergun Values	150	1.75

(a) These values were obtained when the test section was repacked.

An examination of Table IV shows a much greater variation in k_1 than k_2. This is understandable since all data were taken for Rem > 20. For Rem $\cong$ 100 the contributions of the viscous and kinetic terms to the frictional pressure gradient are approximately equal. For Rem $\cong$ 0.15 viscous effects account for 99.8% of the frictional pressure gradient. As a result most of the data fall in the region where kinetic losses are dominant, so the coefficient of the viscous term is less well known. The values given in Table IV are however those which best fit the data. In this thesis the values of k_1 and k_2 presented in Table IV are used in place of the Ergun values unless otherwise noted.

Figure 7 is an example of the type of plot used to evaluate k_1 and k_2. It should be noted that the data for both fluids fall on one line. For this reason the variation in the values of k_1 and k_2 presented in Table IV are believed to be due to bed variations only. That is, k_1 and k_2 are not functions of either velocity or fluid properties.

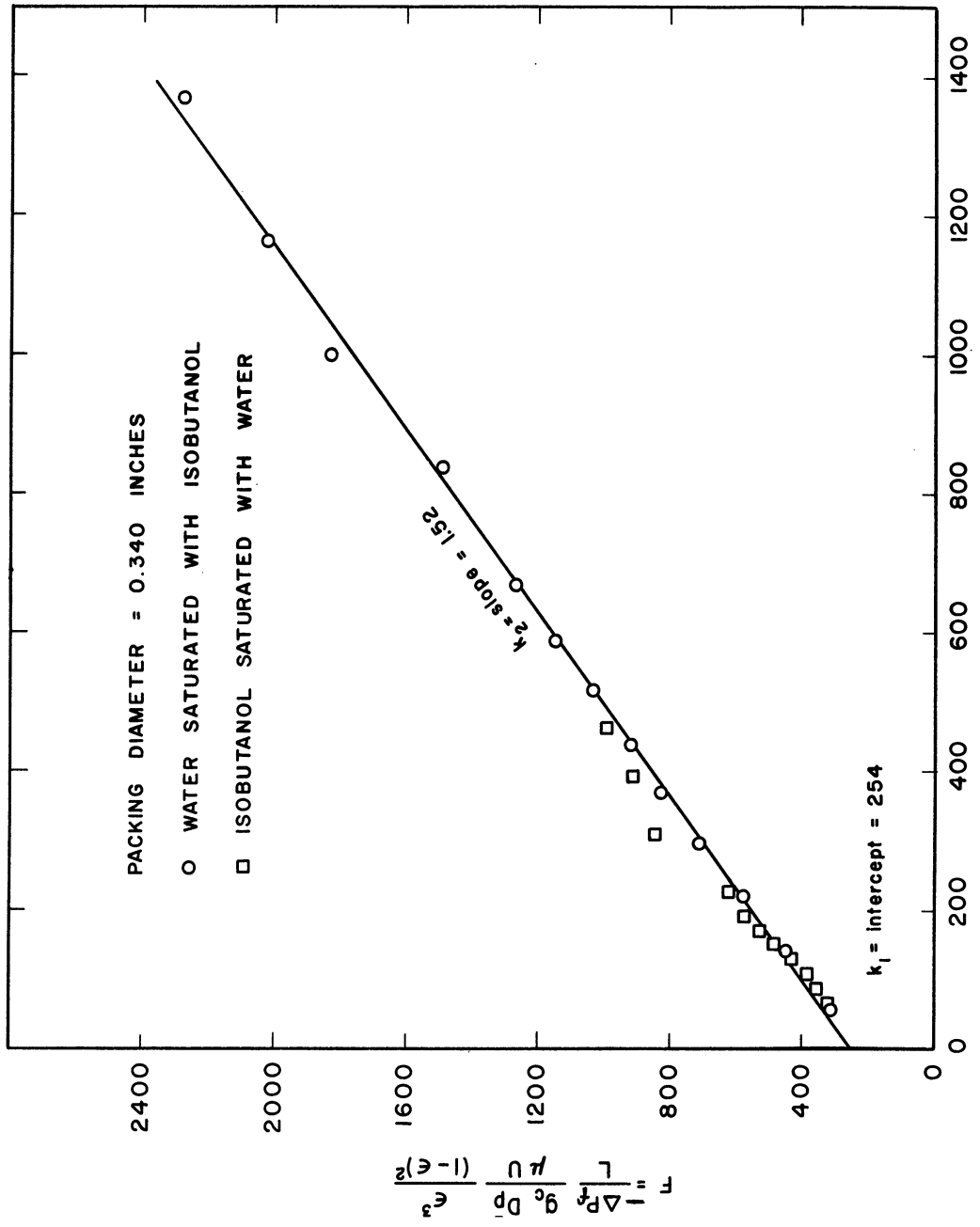

Figure 7. Fit of Single-Phase Data to Ergun Type Equation.

In order to evaluate the accuracy and reliability of the experimental techniques used here, all of the single-phase data were compared with the Ergun equation. Figure 8 illustrates this comparison. A logarithmic plot is used to cover a wider range of variables. The solid line in Figure 8 is Equation (35) with $k_1 = 150$ and $k_2 = 1.75$.

The single-phase data at large values of Rem are lower than those predicted by the Ergun equation. An examination of the data Ergun used to evaluate k_1 and k_2,[24] however, shows the same effect. It is very possible, therefore, that some phenomenon other than those accounted for in the Ergun equation occurs at high values of Rem.

3.2 Two-Phase Pressure Gradient

Before two-phase pressure-gradient measurements could be recorded, steady state operation had to be achieved. The procedure described in the section on experimental apparatus showed that a varying length of time was required to reach steady state. This time varied from about 10 minutes at high flowrates to as much as 35 minutes for low flowrates. The two-phase pressure-gradient results in Tables I - VI, Appendix D, were all obtained at steady state.

With the system water-isobutanol-0.501-in. spheres an attempt was made to determine whether a hysteresis effect existed. Flowrates of the two phases were established and steady state pressure gradient data were recorded. One of the flowrates was then drastically changed and after a length of time returned to its initial setting. In all cases the pressure gradient returned to its steady state value within 30 minutes.

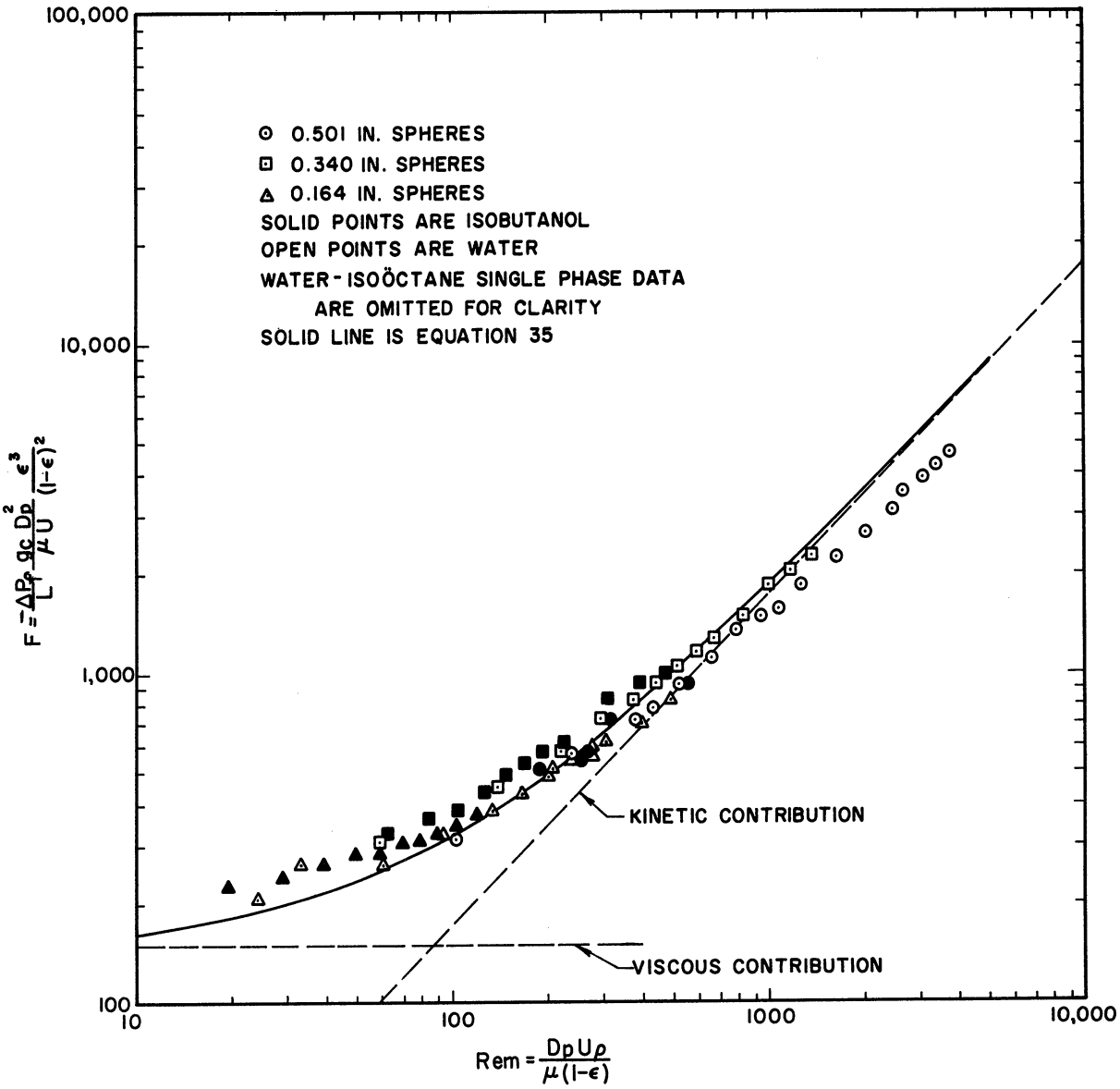

Figure 8. Comparison of Single-Phase Data with Ergun Equation.

For most runs four valuse of total pressure gradient were measured: the entrance pressure gradient and three pressure gradients inside the test section. These values are presented in Appendix D with the arithmetic average of the three inside pressure gradients. An examination of Appendix D shows the variation of pressure gradient with column length to be insignificant, as a result the average values were used in all graphs and correlations.

Plots of average total pressure gradient as a function of water phase flowrate with parameters of organic phase flowrate are presented in Figures 9-14. The total pressure gradient is composed of a static gradient plus a frictional gradient. However in a system involving two fluid phases there is some question as to the value to be used for the static gradient (as discussed on pages 100-103). For this reason the total pressure gradient (a measure value) rather than the pressure gradient due to friction (a derived value) is plotted in Figures 9-14. Figure 9a shows only average pressure gradient. Figure 9b, on the other hand, includes an indication of the flow patterns observed. Consider, for instance, the line representing an isobutanol flowrate of 5.78 gpm in Figure 9b. The point at water phase flowrate =0 gpm is, a single-phase point. As the water phase flowrate is increased a point exhibiting slug flow is observed followed by points exhibiting bubble, homogeneous, slug, homogeneous, and homogeneous flow, respectively. Despite apparent randomness in flow pattern, the data follows a smooth curve. To save space in Figures 10-14 the type of information presented in Figures 9a and 9b will be presented in only one graph.

Originally it was presumed that pressure gradients for the cocurrent flow of immiscible liquids in packed beds could be correlated by the Ergun equation [Equation (35)] if the proper mean values of density and viscosity and the total velocity were used. Figure 9c presents a comparison of the

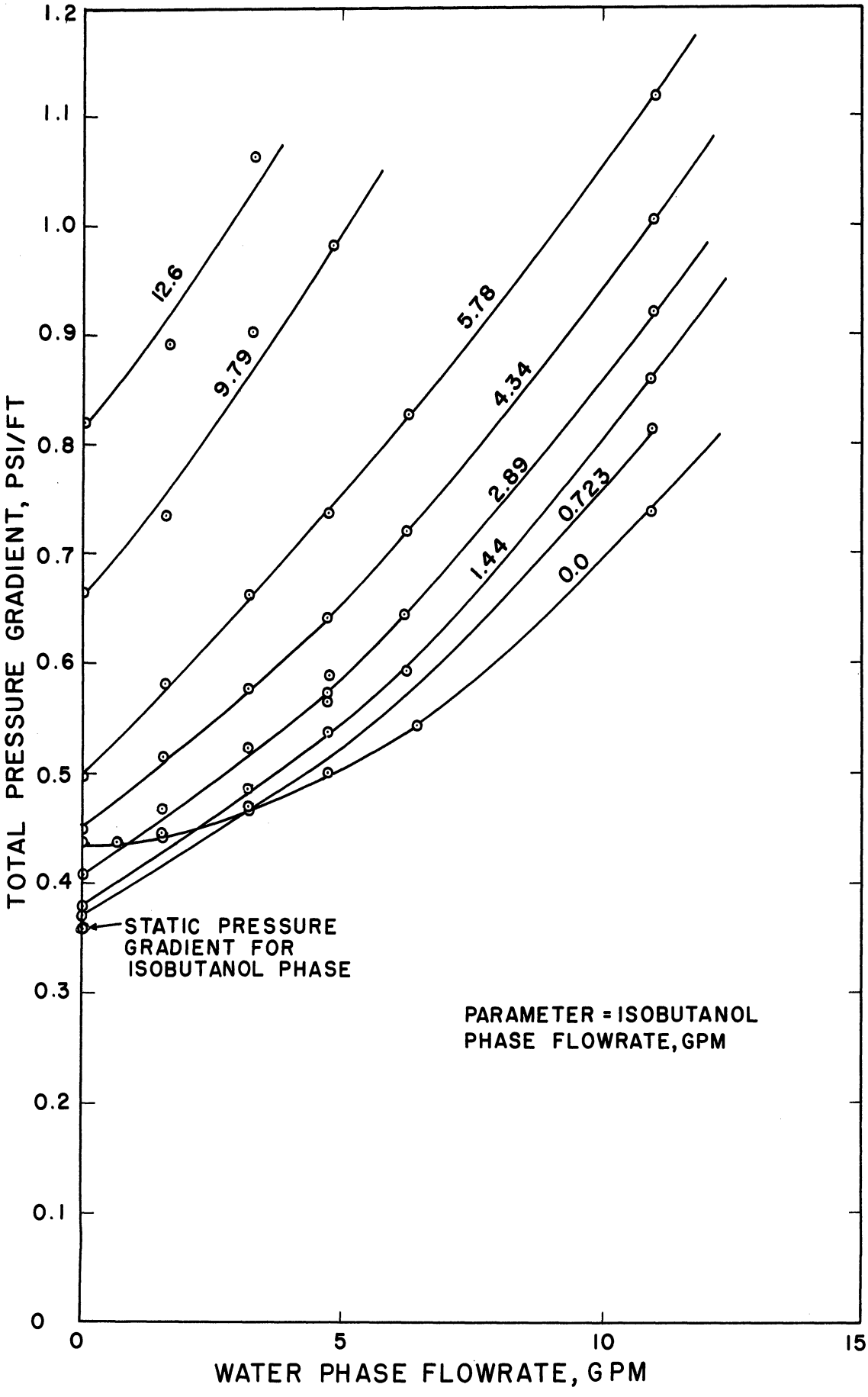

Figure 9a. Total Pressure Gradient in the System Isobutanol -Water-0.501 Inch Spheres.

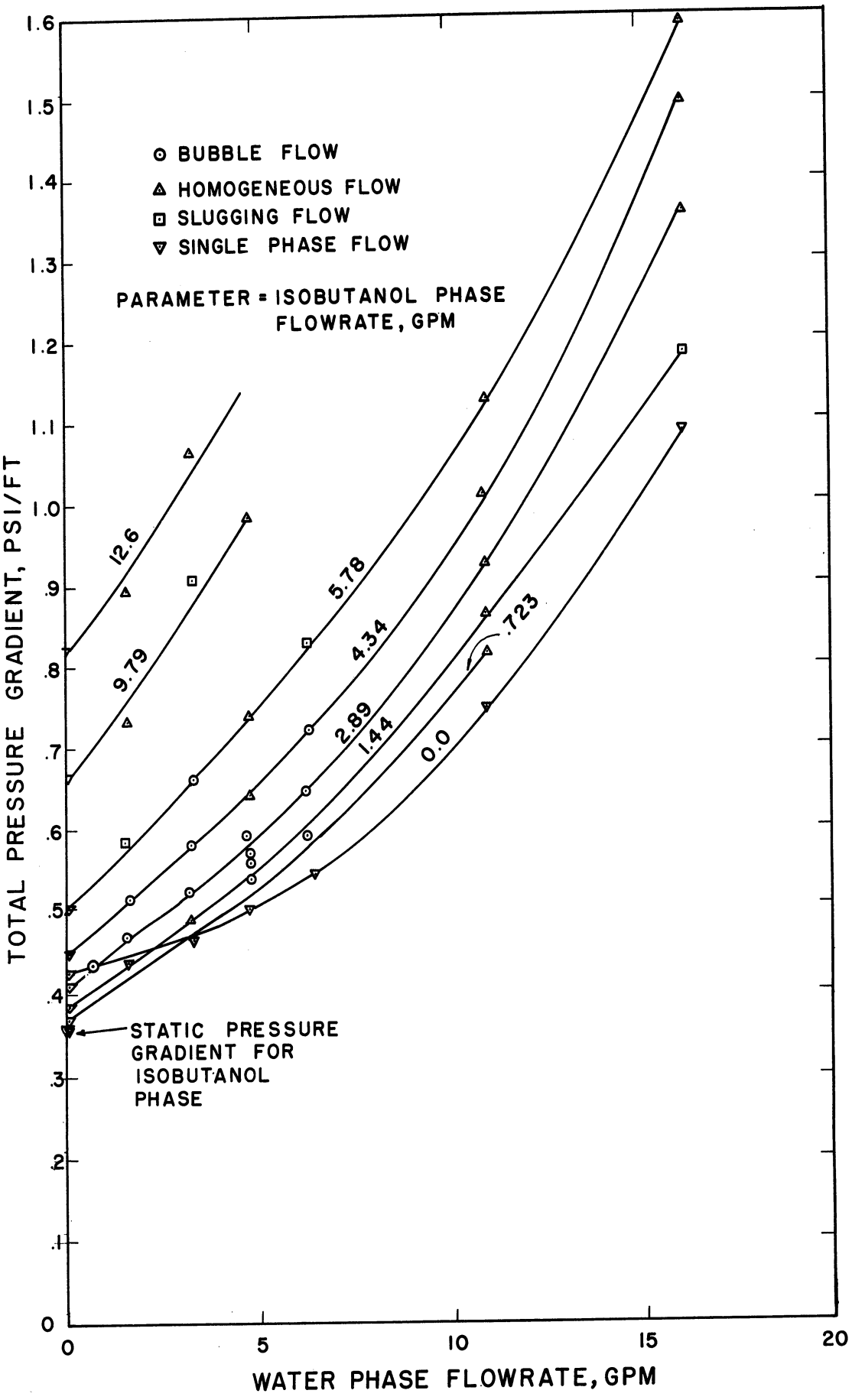

Figure 9b. Total Pressure Gradient in the System Isobutanol -Water-0.501 Inch Spheres.

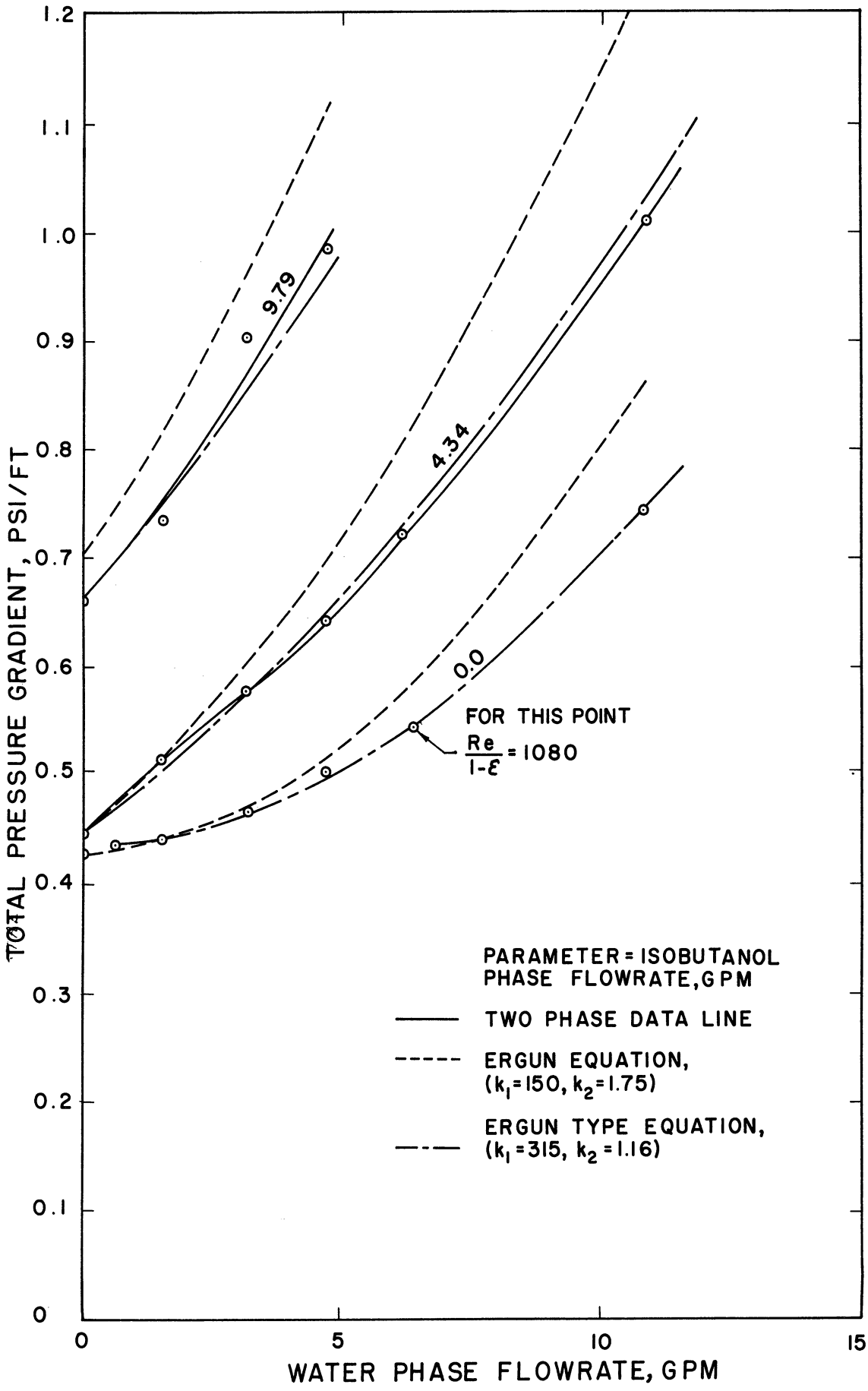

Figure 9c. Total Pressure Gradient in the System Isobutanol -Water-0.501 Inch Spheres.

two-phase pressure-gradient data, the total pressure gradient predicted by the Ergun equation ($k_1 = 150$, $k_2 = 1.75$), and the total pressure gradient predicted by an Ergun type equation with k_1 and k_2 evaluated experimentally. The following mean values were used in the Ergun and Ergun type equations:

$$\mu_m = \frac{U_w\mu_w + U_o\mu_o}{U_w + U_o} \tag{41}$$

where U = individual phase superficial velocity and the subscripts indicate the water phase and the organic phase, and

$$\rho_m = \frac{U_w\rho_w + U_o\rho_o}{U_w + U_o} \tag{42}$$

The static pressure gradient was computed using ρ_m. In Figures 10-14 the comparison between actual two-phase pressure gradient and the Ergun type equation is presented as Figures 10b-14b.

The pressure-gradient data presented in this section are all total pressure gradients. The separation of these pressure gradients into static and frictional components is discussed in detail in the next section.

Even though the data plots show that two-phase mixture does not behave as a single-phase fluid (i.e., a single-phase equation cannot be used), they do point up some interesting results. The data approach the "single-phase" curves at both extremes of flow ratio. This means at extremes of flow ratio the two-phase mixture behaves as a single-phase fluid with respect to pressure gradient. However at intermediate flow ratios the actual pressure gradient is considerably greater than that predicted by the "single-phase" assumption. An examination of the data plots shows that this difference increases with the interfacial tension of the system

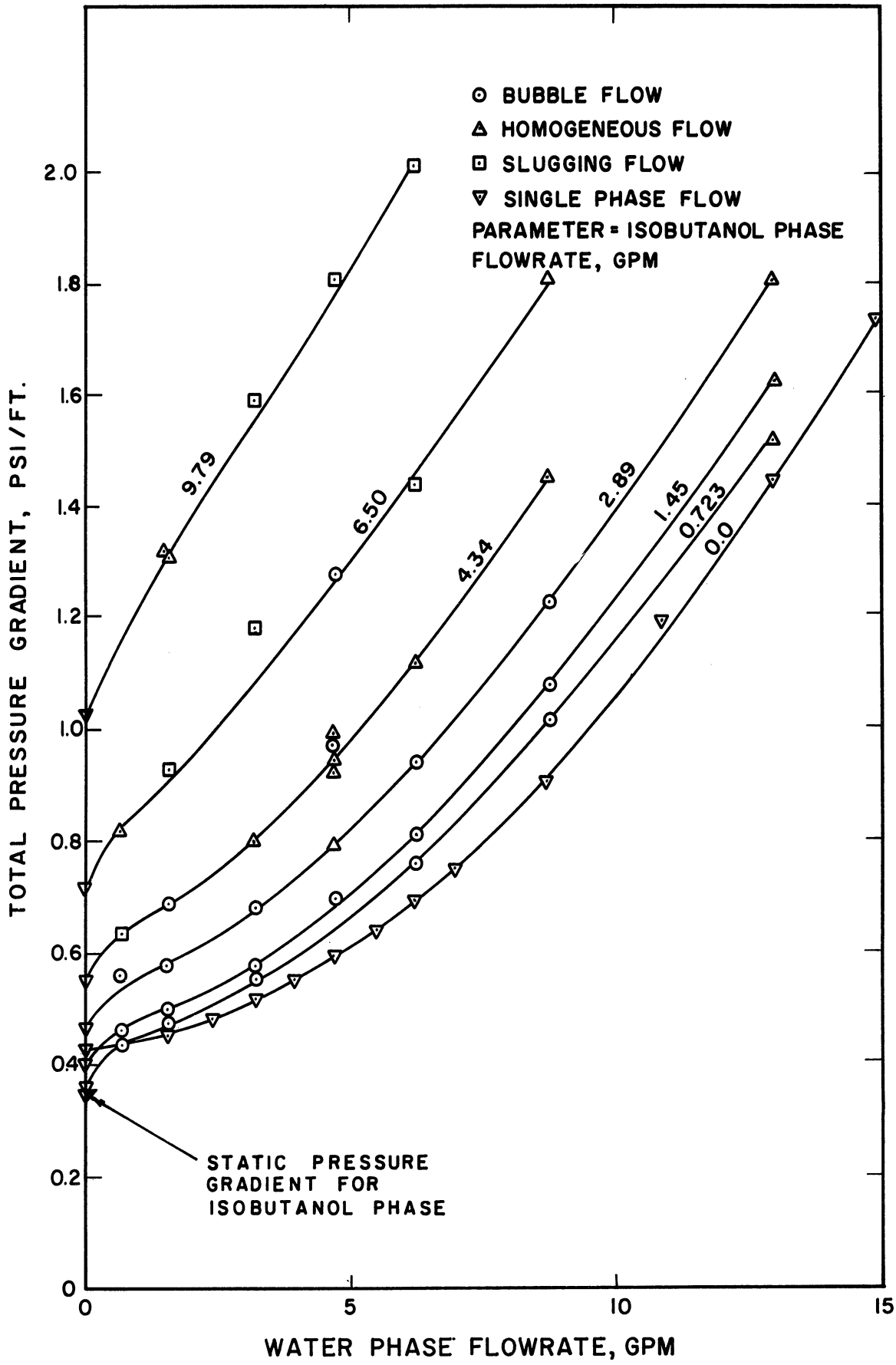

Figure 10a. Total Pressure Gradient in the System Isobutanol -Water-0.340 Inch Spheres.

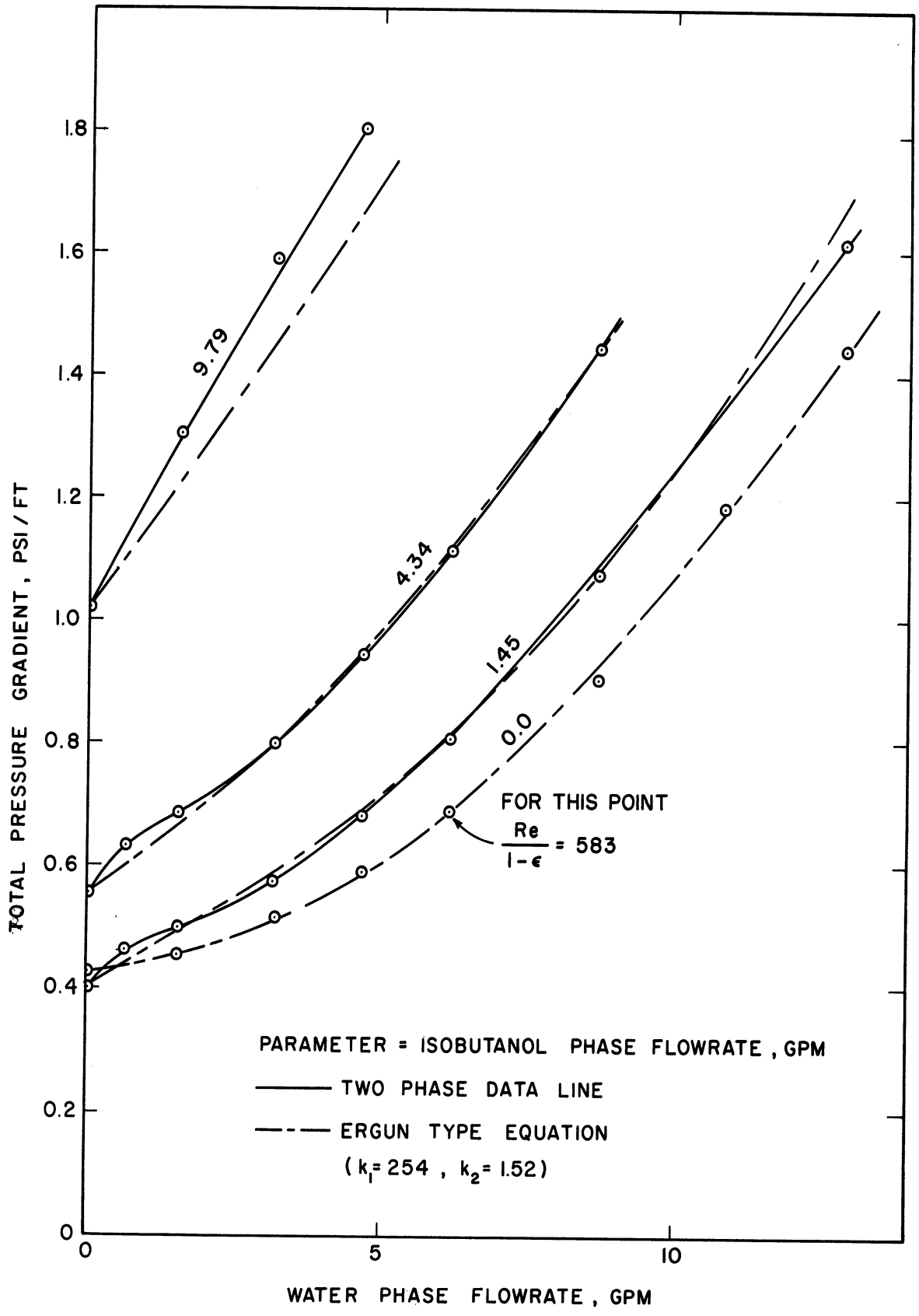

Figure 10b. Total Pressure Gradient in the System Isobutanol-Water -0.340 Inch Spheres.

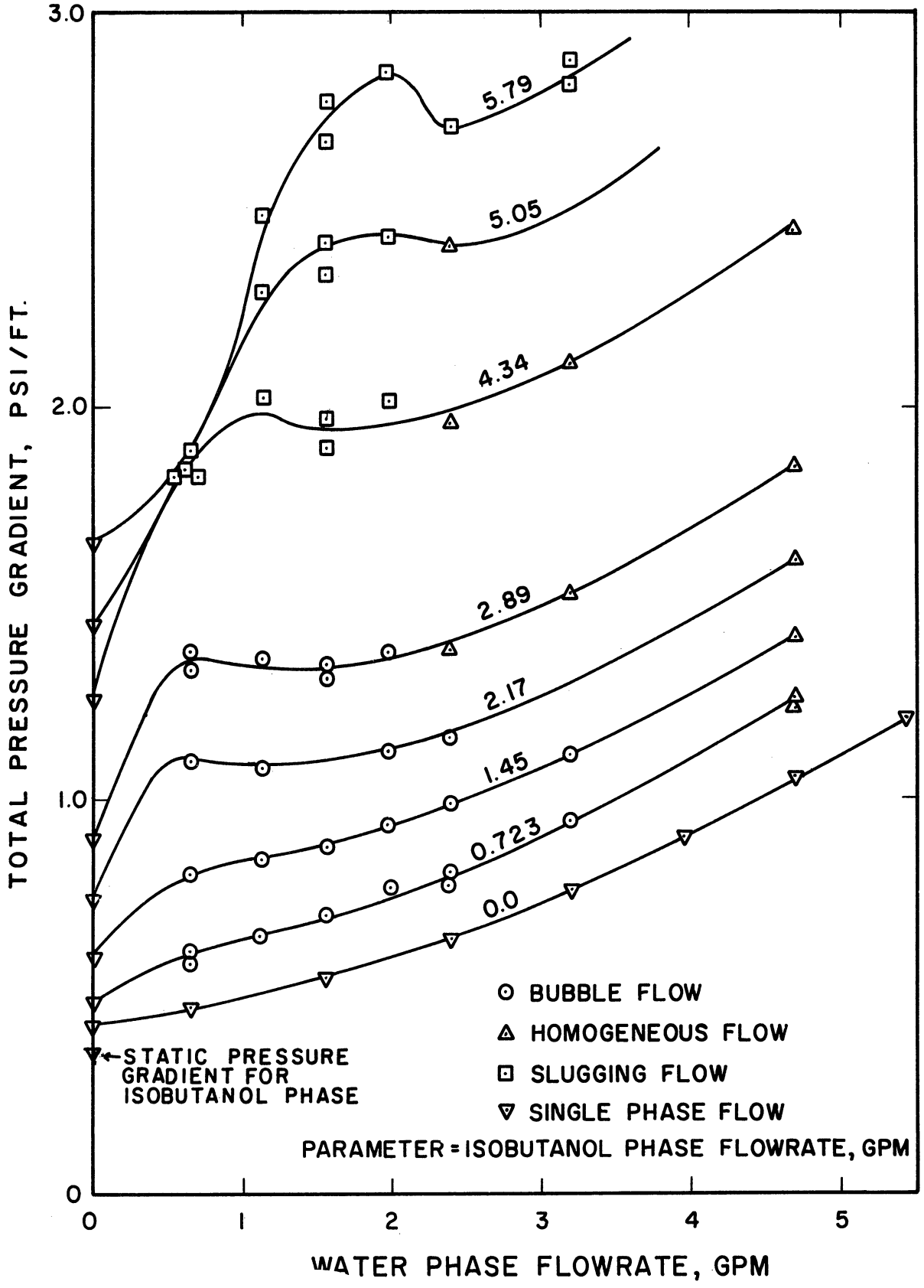

Figure 11a. Total Pressure Gradient in the System Isobutanol -Water-0.164 Inch Spheres.

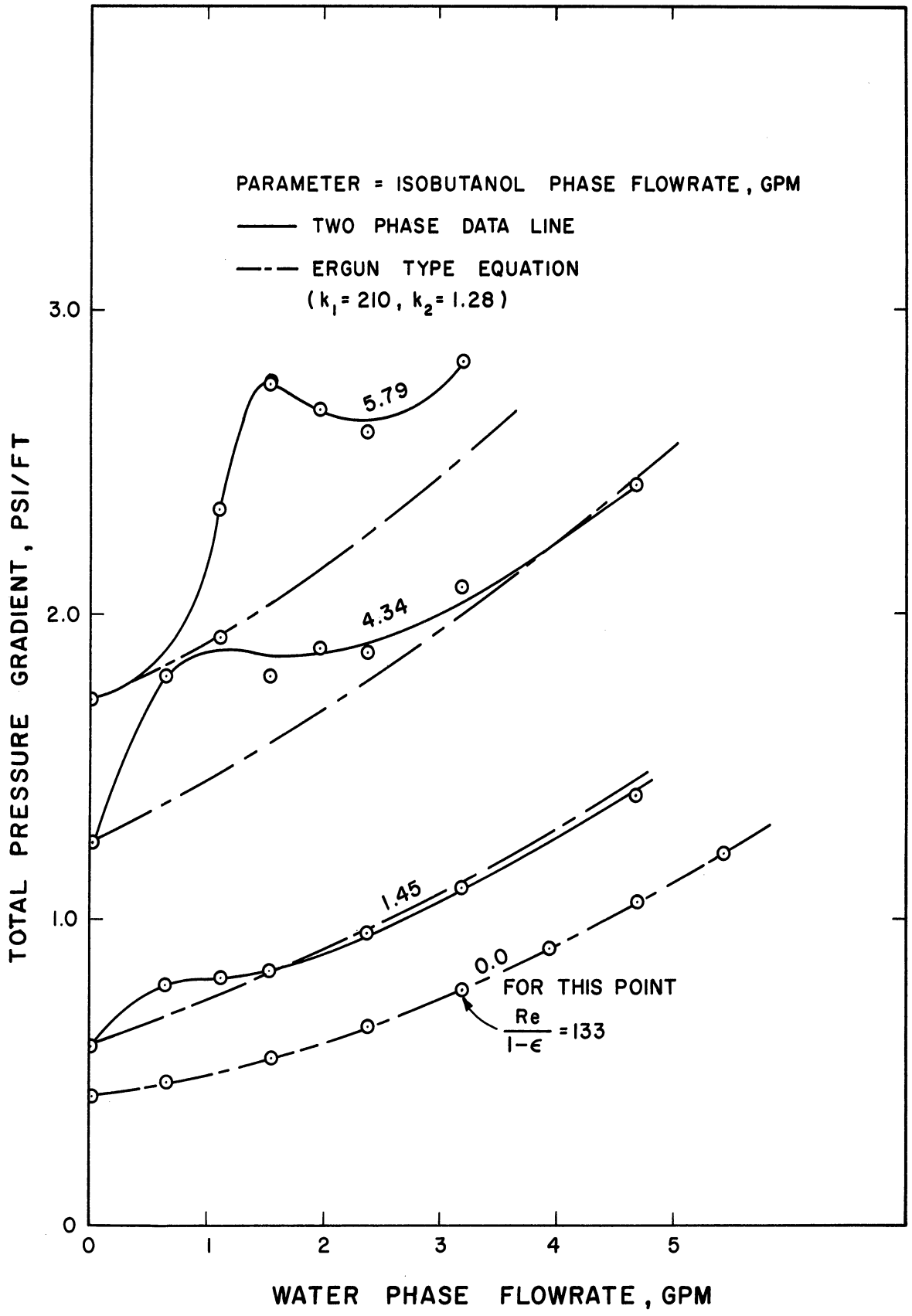

Figure 11b. Total Pressure Gradient in the System Isobutanol -Water -0.164 Inch Spheres.

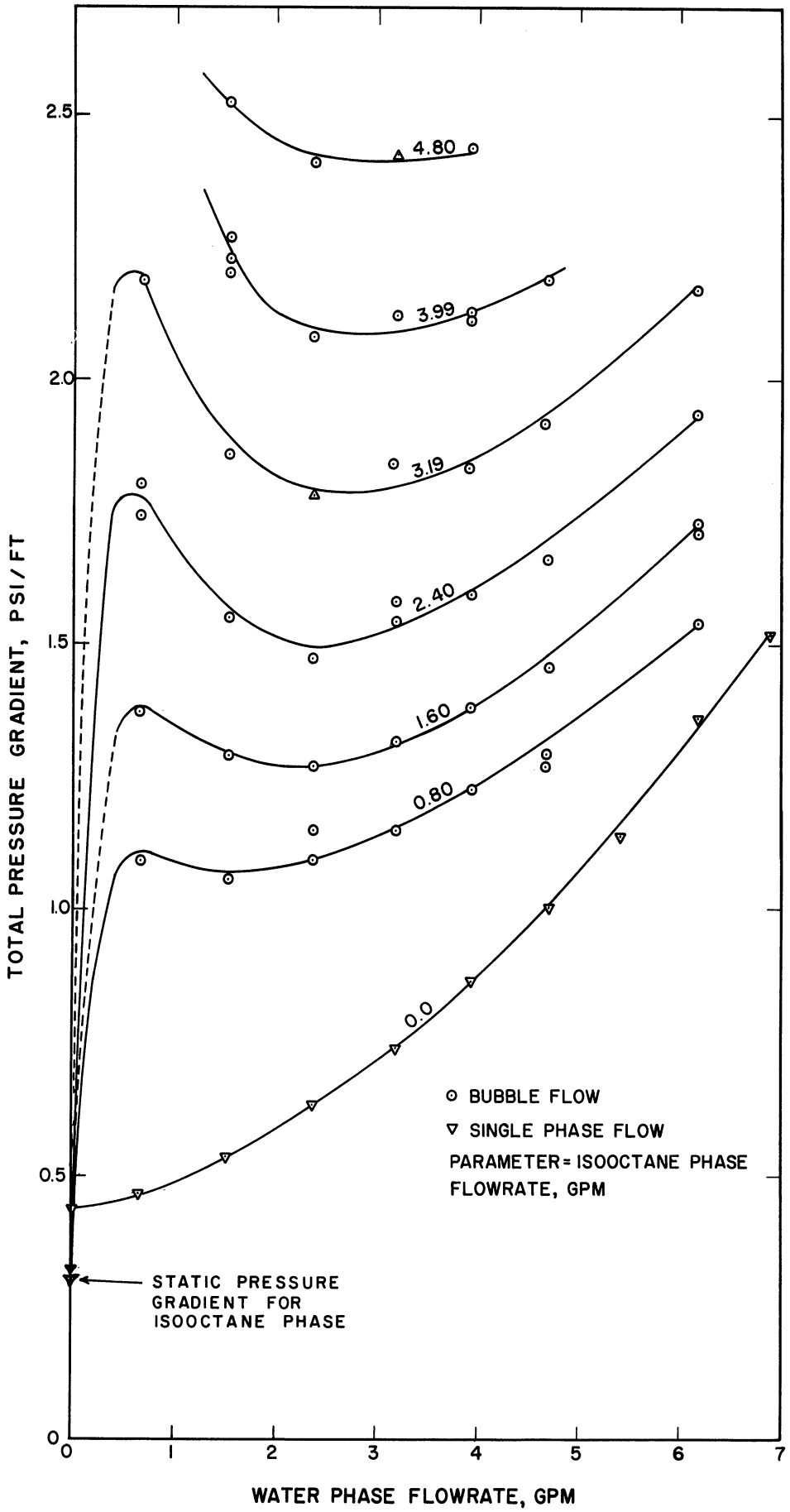

Figure 12a. Total Pressure Gradient in the System Isooctane -Water-0.164 Inch Spheres.

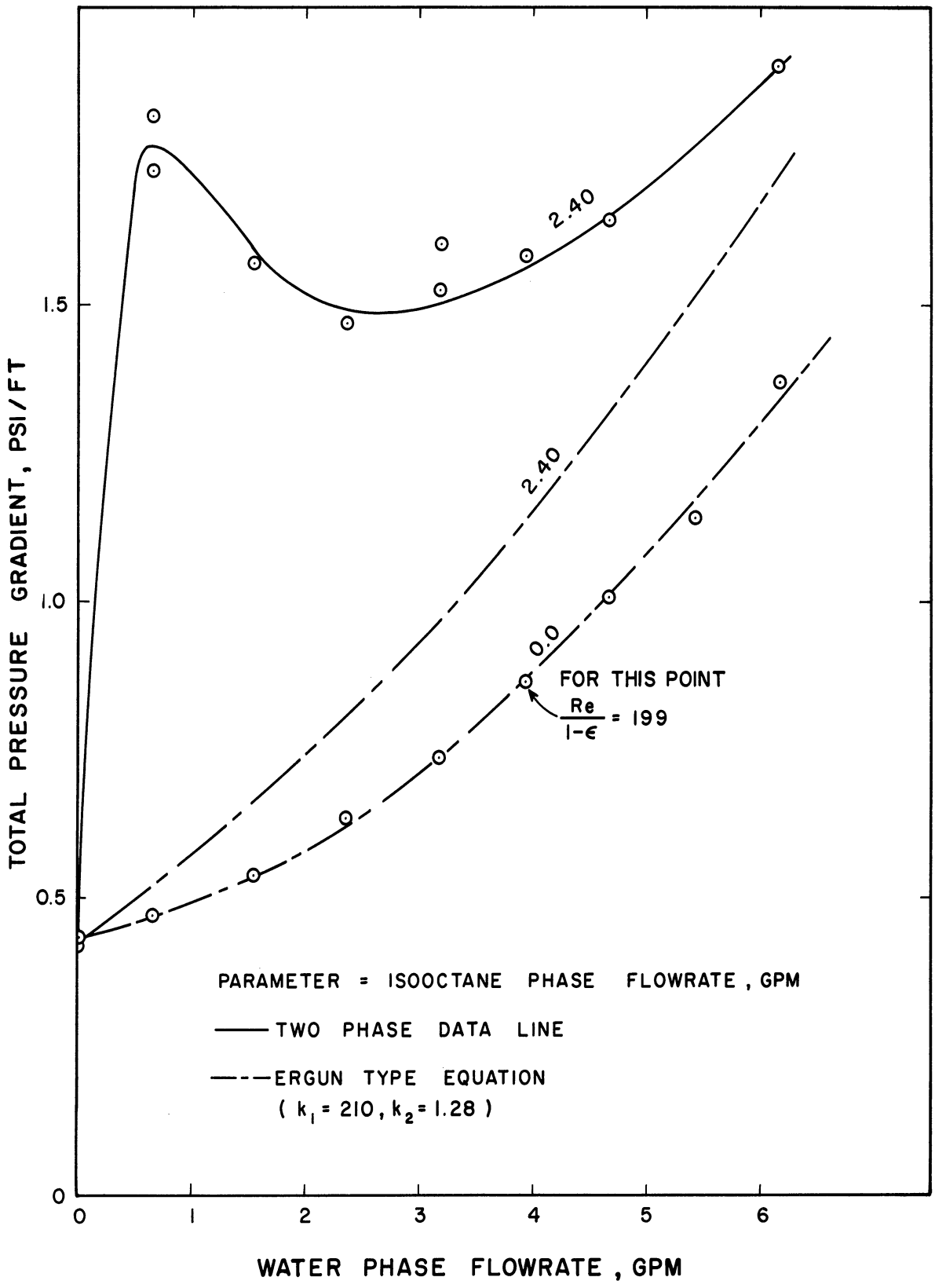

Figure 12b. Total Pressure Gradient in the System Isooctane-Water -0.164 Inch Spheres.

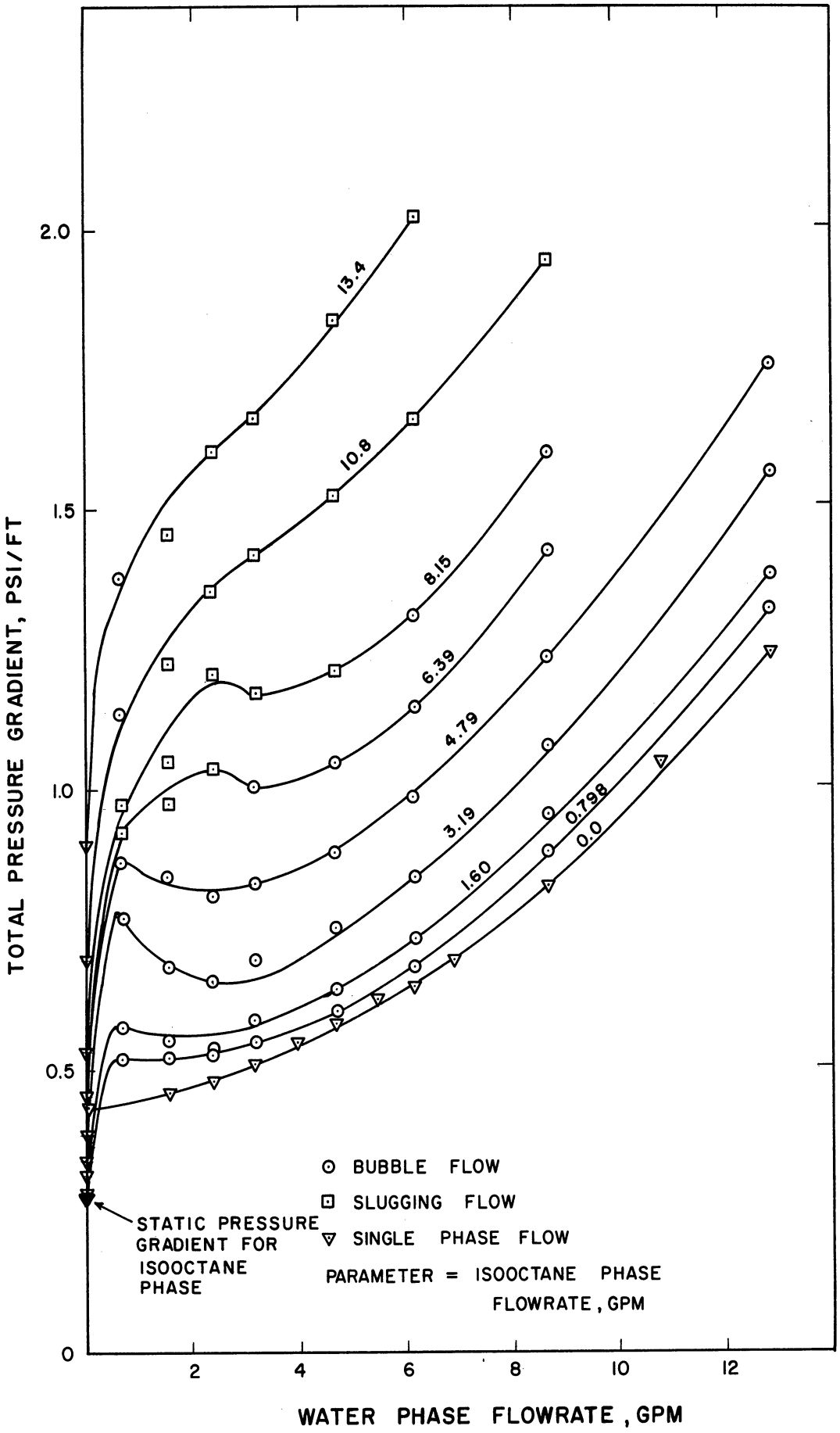

Figure 13a. Total Pressure Gradient in the System Isooctane -Water-0.340 Inch Spheres.

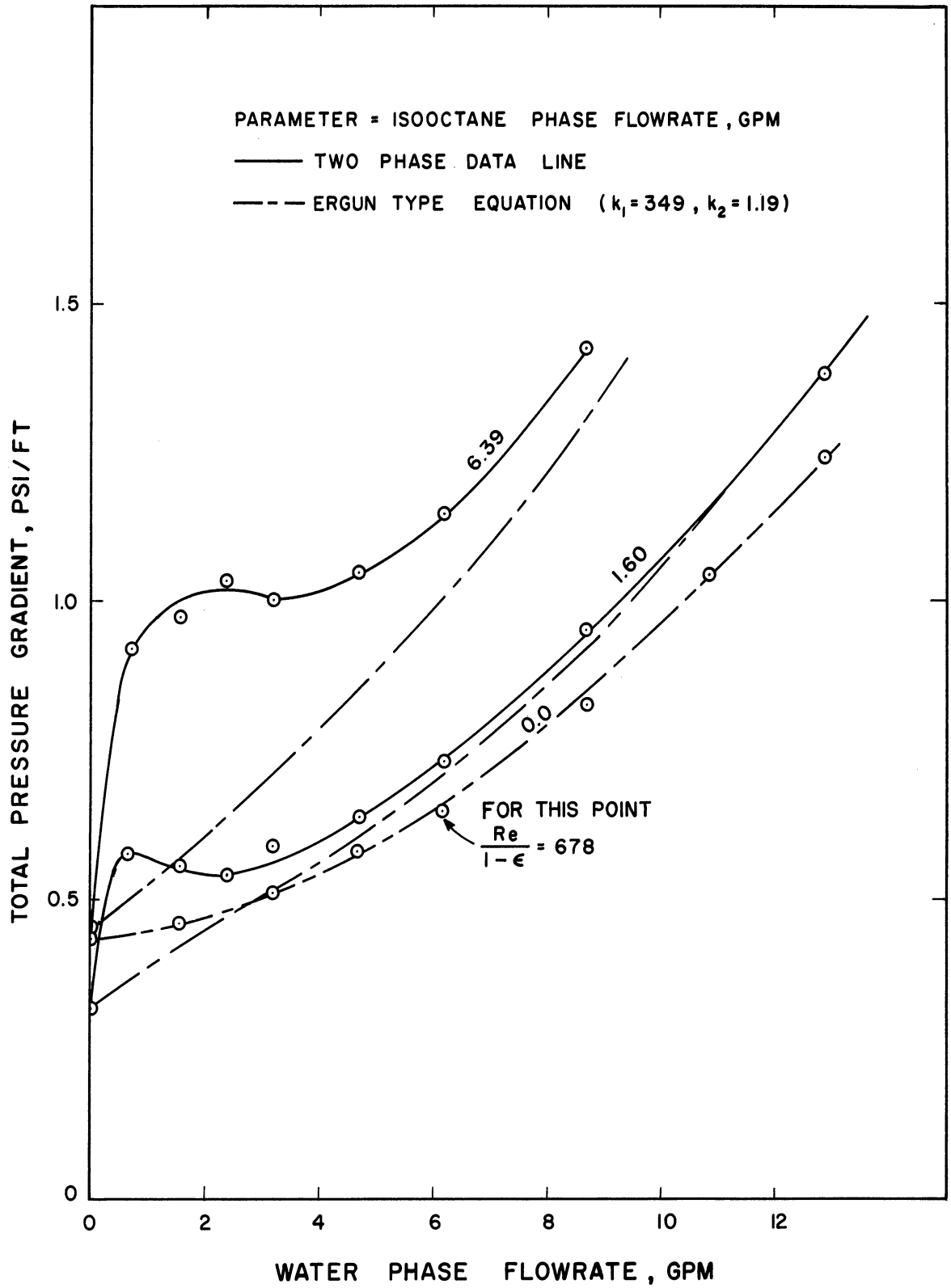

Figure 13b. Total Pressure Gradient in the System Isooctane -Water -0.340 Inch Spheres.

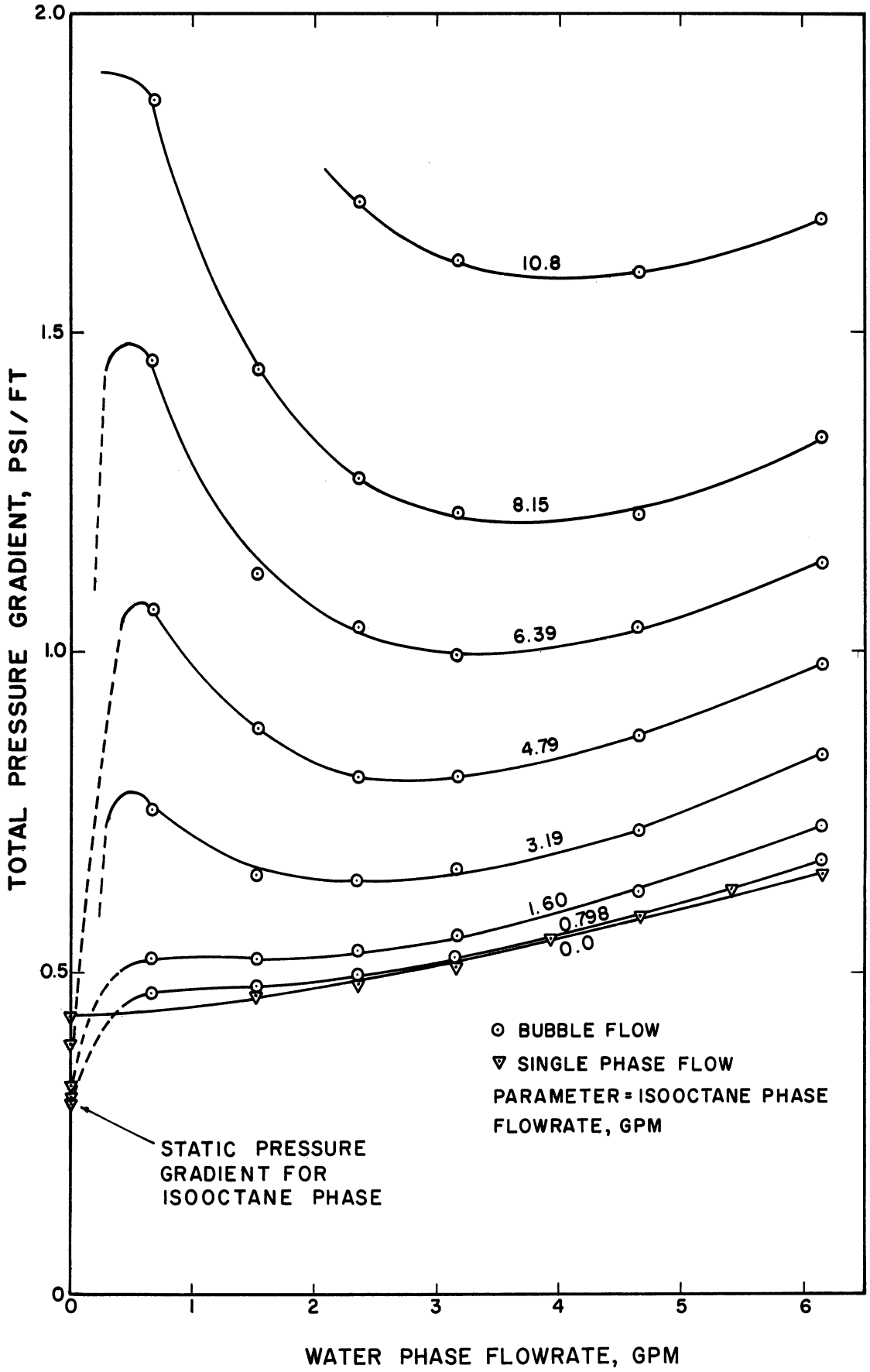

Figure 14a. Total Pressure Gradient in the System Isooctane-Alkaterge "C" -Water-0.340 Inch Spheres.

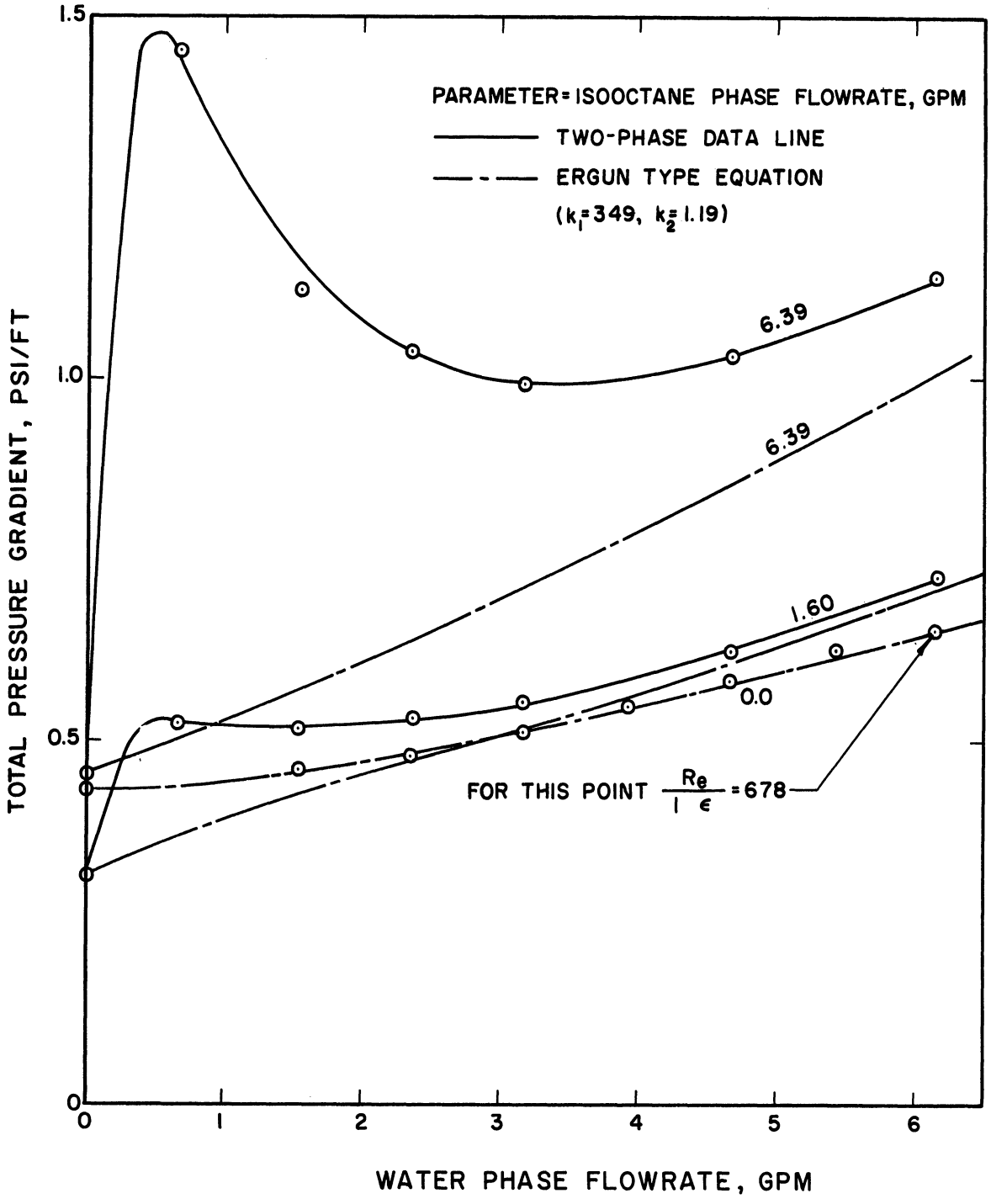

Figure 14b. Total Pressure Gradient in the System Isooctane-Alkaterge "C" -Water-0.340 Inch Spheres.

and decreases as the packing size increases. This phenomenon may be similar to the Jamin effect observed in two-phase flow in porous media.[48,66] The Jamin effect concerns the situation where droplets of the dispersed phase which are too large to pass through the openings in the packing must be stretched or broken in order to allow flow to continue. This conversion of energy is observed as increased pressure drop.

The maximum difference between the actual and predicted pressure drops occurs at mixture compositions of 70 - 80 volume per cent of non-wetting phase. This observation together with the visual observation of flow patterns and settling patterns indicates that a phase reversal may take place at mixture compositions of 70 - 80 volume per cent of the non-wetting phase, i.e. the non-wetting phase may become continuous at this concentration. This point will be discussed further in the section on data correlation.

A comparison of Figures 13 and 14 points out an interesting result. Since the interfacial tension for the system with the surfactant (Alkaterge "C") present is lower than that without it, one might expect the pressure drop to be considerably reduced by addition of the surfactant. In reality, however, this does not happen. A possible reason for this is as follows: During a static interfacial tension measurement (such as with the use of a ring tensiometer) the surfactant concentrates at the interface causing a reduction in measured interfacial tension. In a highly dispersed state, however, this high concentration at the interface cannot occur, because of the large ratio of surface area to volume. As

a result the effective interfacial tension during flow is not the same as the statically measured interfacial tension. This means that any flow data taken with a surfactant present is of questionable significance.

As was mentioned before, the entrance pressure drop was measured in addition to the pressure drop inside the test section. An examination of Appendix D shows that in all cases including single-phase flow the entrance pressure drop is less than the average test section drop. Ordinarily the reverse would be expected. This effect is probably associated with the inlet configuration and merits separate study. Because of this observation only internal pressure drops were used in correlation work.

4. Phase Holdup

The term "phase holdup" ordinarily means the fraction of the void volume of the test section which is occupied by the discontinuous phase. The difficulty encountered in defining which phase was discontinuous required that here "phase holdup" be used to indicate the fraction of the void volume of the test section which was occupied by the non-wetting phase (in all cases the organic phase).

The length of time required to establish or re-establish operating holdup is an important consideration in any commercial application of cocurrent liquid-liquid extraction. A series of runs was performed to establish this time dependence. These results are presented in Table V. Figure 15 shows the results of Part A graphically. Since the data appeared to follow an exponential decay curve, the following treatment

TABLE V

TIME DEPENDENCE OF PHASE HOLDUP

A. Isobutanol-Water-0.501 Inch Spheres (Runs 79 - 87)
Water Flowrate = 4.67 gpm, Isobutanol Flowrate = 4.34 gpm

Time (min.)	Isobutanol Phase Holdup
0.0	0.0
0.25	0.16
0.50	0.38
1.00	0.43
2.00	0.43
4.00	0.46
0.0	1.00
0.25	0.73
0.50	0.57
1.00	0.47
2.00	0.45

B. Isobutanol-Water-0.340 Inch Spheres (Runs 173 - 195)
Water Flowrate = 4.67 gpm, Isobutanol Flowrate = 4.34 gpm

Time (min.)	Isobutanol Phase Holdup
0.0	0.0
0.25	0.26
0.50	0.40
1.00	0.44
2.00	0.43
4.00	0.46
0.0	1.00
0.25	0.82
0.33	0.64
0.50	0.48
1.00	0.47
2.00	0.47

TABLE V (CONT'D)

Water Flowrate = 1.54 gpm, Isobutanol Flowrate = 1.45 gpm

Time (min.)	Isobutanol Phase Holdup
0.0	0.0
0.50	0.21
0.75	0.31
1.00	0.37
2.00	0.37
4.00	0.38
10.00	0.42
0.0	1.00
0.75	0.81
1.00	0.62
1.50	0.44
2.00	0.43
4.00	0.43

C. Isobutanol-Water-0.164 Inch Spheres (Runs 251 - 255) Water Flowrate = 1.54 gpm, Isobutanol Flowrate = 1.45 gpm

Time (min.)	Isobutanol Phase Holdup
0.0	1.00
0.75	0.91
1.00	0.62
1.50	0.38
2.00	0.38
4.00	0.38

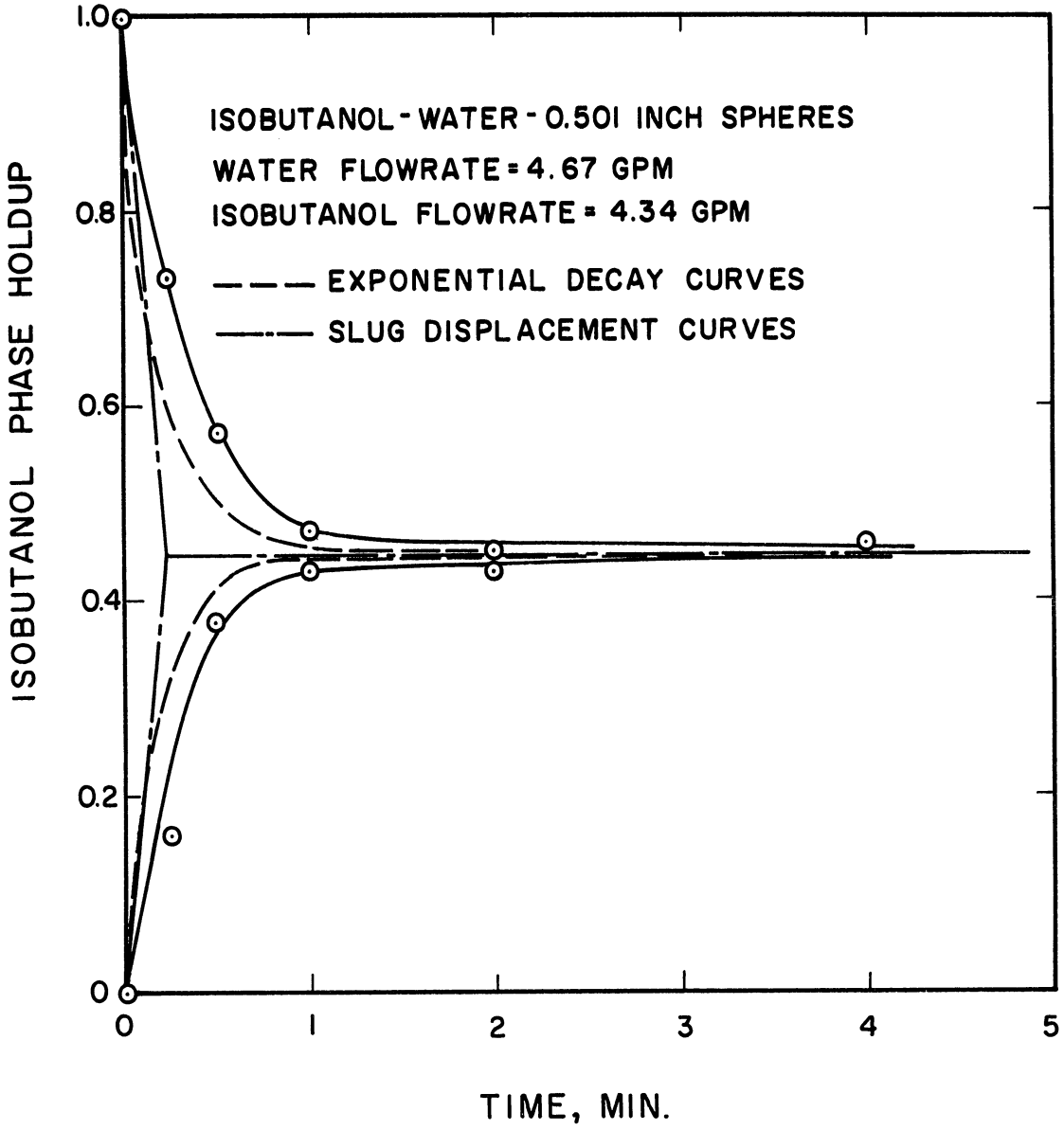

Figure 15. Time Dependence of Phase Holdup.

was used. The dotted lines in Figure 15 are exponential decay curves defined by

$$\Delta RI = RI_f \, e^{-\frac{t}{K}} \tag{43}$$

where

RI = isobutanol phase holdup

RI_f = value of RI as $t \rightarrow \infty$

$\Delta RI = |RI - RI_f|$

t = time, min.

K = time constant, min.

For the curves in Figure 15, K was chosen as the minimum time required to refill the column to a holdup of RI_f, or

$$K = \frac{\text{total void volume of test section x } RI_f}{\text{flowrate of missing phase}} \tag{44}$$

For the upper curve in Figure 15 where isobutanol is being replaced with water K = 0.22 min. For the lower curve K = 0.195 min. Figure 15 indicates that the time dependence of holdup can be loosely approximated by an exponential decay curve. It seems likely that some other value of K would give a better fit of the experimental data. It would, however, have little physical significance. If the second phase were assumed to displace the first phase as a slug, a linear change in holdup with time would occur. Curves of this type (called slug displacement curves) are included in Figure 15 for comparison purposes. It should be noted that this is not nearly as good an approximation of the data as the exponential decay curves.

The steady state values of phase holdup (in all cases organic phase holdup) are presented in Tables I - VI, Appendix D, along with the pressure-drop data. Zero values of holdup in the tables indicate that holdup was not measured for those runs. The holdup data are presented graphically in Figures 16 - 20. Reproducibility is again indicated by the presence of duplicated points on the graphs.

5. Drop Sizes

In any application of the results of this thesis to cocurrent liquid-liquid extraction, quantitative information about the amount of interfacial area produced would be desirable. The interfacial area produced in a given system determines, to a great extent, the rate of mass transfer from one phase to the other. To a lesser extent it is also important to know how this area is distributed between small drops and large drops in the liquid mixture.

A number of methods have been used to present information of this type, e.g. an equivalent drop diameter, surface area per unit volume of discontinuous phase, surface area per unit volume of mixture, etc. Since in the present case phase holdup is a known quantity and since interfacial area was determined by measuring drop diameters, data on interfacial area is presented as an equivalent drop diameter.

A number of equivalent drop sizes have also been proposed, e.g. the arithmetic average diameter, the median diameter (that diameter such that half of the total population of drops are larger than it), the Sauter mean diameter, etc. By far the most important in mass transfer

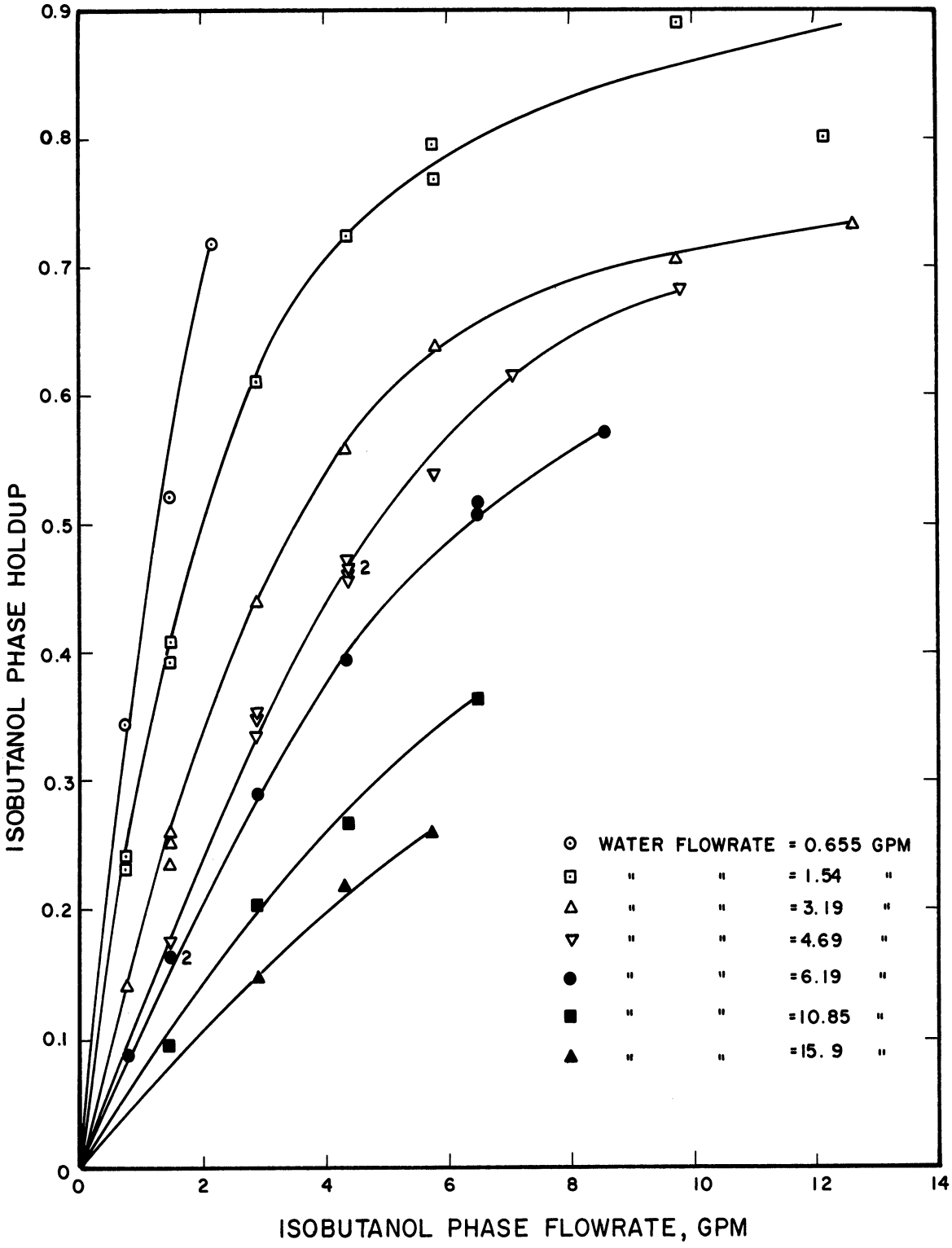

Figure 16. Isobutanol Phase Holdup in the System Isobutanol -Water-0.501 Inch Spheres.

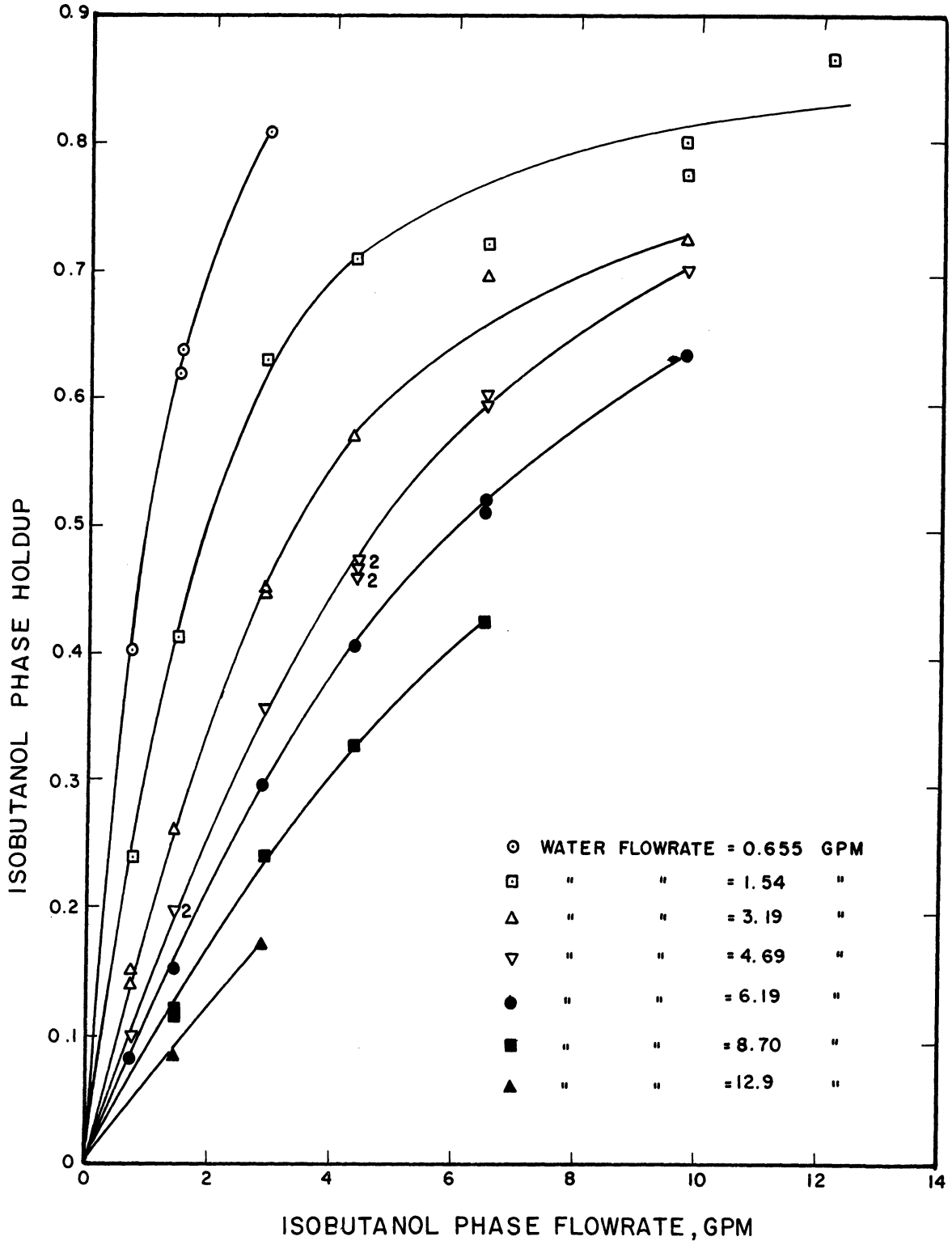

Figure 17. Isobutanol Phase Holdup in the System Isobutanol -Water-0.340 Inch Spheres.

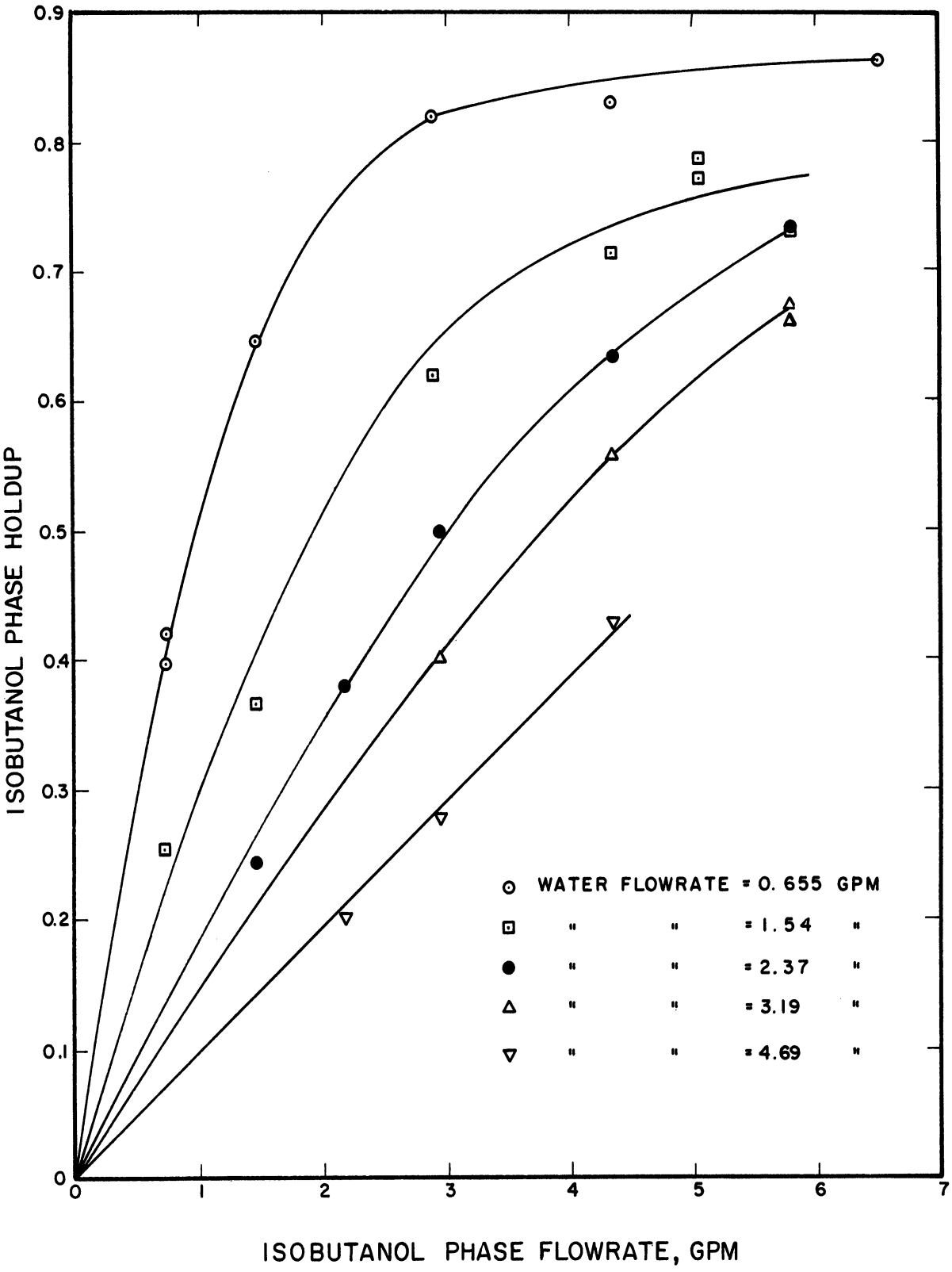

Figure 18. Isobutanol Phase Holdup in the System Isobutanol -Water-0.164 Inch Spheres.

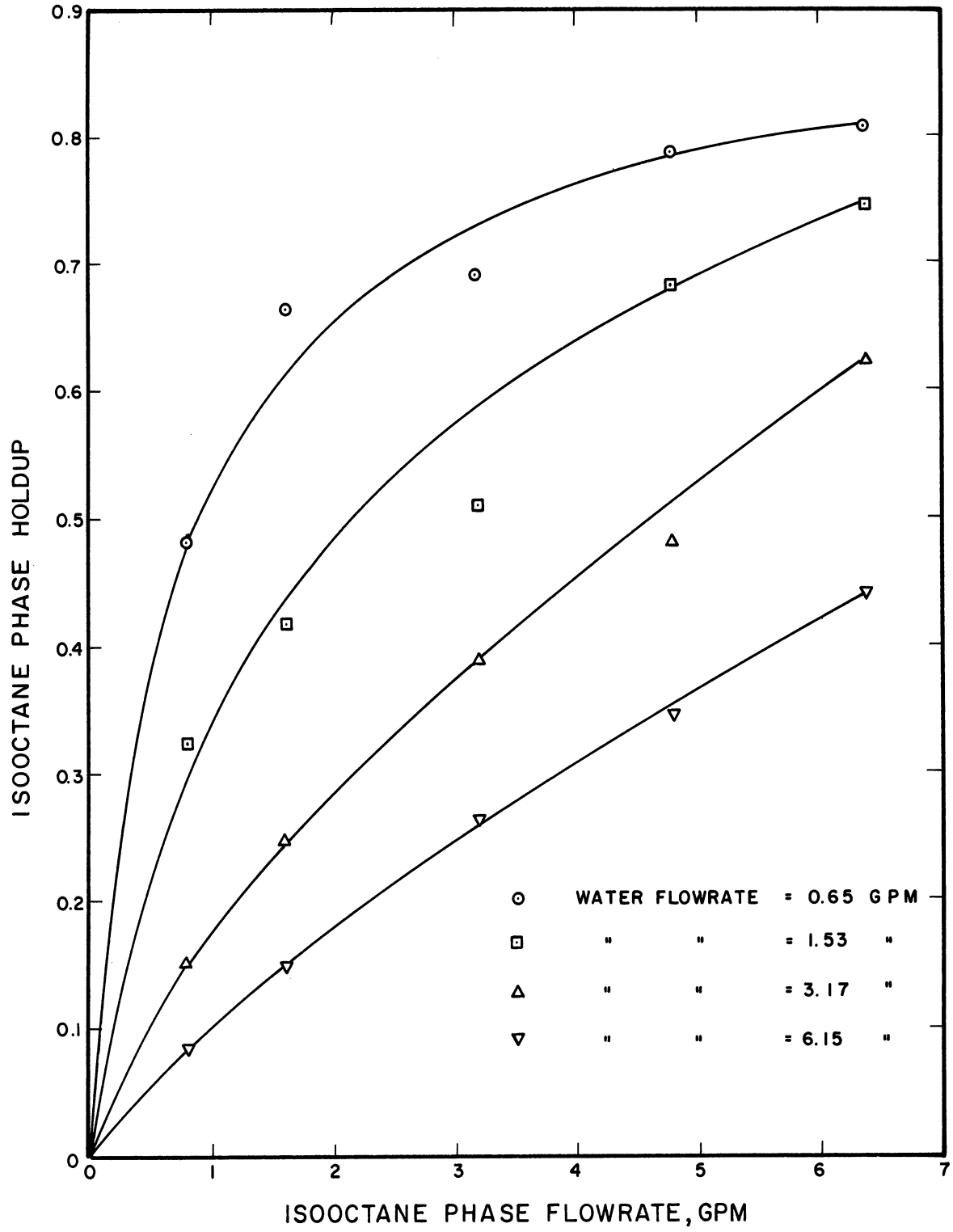

Figure 19. Isooctane Phase Holdup in the System Isooctane -Water-0.340 Inch Spheres.

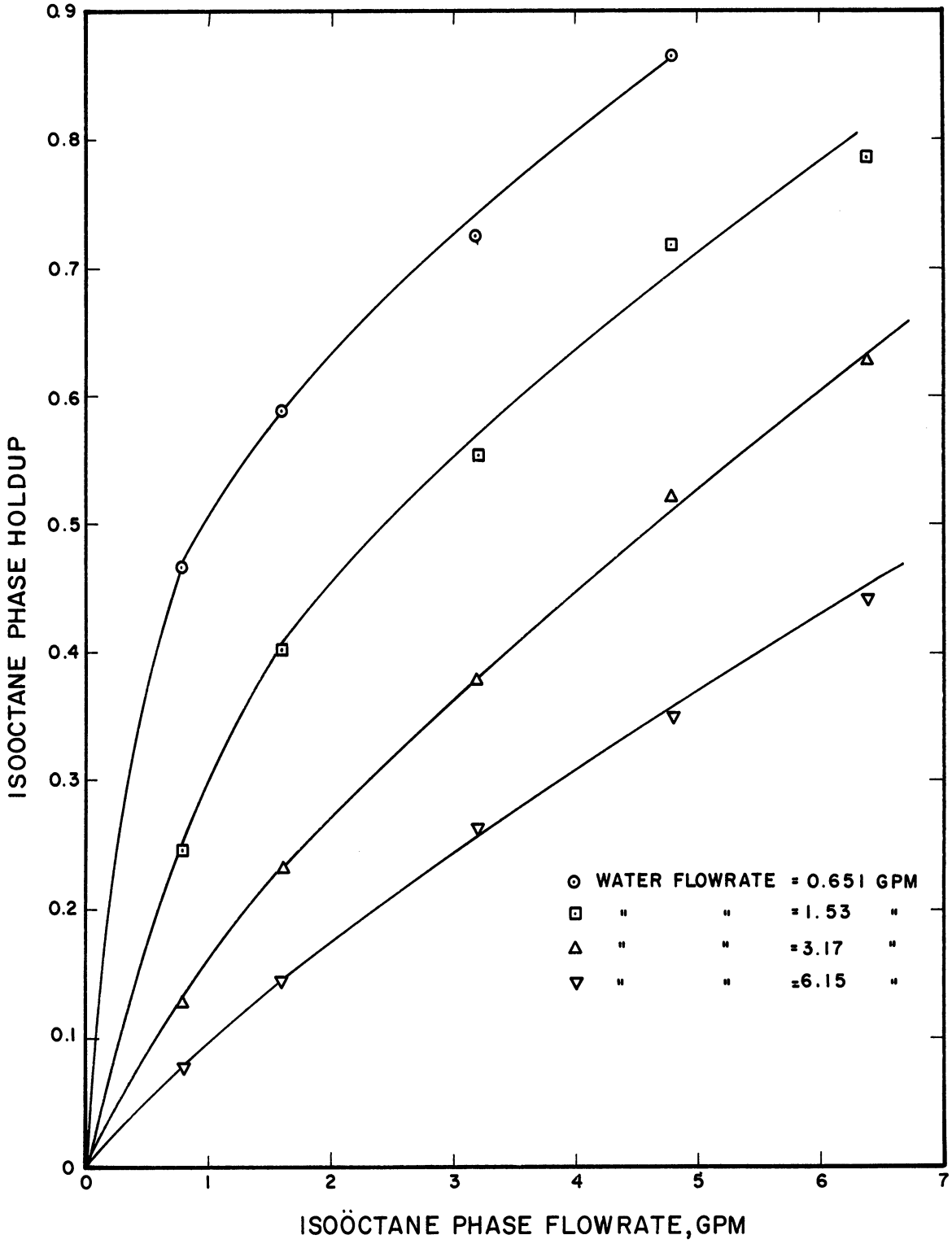

Figure 20. Isoöctane Phase Holdup in the System Isoöctane - Alkaterge "C" -Water-0.340 Inch Spheres.

is the Sauter mean diameter, since it is the diameter of a drop which has the same ratio of surface area to volume as the total population of measured drops. Let d_{32} be the Sauter mean diameter. Then the ratio of volume to surface area for a drop of this diameter is given by

$$R_{32} = \frac{\frac{\pi}{6} d_{32}^3}{\pi d_{32}^2} = \frac{d_{32}}{6} \tag{45}$$

For the total population of measured drops this ratio is given by

$$R_T = \frac{\sum_{i=1}^{N} \frac{\pi}{6} d_i^3}{\sum_{i=1}^{N} \pi d_i^2} = \frac{1}{6} \frac{\sum_{i=1}^{N} d_i^3}{\sum_{i=1}^{N} d_i^2} \tag{46}$$

where N = the total number of drops. Equating these two ratios gives

$$d_{32} = \frac{\sum_{i=1}^{N} d_i^3}{\sum_{i=1}^{N} d_i^2} \tag{47}$$

Equation (47) defines the Sauter mean diameter as it is used here. This diameter together with the value for phase holdup enables the computation of interfacial area.

Typical examples of the photographs taken in this research are shown in Figures 21 - 24. The drop diameters measured from each such photograph were divided into twenty size classes, the sizes of which depended on the over-all size range found in the photograph. The number of drops in each size class was then punched on an IBM card along with the photo number and the two rotameter readings. One card was used for each photograph. A group of cards giving the fluid properties, sizes associated

Figure 21. Photograph of Flowing Water-Isobutanol Mixture in Bed of 0.501 Inch Spheres. Water flowrate = 1.54 gpm. Isobutanol flowrate = 1.45 gpm. Magnification = 2.9X

Figure 22. Photograph of Flowing Water-Isobutanol Mixture in Bed of 0.340 Inch Spheres. Water flowrate = 1.54 gpm. Isobutanol flowrate = 1.45 gpm. Magnification = 2.9X

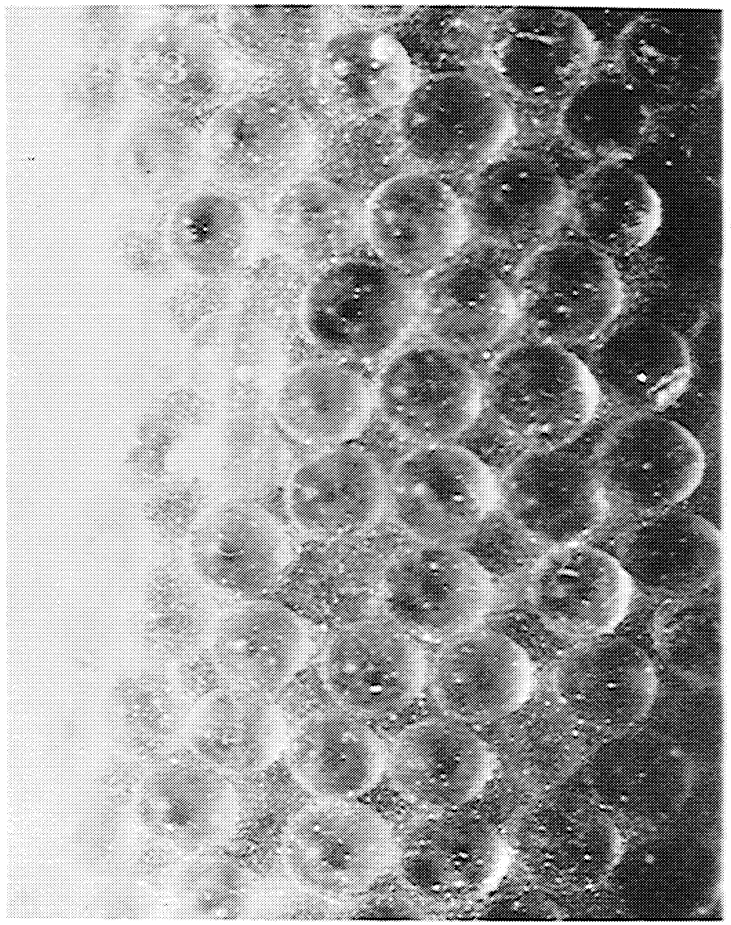

Figure 23. Photograph of Flowing Water-Isobutanol Mixture in Bed of 0.164 Inch Spheres. Water flowrate = 1.54 gpm. Isobutanol flowrate = 1.45 gpm. Magnification = 2.9X

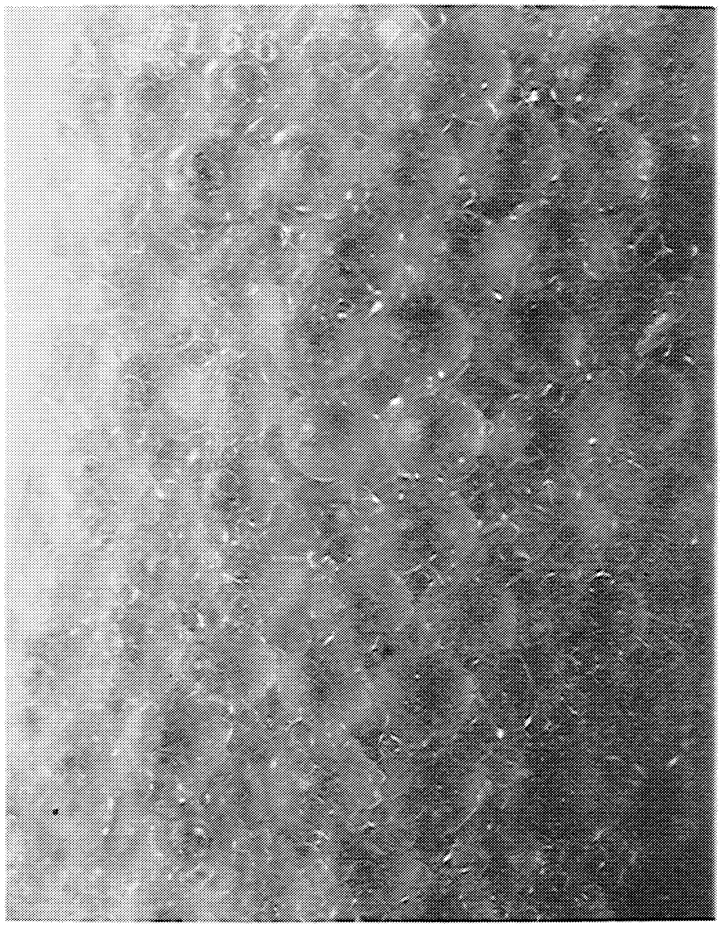

Figure 24. Photograph of Flowing Isooctane-Water Mixture in Bed of 0.164 Inch Spheres. Water flowrate = 1.53 gpm. Isooctane flowrate = 1.60. Magnification = 2.9X

with each size class, etc. was placed before each set of photo cards. Fluid linear velocities and Sauter mean diameters were then computed on the IBM 7090 for each photograph. The results are presented in Tables I - VI, Appendix E. The raw drop count data were omitted since they were quite lengthy and were not considered to be of particular value in raw form.

Due to a clouding of the inside wall of the test section after a period of time, the photographing and counting of drops became rather difficult for the last two systems studied. For this reason only two photographs from each system are included in the data tables.

Up to this point the drop size data have been treated as if they were truly representative of the drop sizes in the interior of the packed bed. This is open to question since the photographs were all taken just inside the wall of the test section. Although there is no means of verification, it is believed that any wall effect on d_{32} is quite small. The effects of packing diameter, velocity, and fluid properties on drop size would be expected to show the same trends at the center of the bed as at the wall. The absolute drop size may, however, change slightly with distance from the column wall, due to the velocity profile and the change in porosity.

The reproducibility of the drop size data can best be illustrated by examining the results for photographs 7, 8, 9, 10, 17, 18, and 81 given in Table I, Appendix E and reproduced below in Table VI for convenience. These data, taken over a two-week period show a maximum deviation of 5.7% from their mean.

TABLE VI

REPRODUCIBILITY OF DROP SIZE MEASUREMENTS

Data Taken for System Isobutanol-Water-0.501 Inch Spheres
Water Flowrate = 1.54 gpm, Isobutanol Flowrate = 1.45 gpm

Photograph Number	Sauter Mean Diameter (Microns)
7	875
8	921
9	868
10	931
17	884
18	932
81	963

In addition to mean drop sizes, drop size distributions were computed for each pair of identical photographs. For each such pair the cumulative number of drops below a certain drop diameter was computed. Percentages were then computed from these numbers. In all cases the drops were found to be approximately normally distributed. Several samples of drop distributions are plotted in Figures 25 - 28. In these figures the ordinate is a normal probability scale. As a result data which is normally distributed will appear as a straight line.

Figure 28 shows the largest deviation from a normal distribution. The downward concavity of the curve suggests that these data may better fit a log-normal distribution. (In a log-normal distribution the

logarithms of the drop diameter would be normally distributed.) However, when these data were plotted on log-normal probability paper they produced a curve which was concave upward. Therefore the true distribution is somewhere between the normal and log-normal distributions. It can however by approximated by a normal distribution.

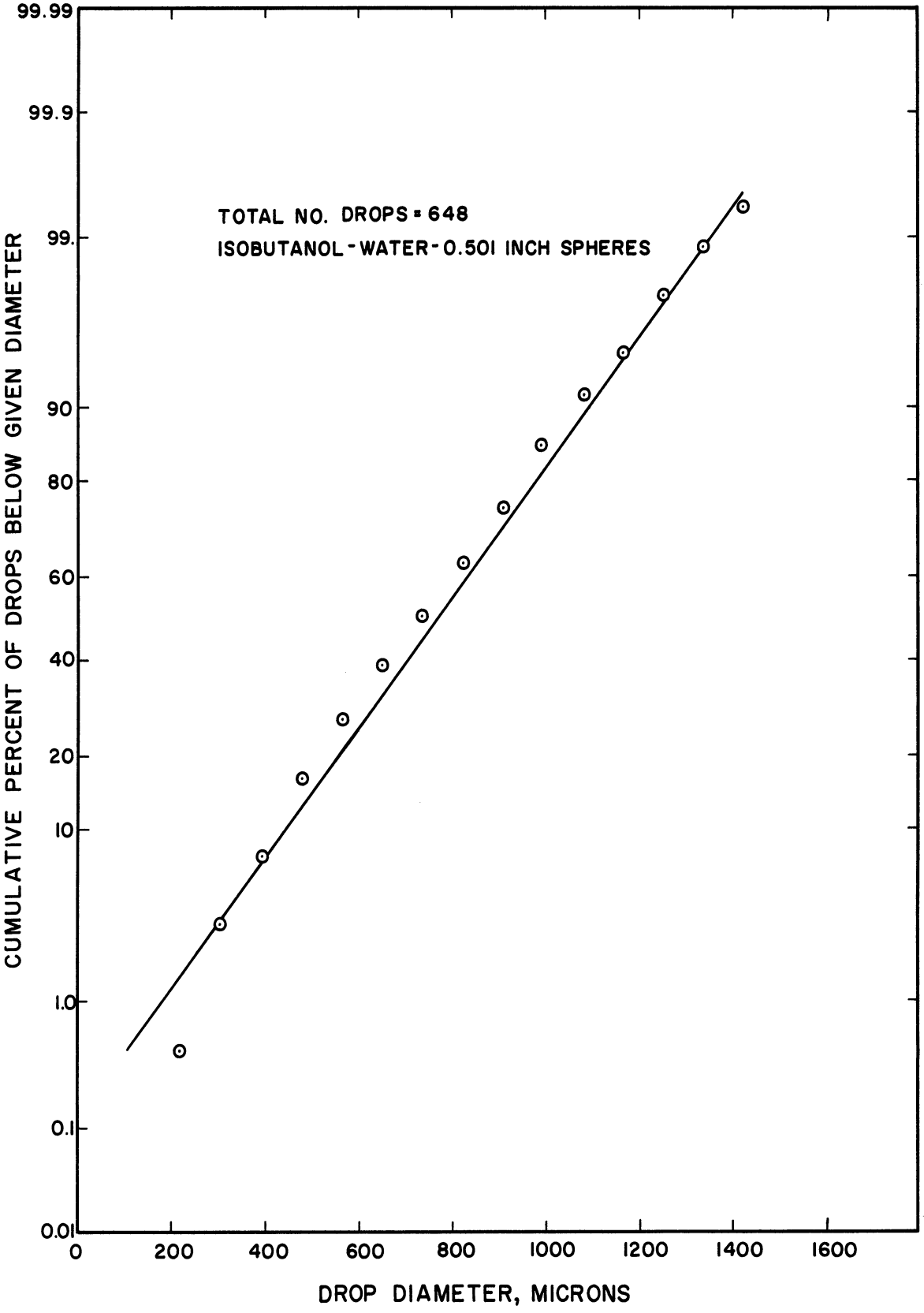

Figure 25. Drop Size Distribution Photographs 7, 8, 9, 10, 17, 18.

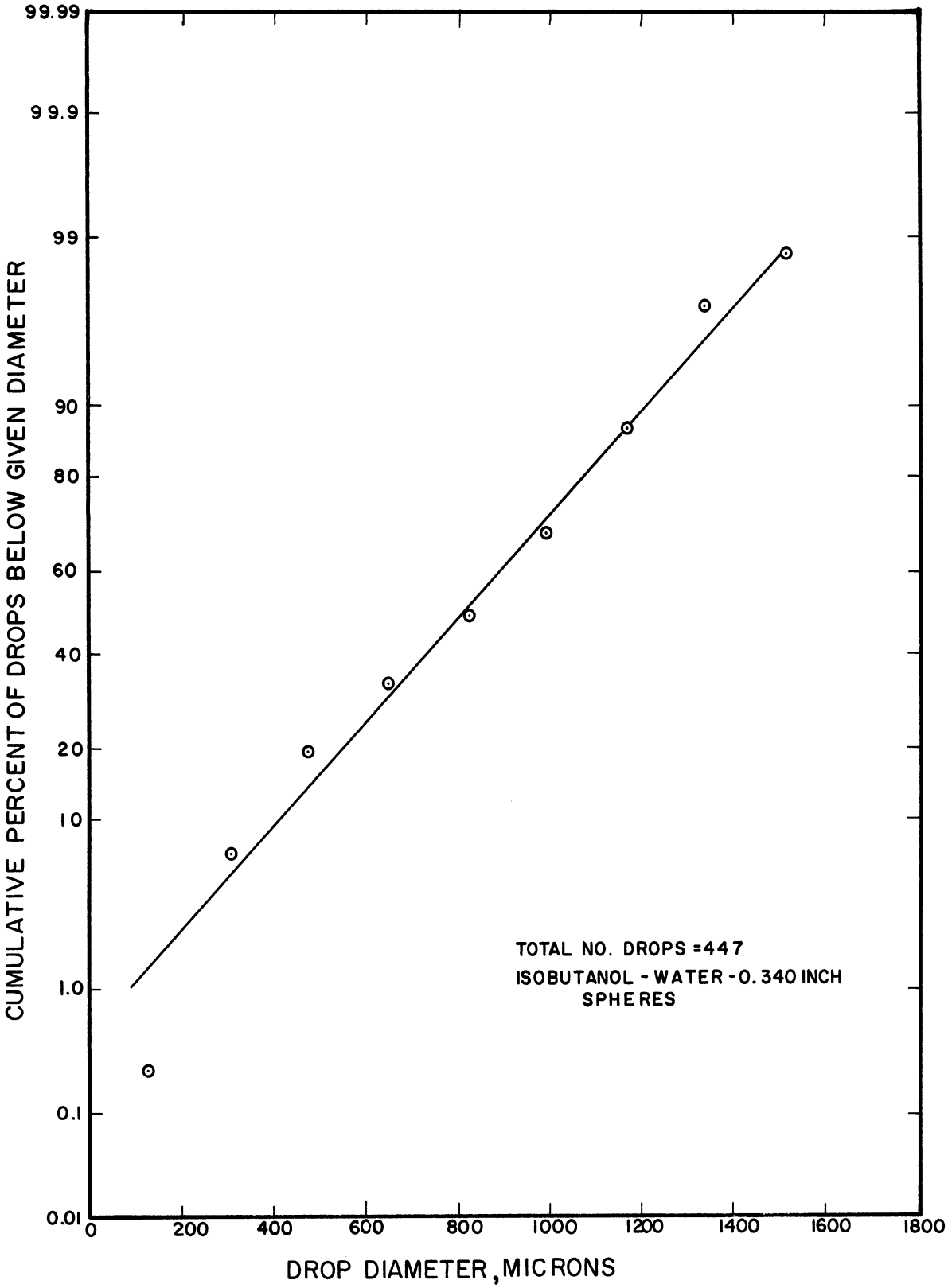

Figure 26. Drop Size Distribution Photographs 99, 101.

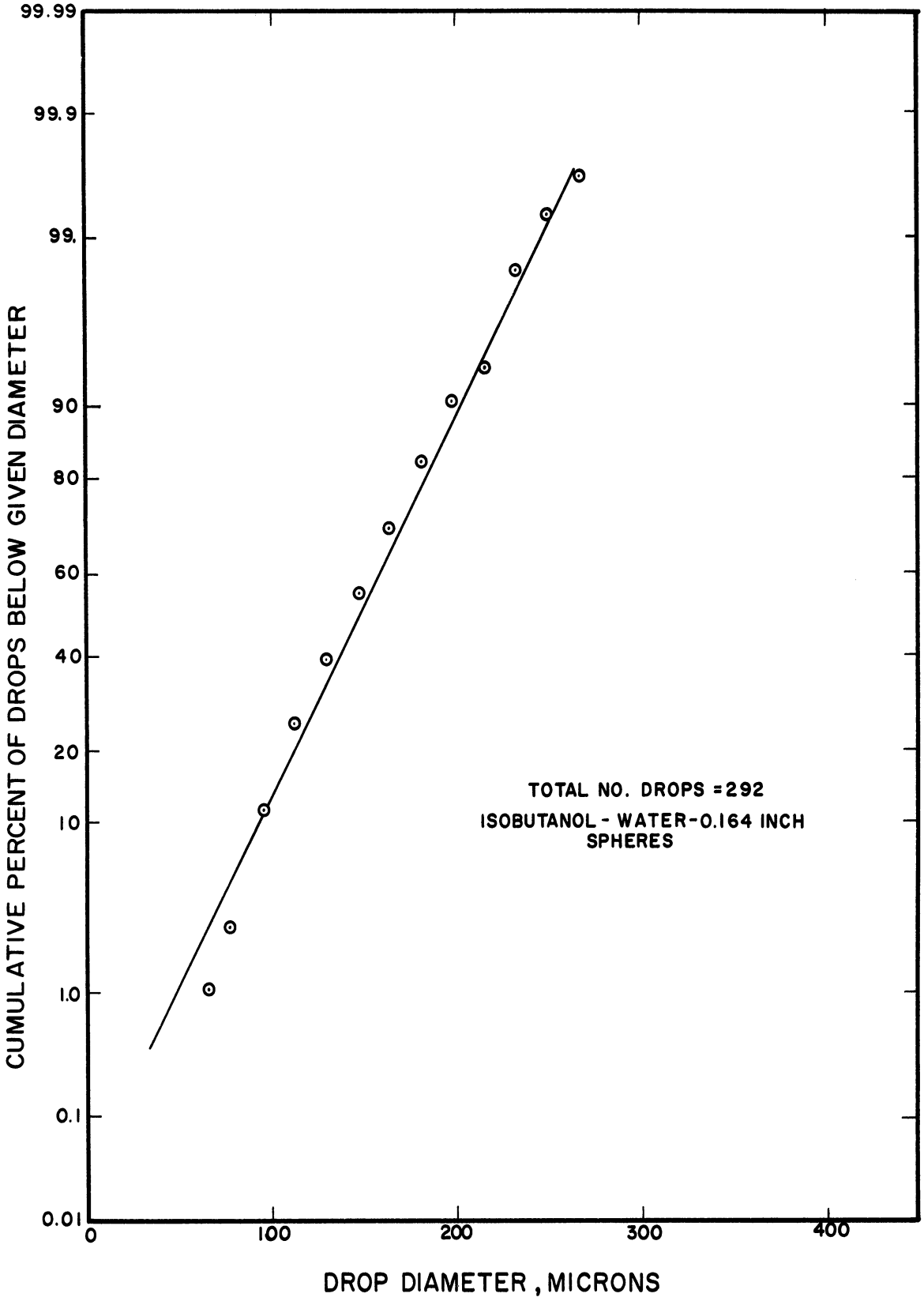

Figure 27. Drop Size Distribution Photographs 151, 152.

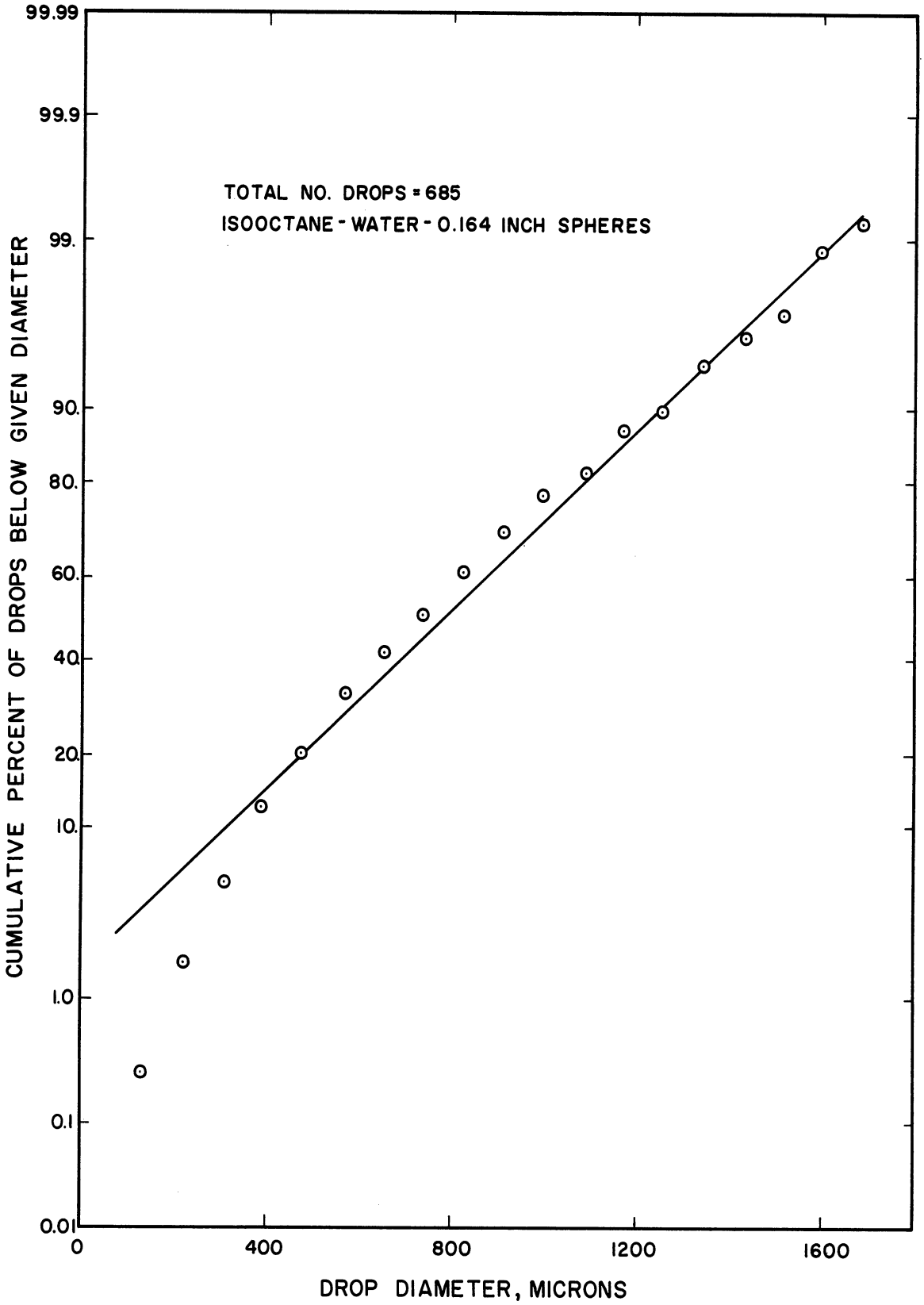

Figure 28. Drop Size Distribution Photographs 157, 158, 183, 184.

VI. CORRELATION OF DATA

The data presented in the previous section are of little value as they stand except for qualitative purposes. Numerical predictions for systems other than those used here would not be possible. Therefore an attempt was made to develop a generalized method for correlating the data of the previous section. Due to the complexity of the system involved, an analytical approach held little hope for success. Therefore a somewhat empirical approach had to be used. The results of that attempt are presented here.

In deriving these correlations, correlations of similar systems were utilized insofar as possible. In the case of pressure drop, single-phase relationships were used as a starting point.

Since it appeared that phase holdup has a strong effect on pressure drop, an attempt was first made to correlate the holdup data.

1. Phase Holdup Correlation

One might assume that the organic phase holdup, RI, could be predicted by an equation of the form

$$RI = \frac{U_O}{U_W + U_O} \tag{48}$$

where

U_O = organic phase superficial velocity

U_W = water phase superficial velocity

However due to the density difference between the two liquids, the less dense liquid rises with respect to the more dense liquid. This relative

velocity, ordinarily called the "slip velocity" can be computed by the following equation for cocurrent liquid flow in packed beds:

$$V_s = \frac{U_o}{\epsilon\ RI} - \frac{U_w}{\epsilon(1 - RI)} \tag{49}$$

where U_w and U_o are both measured in the same direction. For countercurrent flow the same equation applies, but one of the velocities is now negative.

In countercurrent flow the slip velocity has been used quite successfully to correlate holdup data. That is, slip velocities were predicted and then Equation (49) was used to predict RI. In cocurrent flow, however, U_o and U_w are much larger than in countercurrent flow. As a result the slip velocity computed by Equation (49) is the difference between two large numbers and is therefore subject to a great deal of error. In the present study the slip velocities calculated from Equation (49) were, in many cases, of the same order of magnitude as the uncertainties in the data. As a result slip velocities are of little value in correlating holdup data in cocurrent liquid-liquid systems.

The assumption of zero slip velocity was tested and found to be approximately true for the present data. The relative errors, however, were significant enough, particularly at low values of RI, to encourage a search for a more adequate correlation technique.

Wicks and Beckman[78] and Markas and Beckman[52] successfully correlated holdup data in countercurrent liquid-liquid systems by equations of the form

$$RI = A_1(U_D)^r + B_1(U_D)(U_C)^s \tag{50}$$

where U_D and U_C are the dispersed and continuous phase superficial velocities and A_1, B_1, r, and s are constants dependent on the system being studied. This form is obviously unsatisfactory for cocurrent flow because RI is unbounded for large values of either U_D or U_C. In reality RI has a maximum value of 1.

The following modified form of the velocity-power relationship was tested with the data from this investigation:

$$RI = \left(\frac{U_O}{U_O + U_W}\right)^a \tag{51}$$

It should be noted that this equation satisfies the limiting conditions of

$$RI = 0 \quad \text{when} \quad U_O = 0$$

and

$$RI = 1 \quad \text{when} \quad U_W = 0 \ . \tag{52}$$

In addition it is quite simple in that only one empirical constant need be evaluated.

The constant a was evaluated for each data set presented here by first rearranging Equation (51) to the following form:

$$\ln RI = a \ln\left(\frac{U_O}{U_O + U_W}\right) \tag{53}$$

A least squares technique was then used to evaluate the constant a.

Figures 29 - 33 present plots of RI versus $\frac{U_O}{U_O + U_W}$ on a log-log scale. The solid lines represent Equation (53) with a evaluated by the least squares technique. The dotted lines represent Equation (53) for a = 1; this is equivalent to an assumption of zero slip velocity.

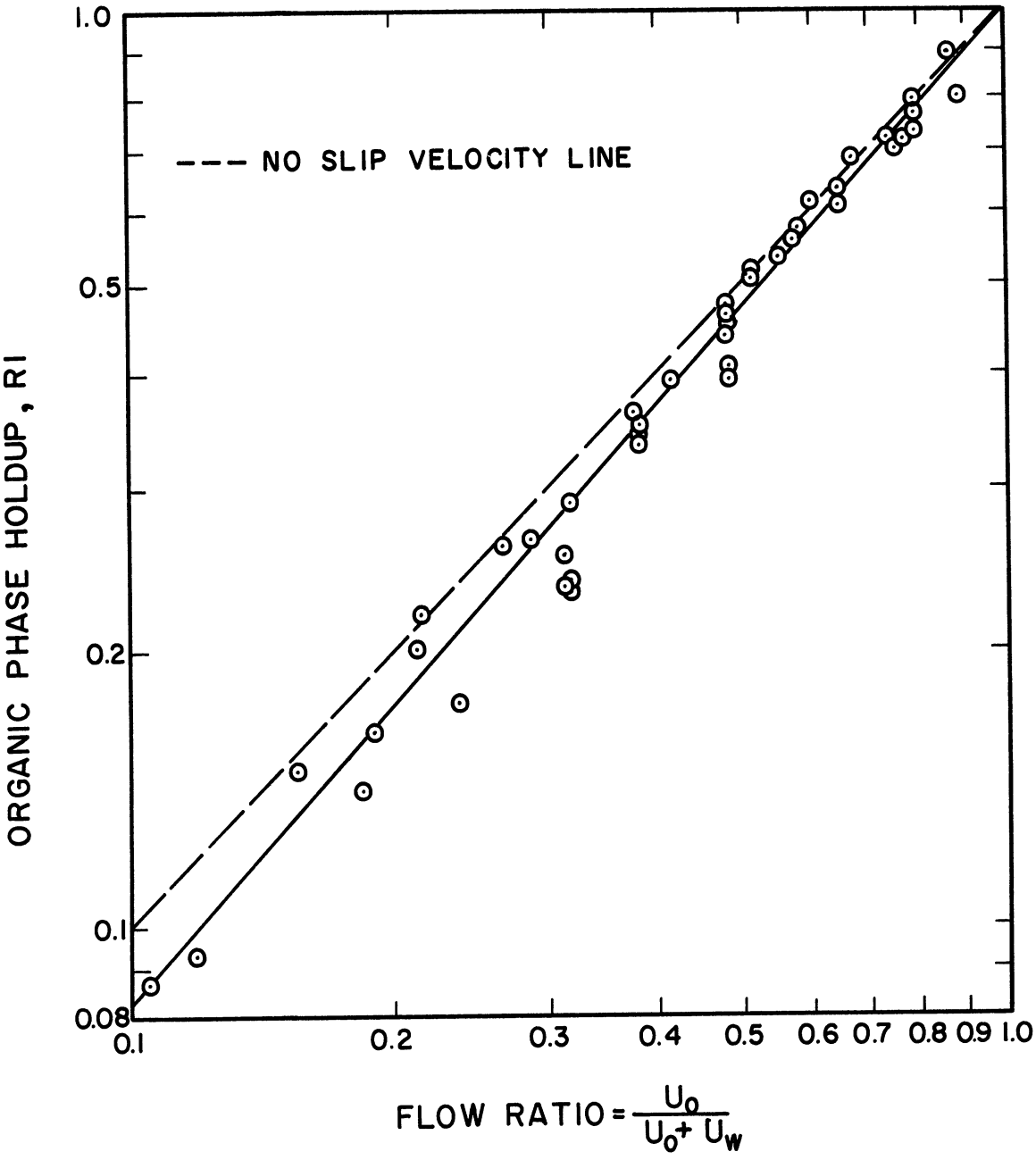

Figure 29. Phase Holdup in the System Isobutanol -Water-0.501 Inch Spheres.

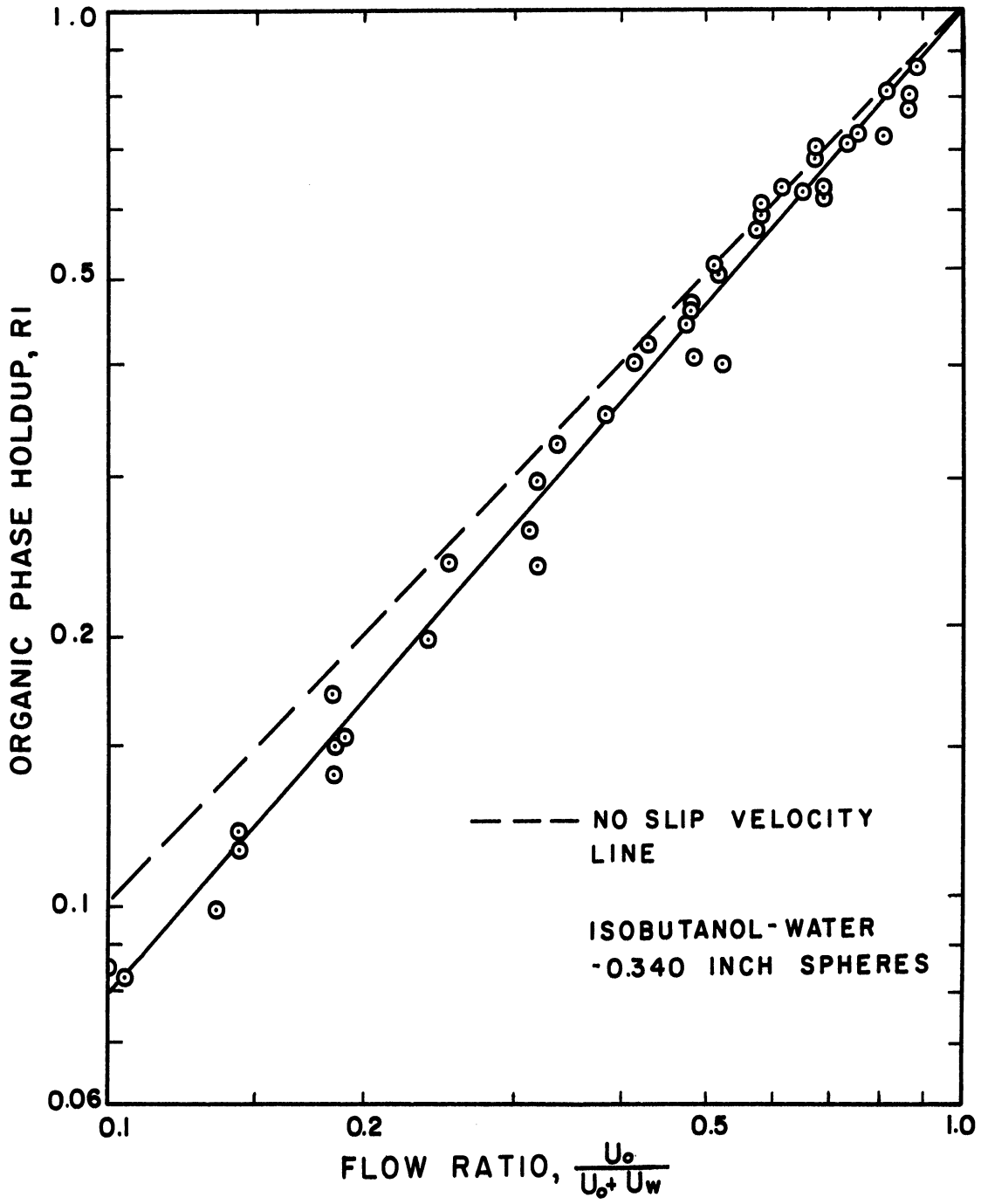

Figure 30. Phase Holdup in the System Isobutanol -Water-0.340 Inch Spheres.

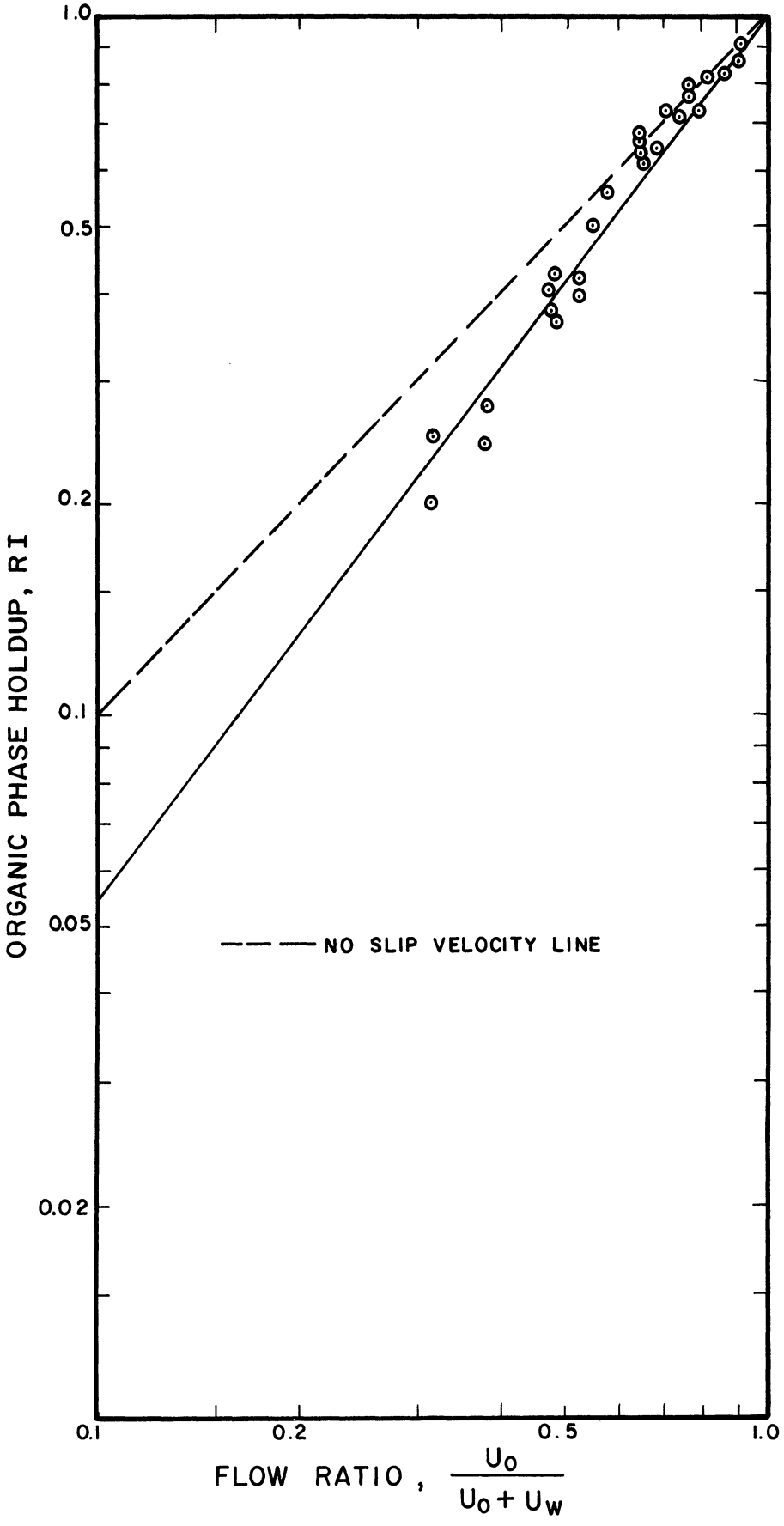

Figure 31. Phase Holdup in the System Isobutanol -Water-0.164 Inch Spheres.

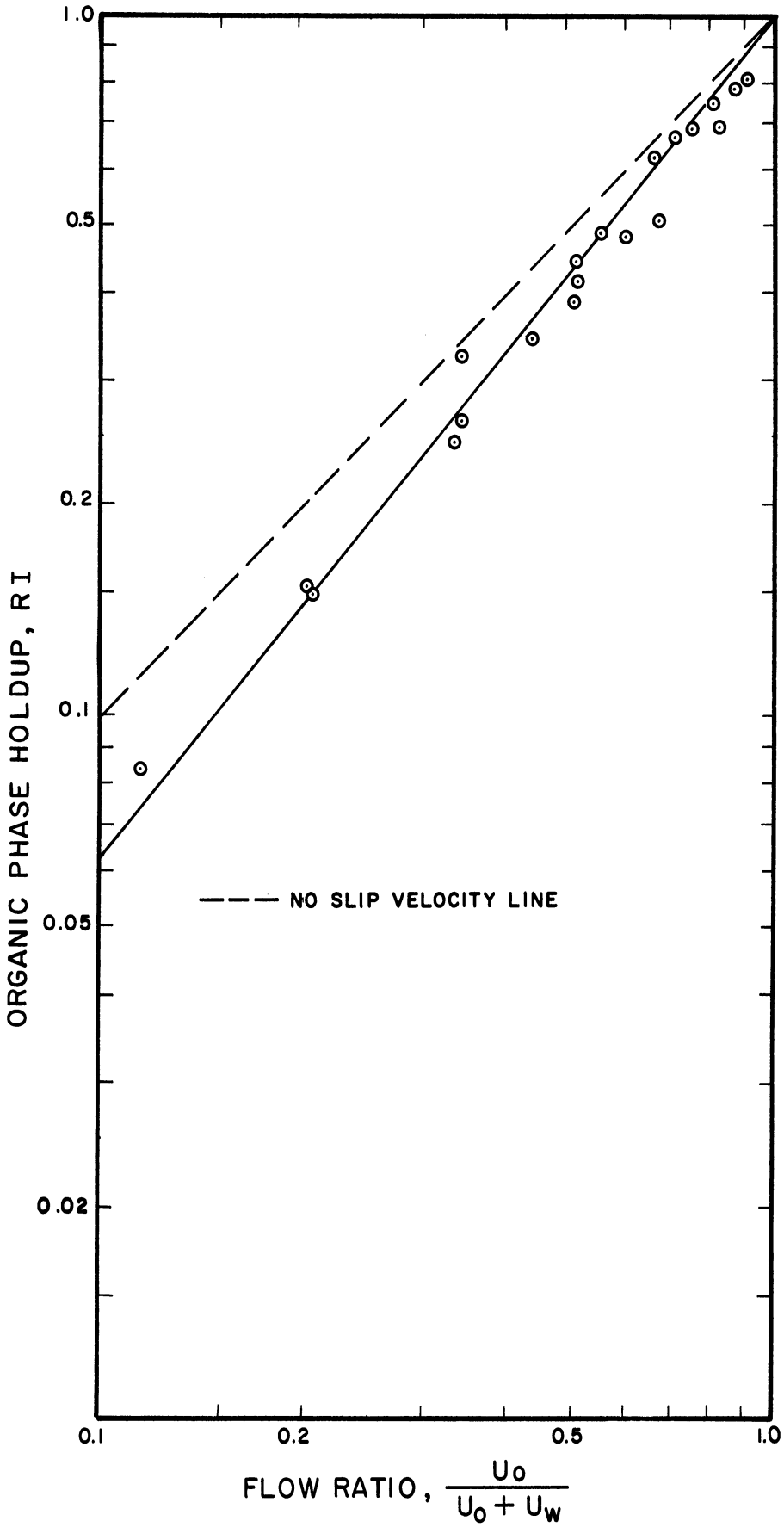

Figure 32. Phase Holdup in the System Isooctane-Water-0.340 Inch Spheres.

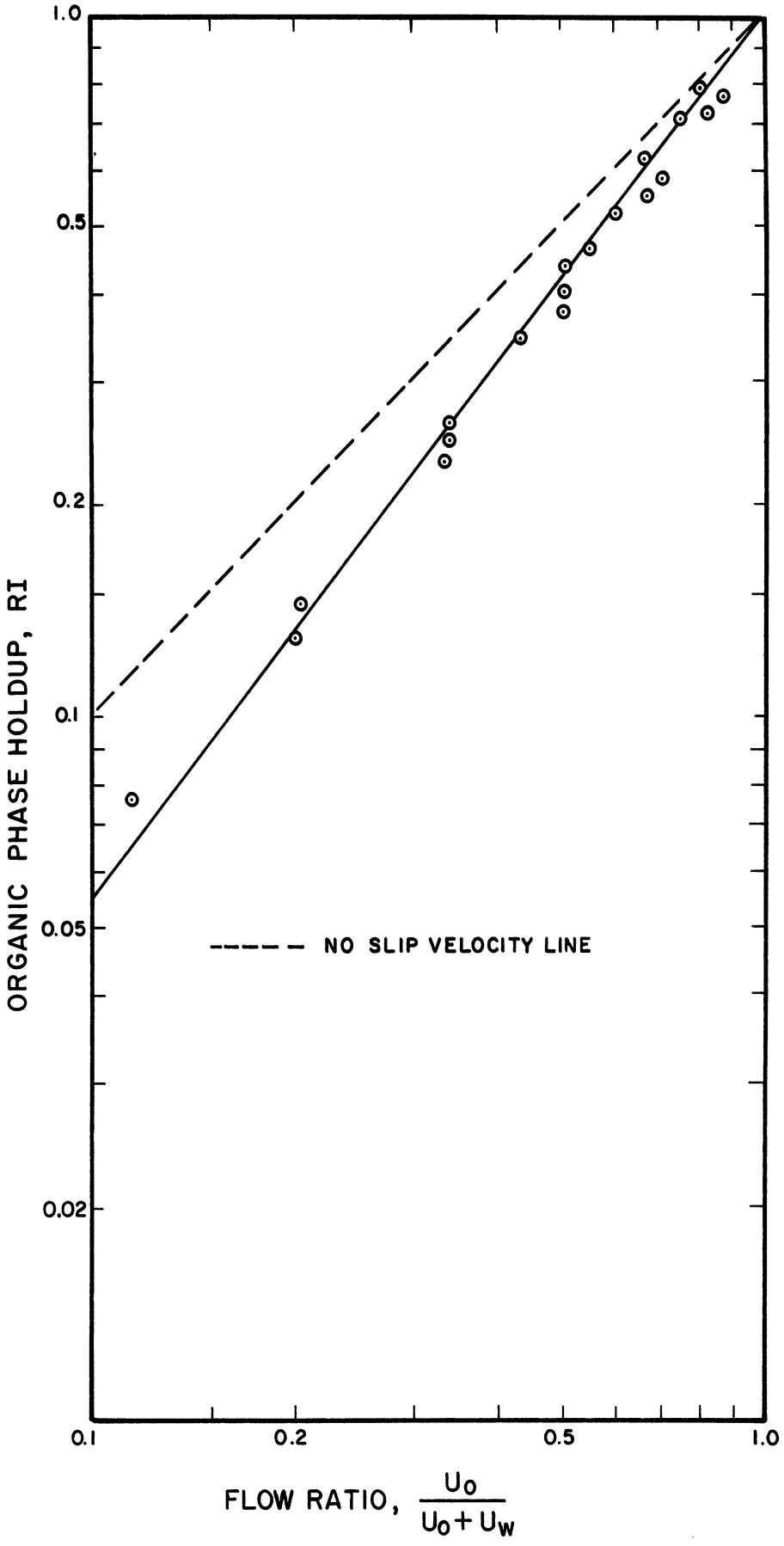

Figure 33. Phase Holdup in the System Isooctane-Alkaterage "C" -Water-0.340 Inch Spheres.

The difference between the solid and dotted lines indicates the error involved in assuming no slip velocity.

Table VII is a summary of the results of the least squares evaluation of a. Also included are correlation coefficients computed on the basis of Equation (53). These indicate a very good fit of the experimental data by Equation (51).

The constant a is probably a function of packing shape, packing size, and physical properties but no correlation of a could be evaluated from the data presented here. Qualitatively, however, it appears that a is inversely proportional to the packing size and is an increasing function of density difference. An interesting future set of experiments would involve the evaluation of a for a large variety of packings and liquid systems.

TABLE VII

RESULTS OF PHASE HOLDUP CORRELATION

System	a	Correlation Coefficient
Isobutanol-Water-0.501 Inch Spheres	1.083	0.988
Isobutanol-Water-0.340 Inch Spheres	1.102	0.994
Isobutanol-Water-0.164 Inch Spheres	1.269	0.977
Isooctane-Water-0.340 Inch Spheres	1.204	0.988
Isooctane-Alkaterge "C" -Water-0.340 Inch Spheres	1.256	0.995

2. Pressure Gradient Correlation

2.1 Separation of Static and Frictional Pressure Gradients

The two-phase pressure gradients reported in Appendix D are total pressure gradients in a vertical test section. To separate the effects of static head and frictional pressure losses Bernoulli's equation was applied to each phase individually. The approach presented here is substantially that of Hughmark and Pressburg.(38)

Consider velocities and length, Z, taken in the upward direction in the test section. Bernoulli's equation applied across an element of length, ΔZ, then takes the form

$$\int_{P_1}^{P_2} v\,dP + \frac{\Delta u^2}{2g_c} + \Delta Z + w_f + w_s = 0 \qquad (54)$$

where

P_1, P_2 = upstream and downstream pressures, respectively

v = specific volume of fluid = $1/\rho$

$\Delta u = u_2 - u_1$ = velocity difference

$\Delta Z = Z_2 - Z_1$ = vertical length of element of test section

w_f = frictional energy loss per pound of fluid

w_s = shaft work loss per pound of fluid

Shaft work here includes that work performed by one liquid on the other liquid. Now let the subscript w represent the water phase and let the subscript o represent the organic phase. If each phase is considered to form a continuum, Equation (54) may be applied to each phase individually. Then the equations

$$W_w \int_{P_1}^{P_2} v_w\,dP + W_w \frac{\Delta u_w^2}{2g_c} + W_w \Delta Z + W_w w_{fw} + W_w w_{sw} = 0 \qquad (55)$$

and

$$W_o \int_{P_1}^{P_2} v_o dP + W_o \frac{\Delta u_o^2}{2g_c} + W_o \Delta Z + W_o w_{fo} + W_o w_{so} = 0 \qquad (56)$$

apply across the element of length, ΔZ, where

W_w, W_o = mass flow rates of water phase and organic phase, respectively.

Since liquids are, for practical purposes, incompressible

$$\int_{P_1}^{P_2} v dP = v\Delta P = \frac{\Delta P}{\rho} \qquad (57)$$

In addition, if phase holdup is considered to be constant throughout the length of the test section

$$\Delta u_w = \Delta u_o = 0 \qquad (58)$$

Equations (55) and (56), therefore, reduce to

$$W_w \frac{\Delta P}{\rho_w} + W_w \Delta Z + W_w w_{fw} + W_w w_{sw} = 0 \qquad (59)$$

and

$$W_o \frac{\Delta P}{\rho_o} + W_o \Delta Z + W_o w_{fo} + W_o w_{so} = 0 \qquad (60)$$

If Equations (59) and (60) are added and simplified the resulting equation is

$$[\frac{W_w}{\rho_w} + \frac{W_o}{\rho_o}]\Delta P + [W_w + W_o]\Delta Z + [W_w w_{fw} + W_o w_{fo}] + [W_w w_{sw} + W_o w_{so}] = 0 \qquad (61)$$

Since no shaft work is performed on the surroundings by the fluids in the test section

$$W_w w_{sw} + W_o w_{so} = 0 \qquad (62)$$

and, therefore

$$[\frac{W_w}{\rho_w} + \frac{W_o}{\rho_o}]\Delta P + [W_w + W_o]\Delta Z + [W_w w_{fw} + W_o w_{fo}] = 0 \qquad (63)$$

Since $\Delta P = P_2 - P_1$, and $\Delta Z = Z_2 - Z_1$, Equation (63) can be rearranged to give

$$\frac{P_2 - P_1}{Z_2 - Z_1} + \frac{[W_w + W_o]}{[\frac{W_w}{\rho_w} + \frac{W_o}{\rho_o}]} + \frac{[W_w w_{fw} + W_o w_{fo}]}{\Delta Z[\frac{W_w}{\rho_w} + \frac{W_o}{\rho_o}]} = 0 \qquad (64)$$

The first term in Equation (64) is the negative of the measured pressure gradient which is presented in Appendix D. The second term is considered to be the static contribution to the total pressure gradient while the third term represents frictional pressure losses. Equation (64) can be simplified to

$$\frac{P_1 - P_2}{Z_2 - Z_1} = \rho_m + \delta_f \qquad (65)$$

where

$$\rho_m = \frac{[W_w + W_o]}{[\frac{W_w}{\rho_w} + \frac{W_o}{\rho_o}]} = \frac{\rho_w U_w + \rho_o U_o}{U_w + U_o} = \text{"mean" density}$$

U_w, U_o = superficial liquid velocities

$$\delta_f = \frac{[W_w w_{fw} + W_o w_{fo}]}{\Delta Z[\frac{W_w}{\rho_w} + \frac{W_o}{\rho_o}]}$$

Equation (65) is the form commonly used to correlate two-phase pressure-drop data. Ordinarily, however, the mean density, ρ_m, is arbitrarily defined as

$$\rho_m = \rho_w(1\text{-}RI) + \rho_o RI \qquad (66)$$

where RI is the phase holdup. The ρ_m defined immediately below Equation (65) appears to have more theoretical justification than that defined by Equation (66)

Values for ρ_m and δ_f were computed for each run and are presented in Table I, Appendix G. In all cases the average of the three interior pressure gradients was used in the computation.

2.2 Correlation of Frictional Pressure Gradient

In attempting to correlate frictional pressure-gradient data a method analogous to that used in porous media flow was used. In two-phase flow in porous media a "relative permeability" is computed for each phase by means of Equations (17) - (19), Section II-4. This in reality is inversely proportional to the ratio of actual frictional pressure gradient to the frictional gradient if that phase were flowing alone in the medium. This relative permeability is then correlated as a function of water "saturation" or water holdup.

The presence of the kinetic energy term in the equation for packed bed flow complicates the situation somewhat. However, if a predicted frictional gradient based on the assumption that the two-phase mixture can be treated as a single phase is computed, the actual frictional pressure gradient can be related to this predicted one. The variation between these two pressure gradients can then be attributed entirely to interaction between the two phases.

For the present data the Ergun type equation was used with volumetric average properties to predict the "single-phase" frictional

pressure gradient:

$$\delta_{fp} g_c = k_1 \frac{(1-\epsilon)^2}{\epsilon^3} \frac{\mu_m U_m}{D_p^2} + k_2 \frac{(1-\epsilon)}{\epsilon^3} \frac{\rho_m U_m^2}{D_p} \tag{67}$$

where

δ_{fp} = predicted frictional pressure gradient

subscript m = mean value of variable

The "mean" values used were

$$\mu_m = \frac{U_o \mu_o + U_w \mu_w}{U_o + U_w} \tag{68}$$

$$\rho_m = \frac{U_o \rho_o + U_w \rho_w}{U_o + U_w} \tag{69}$$

$$U_m = U_o + U_w \tag{70}$$

The ratio of the actual frictional pressure gradient to the predicted frictional pressure gradient was then computed:

$$P_{RATIO} = \frac{\delta_f}{\delta_{fp}} \tag{71}$$

Values of δ_f, δ_{fp} and P_{RATIO} are presented for comparison in Appendix G. The values of P_{RATIO} varied from approximately unity to as great as 10. A value of unity indicates the "single-phase" assumption to be correct while a value of 10 indicates a high degree of interaction between the phases. An attempt was next made to correlate P_{RATIO} with the physical properties and flow properties of the system.

In the past other authors have suggested a variety of mechanisms for phase interaction in two phase flow. Larkins[44] suggested that in gas-liquid flow the increased pressure gradient is due to the compressibility

of the gaseous phase, i.e. irreversible compression work is performed on the gaseous phase. Cengel,[14] on the other hand, suggested that in the flow of liquid dispersions the increase in pressure gradient could be attributed to an increase in effective viscosity. Neither of these mechanisms provide an adequate explanation for the results observed here.

Surface energy effects are probably the largest contributor to pressure loss due to phase interaction. First the energy required to form a dispersion in flow through a packed bed appears as a pressure loss. When coalescence occurs the energy stored as surface energy is not recovered as pressure but is primarily converted to thermal energy. Therefore each time two droplets coalesce and are redispersed, an irreversible energy conversion occurs, resulting in a pressure loss. An additional contributor to pressure losses due to surface energy effects is believed to be the Jamin effect, previously observed in flow in porous media.[48] If a droplet of dispersed phase is too large to pass through a given opening in the bed, it must either be broken or mishaped to allow passage. Either of these processes involves the creation of additional surface area and thus the conversion of energy. Appendix F is a sample calculation which indicates that surface energy effects are indeed important in liquid-liquid flow in packed beds. For the case considered, if the dispersion is assumed to be formed only once per foot of packing and that no coalescence, redispersion, or "stretching" (due to Jamin effect) occurs in that foot of packing, energy dissipation due to surface effects is approximately 12% of that due to viscous and kinetic

energy effects. The assumptions made here are extremely conservative, so that in reality surface energy effects would be much greater than 12% of the viscous and kinetic effects.

Since no information on coalescence and redispersion rates is available, an empirical approach to the problem of correlation was used. The most important factors affecting surface energy effects are the interfacial tension, σ, the phase holdup RI, and the droplet diameter, d_{32}. The droplet diameter is, in turn, a strong function of packing diameter, D_p, interfacial tension, σ, and mean velocity, U_m. The effect of interfacial tension on drop size, drop breakup, etc. is most commonly presented in terms of the dimensionless Weber number defined as

$$We = \frac{u^2 \rho d}{g_c \sigma} \tag{72}$$

where

u = velocity

ρ = density

d = droplet diameter

σ = interfacial tension

g_c = gravity conversion constant

The Weber number is characteristic of the ratio of inertial forces to surface tension forces. A qualitative examination of the data in Appendix G shows that P_{RATIO} indeed increases with σ and decreases with total velocity and packing diameter. The following form of the Weber number was therefore selected for use here:

$$We = \frac{U_m^2 \rho_m D_p}{g_c \sigma} \tag{73}$$

The substitution of packing diameter, D_p, for droplet diameter is fully justified since d is shown later in this section to be directly proportional to D_p. A simple power dependence of P_{RATIO} on We was assumed. Since P_{RATIO} should approach a minimum value of unity the following quantitative dependence was used:

$$P_{RATIO} - 1 \quad \alpha(We)^a \tag{74}$$

The use of the Weber number takes into account all of the important variables except phase holdup, RI. The dependence of P_{RATIO} on RI is best illustrated by the data for the isobutanol-water-0.164 inch spheres system shown in Figure 34. For those runs for which RI was not measured, RI was computed from the correlation presented previously.

The data in Figure 34 scatter a great deal due to the fact that each point represents a different total velocity. It can easily be seen, however, that P_{RATIO} goes through a maximum in the vicinity of RI = 0.75. A possible explanation for this is that a phase reversal may take place at this point, i.e. the discontinuous organic phase becomes the continuous phase when it occupies more than 75% of the void volume of the test section. The most compact arrangement for packing spherical particles (hexagonal close packing) exhibits a void fraction of 25.95%.[67] This corresponds surprisingly well with the maximum in the P_{RATIO} versus RI curve. It is therefore possible that as RI increases, the spherical droplets of organic phase become closer and closer together until at RI $\cong$ 0.75 no closer packing can exist. As RI is increased beyond this point the organic phase becomes continuous. This reduces the interfacial

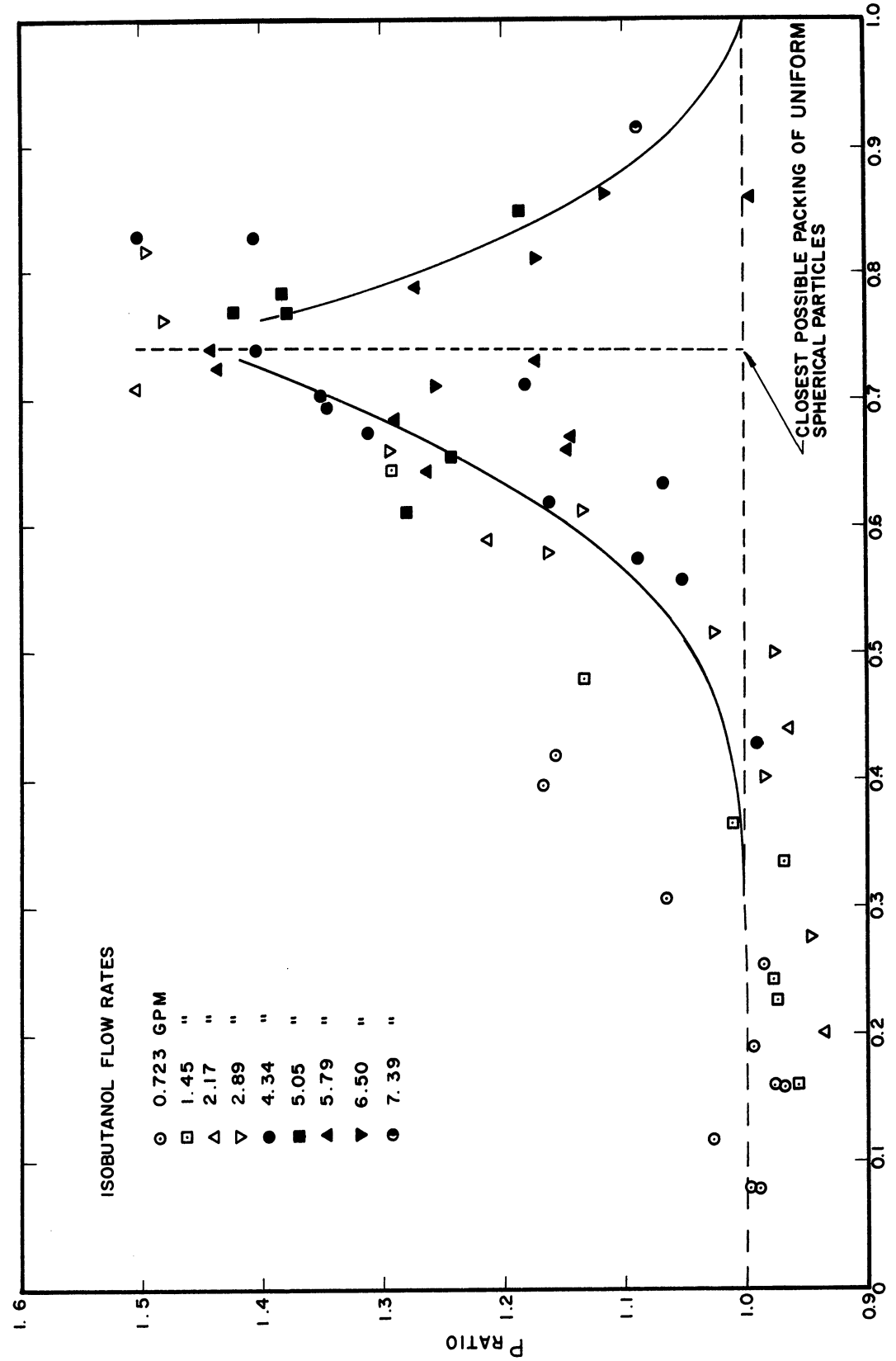

Figure 34. Dependence of P_{RATIO} on Phase Holdup in the System Isobutanol-Water-0.164 Inch Spheres.

area of the dispersion which in turn reduces the pressure losses due to surface effects. As RI approaches 1, the pressure drop approaches that for the pure organic phase.

Due to the shape of the P_{RATIO} versus RI curve the following form for quantitatively predicting the dependence of P_{RATIO} on RI was assumed:

$$P_{RATIO} - 1 \quad \alpha \; e^{-c(RI-c_1)^2} \tag{75}$$

This is the form of the Gaussian distribution curve which approximates the P_{RATIO} versus RI curve. It does not satisfy the end conditions of

$$P_{RATIO} = 1 \quad \text{for RI} = 0$$

and (76)

$$P_{RATIO} = 1 \quad \text{for RI} = 1$$

for all values of c. It does, however, closely approximate these conditions.

Combining Equations (74) and (75) gives the following expression for correlation purposes:

$$P_{RATIO} = 1 + K(We)^a \; e^{-c(RI-c_1)^2} \tag{77}$$

In order to evaluate the empirical constants K, a, c, and c_1, Equation (77) was rearranged to the linear form

$$\ln(P_{RATIO} - 1) = \ln K + a\ln(We) - c(RI-c_1)^2$$

or

$$\ln(P_{RATIO} - 1) = (\ln K - cc_1^2) + a\ln(We) - cRI^2 + 2cc_1RI \tag{78}$$

A least squares regression analysis was used on the IBM 7090 digital computer to evaluate the constants in Equation (78). A lack of sufficient data for RI > 0.75, however, prevented an adquate determination of c_1. Therefore c_1 was, on the basis of the preceding arguments, arbitrarily chosen as 0.75. The regression analysis was then applied to

$$\ln(P_{RATIO} - 1) = \ln K + a\ln(We) - c(RI-0.75)^2 \qquad (79)$$

Since logarithms do not exist for negative numbers, values of $P_{RATIO} < 1$ were omitted from the analysis. This results in a small unavoidable bias in the values of the constants. Values of RI were computed for those runs in which RI was not measured. The results of the correlation are presented in Table VIII.

TABLE VIII

RESULTS OF P_{RATIO} CORRELATION

Constant	Value	Variance
ln K	-0.32413	0.00535
K	0.723	-
a	-0.624	0.000761
c	5.59	0.145

Correlation Coefficient Based on Equation (79) = 0.846

The variance is the square of the standard deviation of the number and is thus an indication of how well the number is known.

The final form of the pressure drop correlation is thus

$$P_{RATIO} = 1 + 0.723(We)^{-0.624} e^{-5.59(RI-0.75)^2} \qquad (80)$$

The use of four empirical constants was required by the shape of the P_{RATIO} versus RI curve. No physical significance should be attributed to the values presented here. Values of We, RI and P_{RATIO} predicted by Equation (80) are included in the table of processed data in Appendix G. Figure 35a represents a comparison of the measured values of P_{RATIO} with those predicted by Equation (80). For those points with predicted P_{RATIO} less than 1.1, only every tenth point is plotted.

At first appearance Figure 35a exhibits quite a bit of scatter. It should be noted, however, that most of the points exhibiting wide scatter were obtained with the system isooctane-Alkaterge "C"-water-0.340 inch spheres. As was pointed out previously there is some question as to the significance of these data. The concentration of the surfactant at the interface during a static interfacial tension measurement causes a reduction in the measured interfacial tension. On the other hand there is no proof that this is the effective interfacial tension during dynamic flow conditions. Due to the very large ratio of surface area to volume in a dispersion, the concentration of surfactant at the interface is considerably less than that in a static interfacial tension measurement.

The data of Figure 35a are replotted in Figure 35b with isooctane-Alkaterge "C"-water data omitted. This figure indicates a much better fit for Equation (80) than Figure 35a. If the addition of a surfactant has little or no effect on the dynamic interfacial tension, the values predicted by Equation (80) would not be correct for the isooctane-Alkaterge

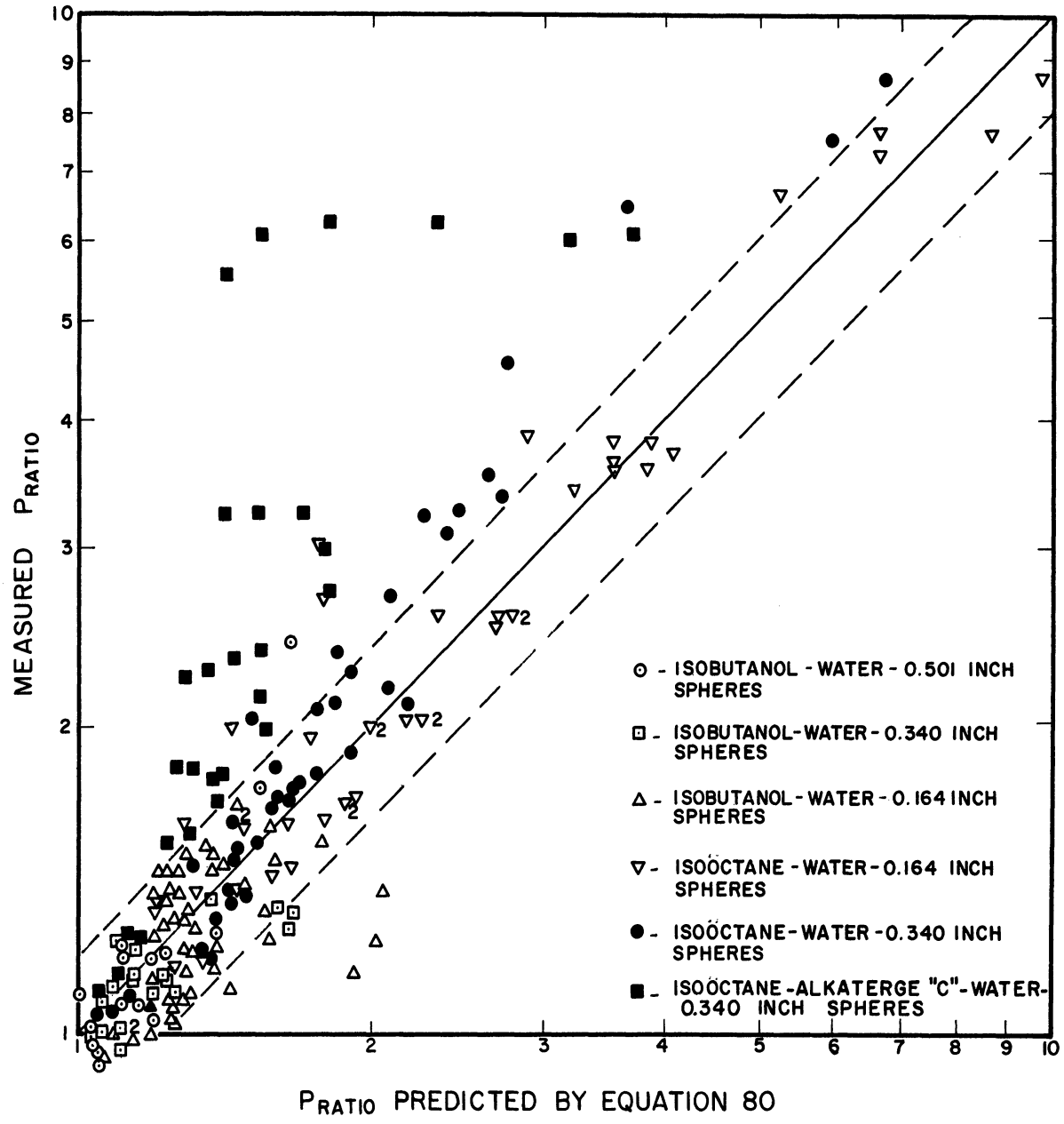

Figure 35a. Comparison of Predicted and Measured P_{RATIO}.

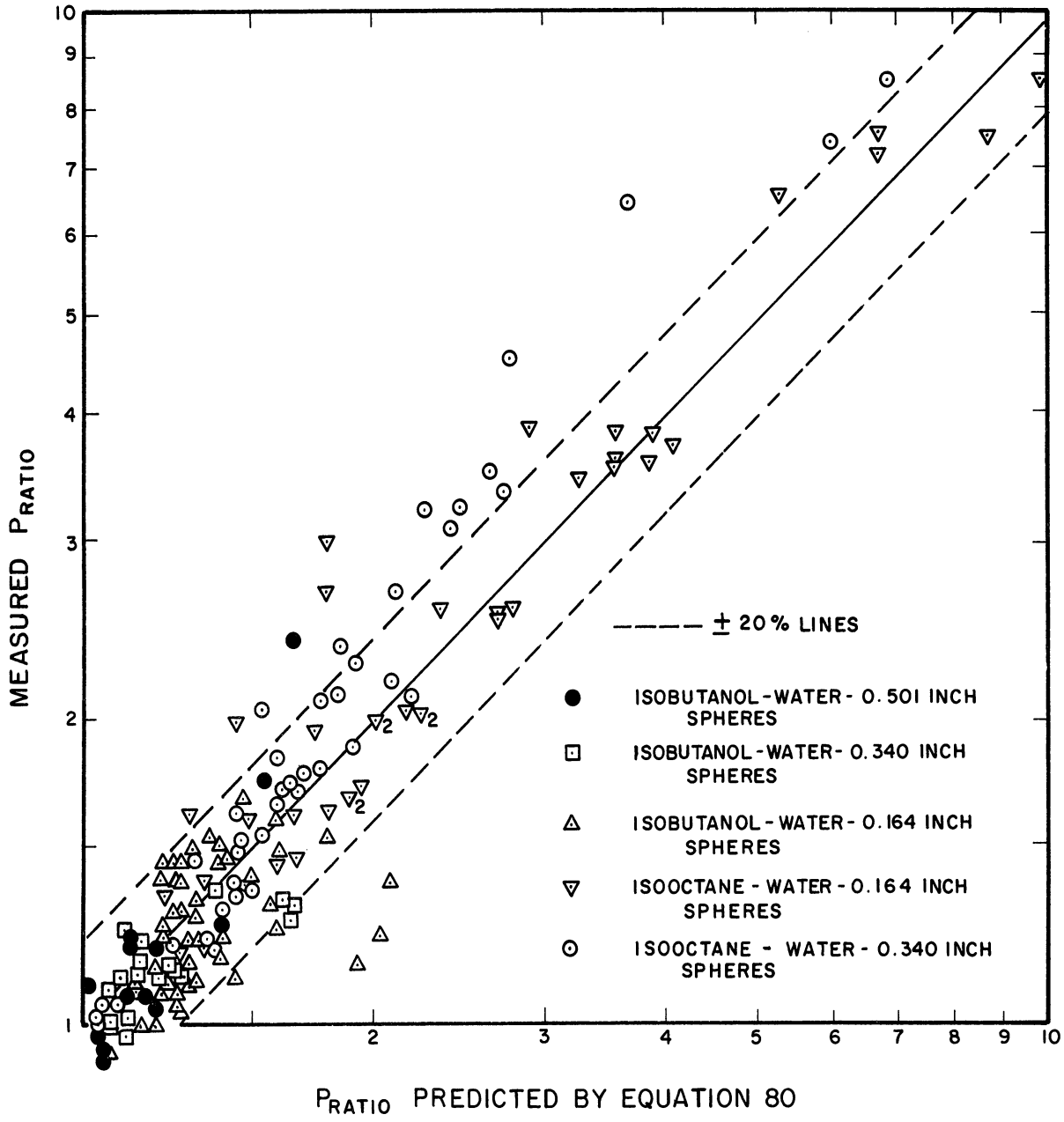

Figure 35b. Comparison of Predicted and Measured P_{RATIO} with Exclusion of Surfactant Data.

"C"-water data. New predicted values of P_{RATIO} were computed for this system by Equation (80) using the normal value of 49.5 dynes/cm for σ. These corrected values are plotted in Figure 35c along with the rest of the data from Figure 35a. The improvement in the correlation indicates that the apparent change in interfacial tension caused by addition of a surfactant is not the actual change in interfacial tension under all degrees of dispersion.

An analysis of the data in Figure 35a shows that 83.4% of the points fall within $\pm$20% of the predicted value. If the data taken with Alkaterge present are neglected 89.9% of the data are within the $\pm$20% limits. Again neglecting the Alkaterge "C" runs 92.2% and 97.4% of the data fall within $\pm$25% and $\pm$40%, respectively, of the predicted value. Even with the inclusion of the Alkaterge "C" runs, 92.2% of the data fall within $\pm$40% of the predicted value.

3. Drop Size Correlation

As was pointed out in the review of the literature very little previous work has been performed on interfacial area measurements in packed beds. As a result a completely empirical approach to the problem of correlation was used here. The characteristic diameter used in the correlation was in all cases the Sauter mean diameter discussed in the previous section.

Since no completely general correlation of drop sizes was found to be adequate, the effect of the individual experimental variables will be discussed separately.

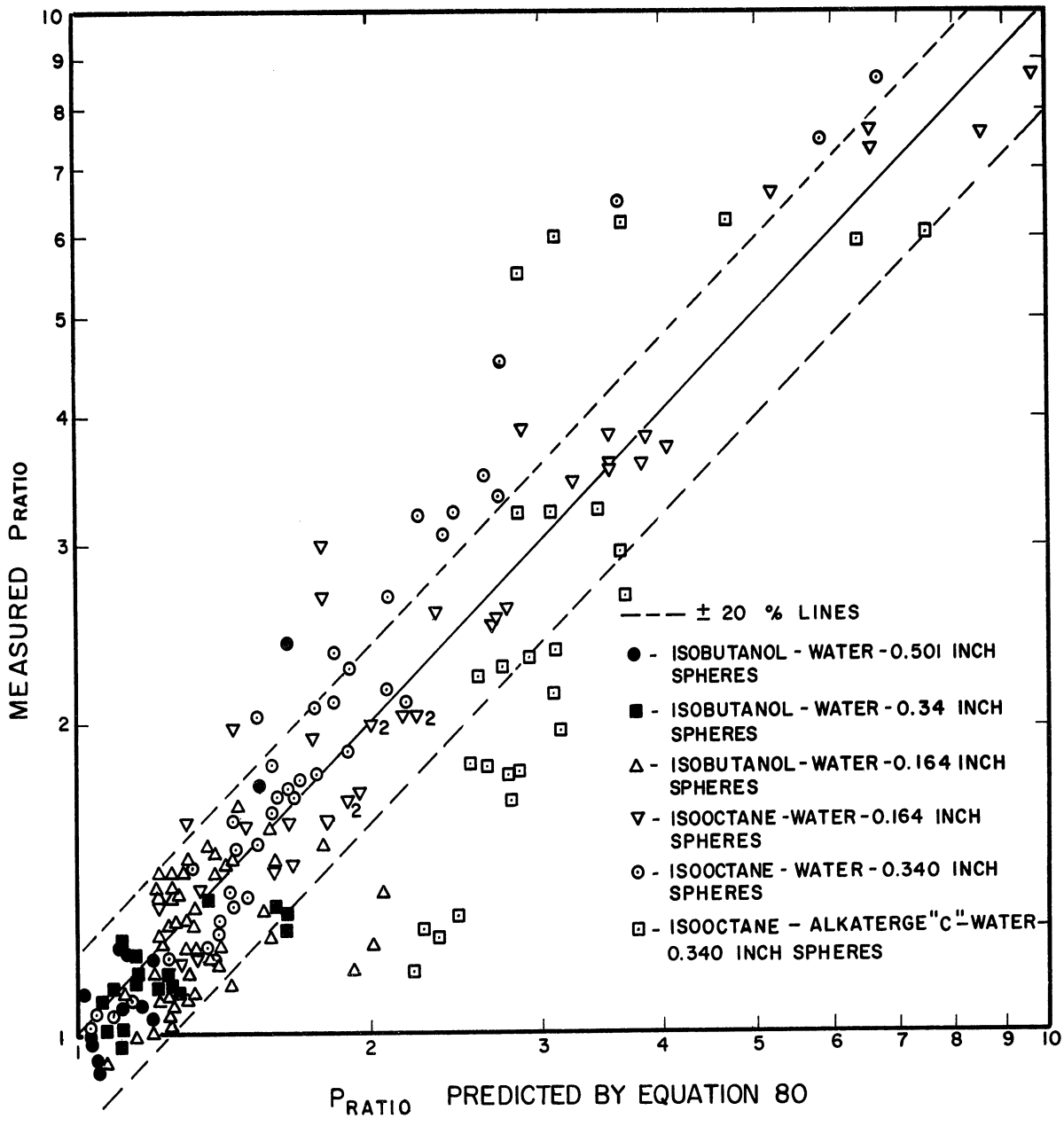

Figure 35c. Comparison of Predicted and Measured P_{RATIO} with Corrected Surfactant Data.

3.1 Effect of Velocity

Several methods were tried before the effect of velocity on drop size was finally obtained. Since the total energy input per volume of liquid mixture is proportional to the total velocity of the mixture,

$$d_{32} = K(U_m)^b \tag{81}$$

was tried as a correlating equation. This proved to be of little value but an equation of the following form

$$d_{32} = Ke^{-cU_m} \tag{82}$$

showed a very good correlation for each individual system. Plots of $\ln d_{32}$ versus U_m are presented in Figure 36 for the isobutanol-water systems. An equivalent plot for the system isooctane-water-0.164 inch spheres appears in Figure 37.

3.2 Effect of Packing Diameter

As can be seen from Figure 36 packing diameter has a strong effect on drop size. A plot of drop diameter, d_{32}, versus packing diameter, D_p, on a logarithmic scale shows that d_{32} is directly proportional to D_p (see Figure 38). Only one set of flow velocities and flow ratios is shown for each liquid system.

3.3 Effect of Fluid Properties

Due to the small number of different fluid systems studied, the effect of fluid properties cannot be determined very well. It was felt, however, that the effect of interfacial tension on drop size was far greater than that of any of the other physical properties. Therefore,

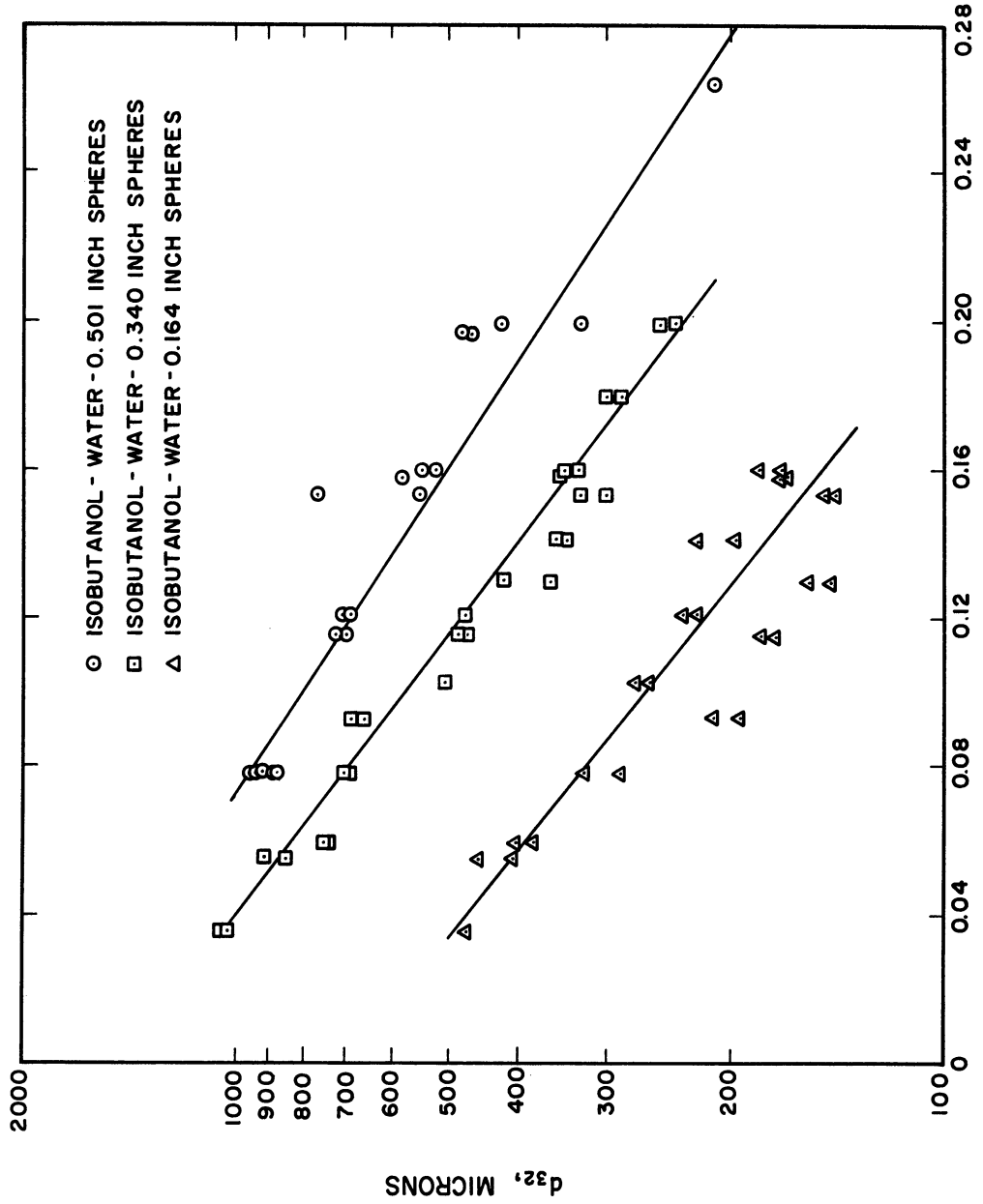

Figure 36. Effect of Velocity on Sauter Mean Drop Diameter.

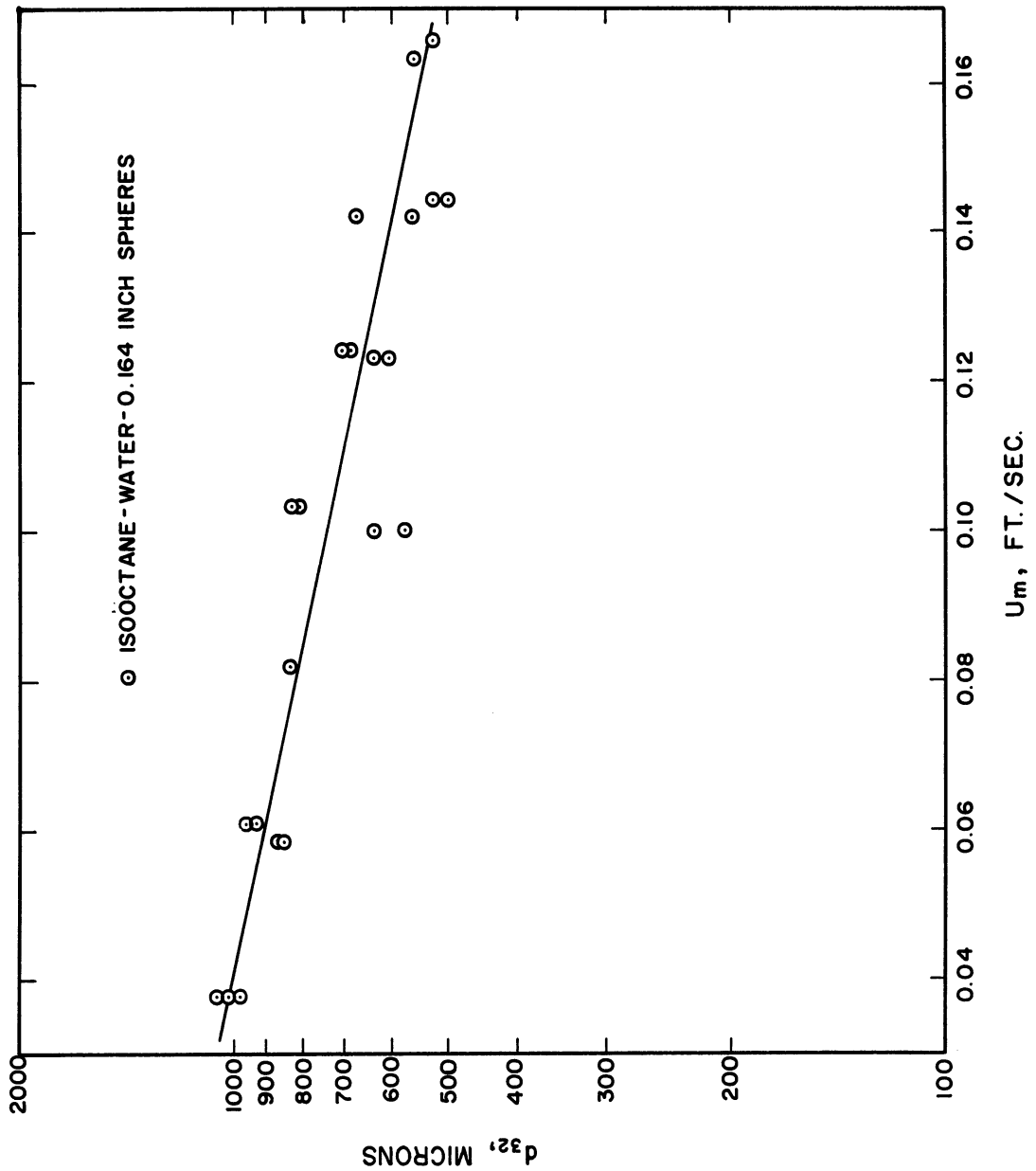

Figure 37. Effect of Velocity on Sauter Mean Drop Diameter.

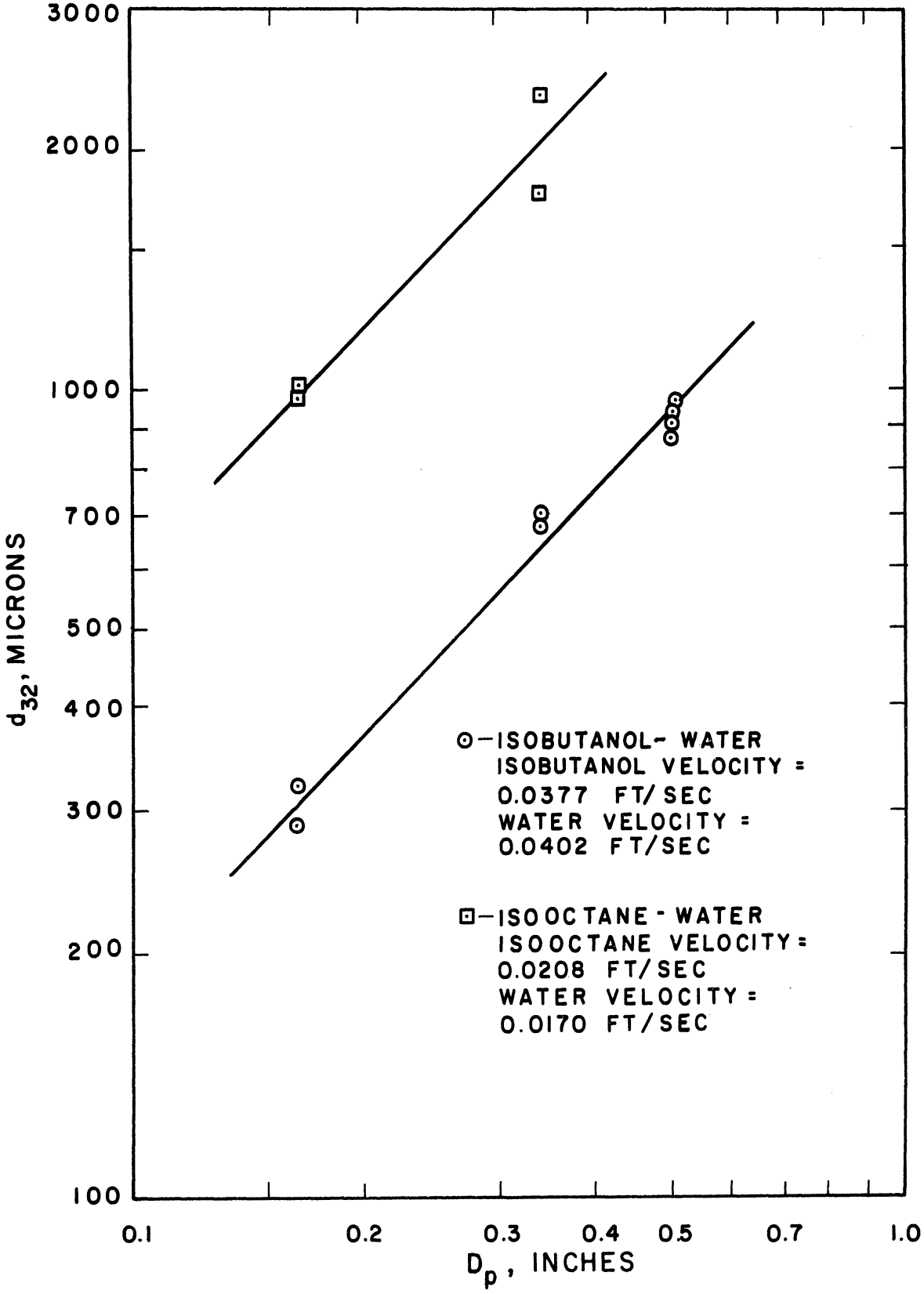

Figure 38. Effect of Packing Diameter on Sauter Mean Drop Diameter.

a plot of drop diameter versus interfacial tension is presented in Figure 39. This indicates that drop size is approximately proportional to the 1/4 power of interfacial tension. This, of course, can not be used for correlation purposes since the effects of the other fluid properties are neglected.

3.4 Summary

In order to summarize the effects mentioned here, a correlating equation of the following form was postulated:

$$\frac{d_{32}}{D_p} = K' e^{-c' U_m} \tag{83}$$

Values of K' and c' were evaluated for each data set by a least squares technique after rearranging Equation (83) to give

$$\ln \frac{d_{32}}{D_p} = \ln K' - c' U_m \tag{84}$$

In addition all of the isobutanol-water data were fitted to Equation (84). The results of this correlation are presented in Table IX. The correlation coefficients are based on Equation (84).

In an attempt to make Equation (83) as general as possible, the technique of dimensional analysis was applied to the data presented here. The following experimental variables were considered to have a significant effect on drop size: interfacial tension, σ; packing diameter, D_p; mean superficial velocity, U_m; mean density, ρ_m; dispersed phase viscosity, μ_d. The gravitational conversion constant, g_c, must also be included to allow dimensional consistency. A dimensional analysis of these variables

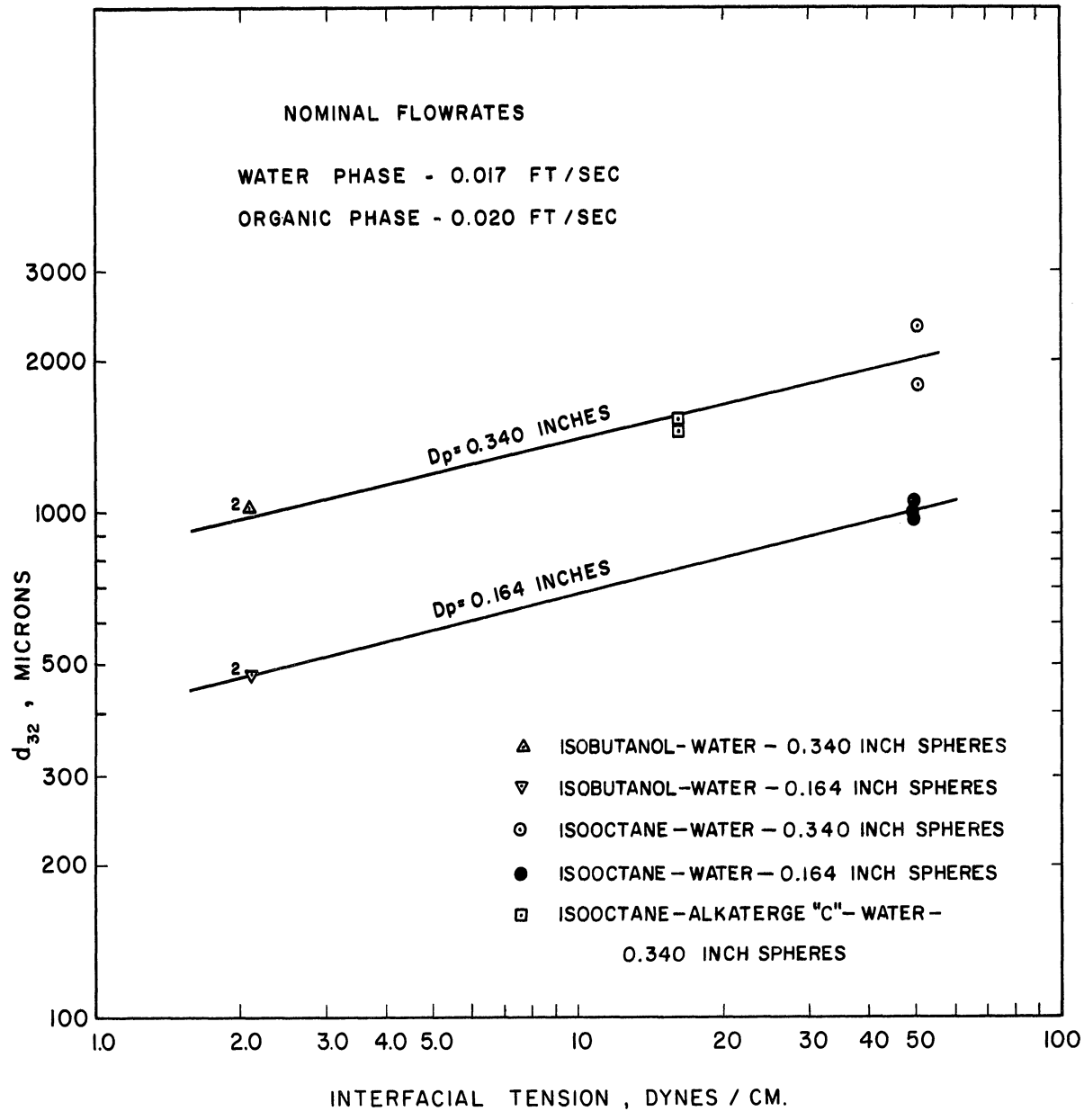

Figure 39. Effect of Interfacial Tension on Sauter Mean Drop Diameter.

TABLE IX

RESULTS OF DROP SIZE CORRELATION

System	K'	c' $\frac{sec}{ft}$	Correlation Coefficient
Isobutanol-Water-0.501 Inch Spheres	0.126	6.88	0.957
Isobutanol-Water-0.340 Inch Spheres	0.158	8.90	0.983
Isobutanol-Water-0.164 Inch Spheres	0.148	8.80	0.913
All Isobutanol-Water Data	0.141	8.00	0.946
Isooctane-Water-0.164 Inch Spheres	0.299	5.31	0.926

gives the following functional relationship:

$$\left(\frac{d_{32}}{D_p}\right) = f\left(\frac{D_p \rho_m U_m}{\mu_m}, \frac{D_p \rho_m U_m^2}{\sigma g_c}\right) \tag{85}$$

or

$$\left(\frac{d_{32}}{D_p}\right) = f(Re, We) \tag{86}$$

where

Re = Reynolds number

We = Weber number

A functional relationship which satisfies the empirical requirements of Equation (83) is

$$\frac{d_{32}}{D_p} = K' e^{-c''\left(\frac{We}{Re}\right)} \tag{87}$$

This equation was rearranged to

$$\ln \frac{d_{32}}{D_p} = \ln K' - c''\left(\frac{We}{Re}\right) \tag{88}$$

and K' and c'' were evaluated for all of the drop size data by a least squares technique. The resulting equation is

$$\frac{d_{32}}{D_p} = 0.168\ e^{-20.5\left(\frac{We}{Re}\right)} \tag{89}$$

The correlation coefficient based on Equation (88) is 0.961. Figure 40 is a plot of $\frac{d_{32}}{D_p}$ versus $\frac{We}{Re}$ on log-log paper. The solid line represents Equation (89).

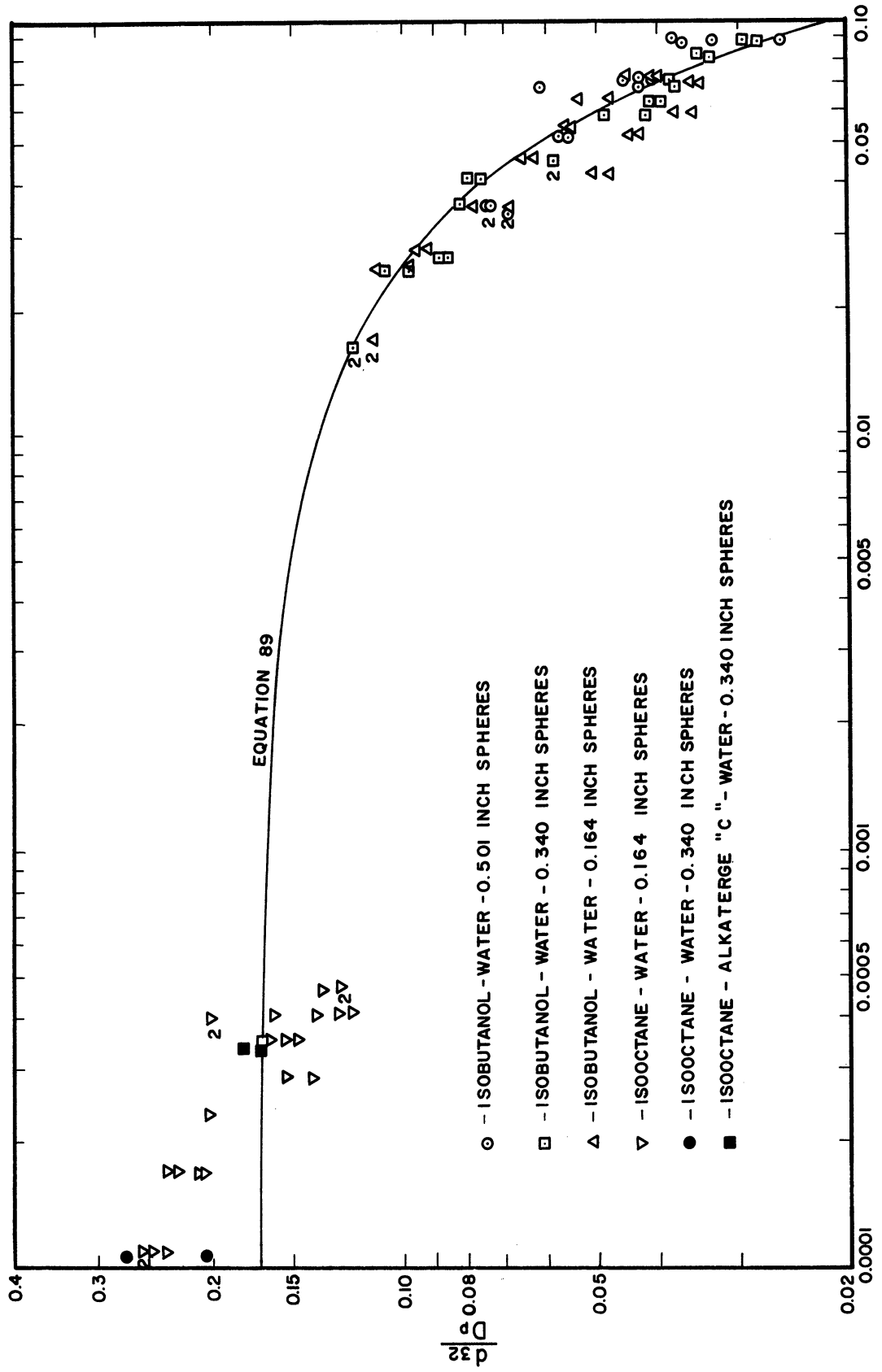

Figure 40. Correlation of Drop Size Data.

VII. CONCLUSIONS

As a result of the investigation presented here, the following conclusions can be drawn:

1. Although the form of the Ergun equation is quite satisfactory, the empirical constants vary for different beds and must be experimentally determined to enable precise single phase pressure drop predictions. Variations in packing arrangement are believed to cause the variations in the constants. On the other hand the values of the empirical constants are not effected by fluid properties.
2. Three flow regimes have been observed in the cocurrent flow of immiscible liquids in packed beds. They are bubble flow, homogeneous flow, and slug flow.
3. A mixture of two immiscible liquids flowing cocurrently through a packed bed cannot be treated as a single phase except at the extremes of flow ratio. At intermediate flow ratios surface energy effects have a significant effect on pressure drop.
4. If P_{RATIO} is defined as the ratio of the actual two-phase pressure gradient to that predicted using the assumption that the two-phase mixture behaves as a single phase, P_{RATIO} exhibits a maximum at approximately 75% holdup of the non-wetting phase. Values of P_{RATIO}, which is a measure of phase interaction, have been observed as high as 10.

5. A phase reversal is believed to occur at a non-wetting phase holdup of $\sim$75%.

6. P_{RATIO} can be approximated by

$$P_{RATIO} = 1 + 0.723(We)^{-0.624} e^{-5.59(RI-0.75)^2} \qquad (90)$$

for the systems studied here. This expression should be approximately true for other liquid-liquid systems in which water is the wetting phase.

7. Phase holdup of the non-wetting phase, RI, can be loosely approximated by assuming no slip velocity. Relative errors due to this assumption can be minimized, particularly at low values of RI, by using

$$RI = \left(\frac{U_o}{U_o + U_w}\right)^a \qquad (91)$$

where a must be evaluated experimentally.

8. The dispersed phase takes the form of spherical droplets. These droplets exhibit a Gaussian distribution with respect to diameter. The Sauter mean drop diameter is directly proportional to the packing diameter. Its dependence on velocity can be expressed by

$$d_{32} \alpha e^{-cU_m} \qquad (92)$$

where U_m = total mixture superficial velocity. The effect of fluid properties on drop size has not been determined, however, increasing interfacial tension increases the drop size noticeably.

VIII. RECOMMENDATIONS FOR FUTURE STUDY

Any investigation of an exploratory nature raises some questions which cannot be answered in a reasonable length of time. The following subjects are therefore suggested as possible areas for future research:

1. Determine the effect of fluid properties on drop sizes. The photographic techniques described here should be adequate for this purpose. In addition the wall effect on drop size should be investigated. A specially designed test section would be required for this study.
2. Determine the effect of fluid properties on phase holdup and P_{RATIO} more precisely.
3. Determine coalescence and redispersion frequencies for liquid-liquid flow in packed beds. High speed photography could probably be used for this purpose. From data of this type an estimate of actual energy consumption due to surface generation could be obtained.
4. Determine the effect of packing material on dispersion formation. A material which is preferentially wetted by the organic phase could be used to increase the tendency for a continuous organic phase. The suspected phase reversal should then occur at 25% organic phase holdup.

LITERATURE CITED

1. Anderson, G. H., and B. G. Mantzouranis, "Two-Phase (Gas-Liquid) Flow Phenomena - I Pressure Drop and Holdup for Two Phase Flow in Vertical Tubes," Chem. Eng. Sci., 12, 109 (1960).

2. Benenati, R. F., and C. B. Brosilow, "Void Fraction Distribution in Beds of Spheres," AIChE J., 8, 359 (1962).

3. Bertuzzi, A. F., M. R. Tek, and F. H. Poettmann, "Simultaneous Flow of Liquid and Gas Through Horizontal Pipe," J. Pet. Tech., 8, January 17, 1956.

4. Blake, F. C., "The Resistance of Packing to Fluid Flow," Trans. AIChE, 14, 415 (1922).

5. Brigham, W. E., E. D. Holstein, and R. L. Huntington, "Two-Phase Cocurrent Flow of Liquids and Air Through Inclined Pipe," Petr. Eng., 29, No. 12, D-39 (1957).

6. Brown, R. A. S., and G. W. Govier, "High-Speed Photography in the Study of Two-Phase Flow," Can. J. Chem. Eng., 39, 159 (1961).

7. Brown, R. A. S., G. A. Sullivan, and G. W. Govier, "The Upward Vertical Flow of Air-Water Mixtures-III Effect of Gas Phase Density on Flow Pattern, Holdup and Pressure Drop," Can. J. Chem. Eng., 38, 62 (1960).

8. Brownell, L. E., H. S. Dombrowski, and C. A. Dickey, "Pressure Drop Through Porous Media - IV New Data and Revised Correlation," Chem. Eng. Prog., 46, 415 (1950).

9. Brownell, L. E., and D. L. Katz, "Flow of Fluids Through Porous Media," Chem. Eng. Prog., 43, 537 (1947).

10. Brownell, L. E., and D. L. Katz, "Flow of Fluids Through Porous Media - II Simultaneous Flow of Two Homogeneous Phases," Chem. Eng. Prog., 43, 601 (1947).

11. Burke, S. P., and W. B. Plummer, "Gas Flow Through Packed Columns," Ind. Eng. Chem., 20, 1196 (1928).

12. Calvert, S., and B. Williams, "Upward Cocurrent Annular Flow of Air and Water in Smooth Tubes," AIChE J., 1, 78 (1955).

13. Carman, P. C., "Fluid Flow Through Granular Beds," Trans. Instn. Chem. Eng. (London), 15, 150 (1937).

14. Cengel, J. A., A. A. Faruqui, J. W. Finnigan, C. H. Wright, and J. G. Knudsen, "Laminar and Turbulent Flow of Unstable Liquid-Liquid Emulsions," AIChE J., 8, 335 (1962).

15. Charles, M. E., G. W. Govier, and G. W. Hodgson, "The Horizontal Pipeline Flow of Equal Density Oil-Water Mixtures," Can. J. Chem. Eng., 39, 27 (1961).

16. Charles, M. E., and P. J. Redberger, "The Reduction of Pressure Gradients in Oil Pipelines by the Addition of Water: Numerical Analysis of Stratified Flow," Can. J. Chem. Eng., 40, 70 (1962).

17. Chenoweth, J. M., and M. W. Martin, "Turbulent Two-Phase Flow," Petr. Ref., 34, No. 10, 151 (1955).

18. Chilton, T. H., and A. P. Colburn, "Pressure Drop in Packed Tubes," Ind. Eng. Chem., 23, 913 (1931).

19. Chisolm, D., and A. D. K. Laird, "Two Phase Flow in Rough Tubes," Trans. ASME, 80, 276 (1958).

20. Church, J. M., and R. Shinnar, "Stabilizing Liquid-Liquid Dispersions by Agitation," Ind. Eng. Chem., 53, 479 (1961).

21. Dixon, J. A., "Binary Solutions of Saturated Hydrocarbons," J. Chem. Eng. Data, 4, 289 (1959).

22. Dodds, W. S., L. F. Stutzman, B. J. Sollami, and R. J. McCarter, "Pressure Drop and Liquid Holdup in Cocurrent Gas Absorption," AIChE J., 6, 390 (1960).

23. Endoh, K., and Y. Oyama, "On the Size of Droplets Disintegrated in Liquid-Liquid Contacting Mixer," Sci. Papers Inst. Phys. Chem. Research (Tokyo), 52, 131 (1958).

24. Ergun, S., "Fluid Flow Through Packed Columns," Chem. Eng. Prog., 48, 89 (1952).

25. Ergun, S., and A. A. Orning, "Fluid Flow Through Randomly Packed Columns and Fluidized Beds," Ind. Eng. Chem., 41, 1179 (1949).

26. Fahien, R. W., and C. B. Schriver, "The Effect of Porosity and Transition Flow on Pressure Drop in Packed Beds," Paper presented at Denver Meeting AIChE (1962).

27. Furnas, C. C., "Flow of Gases Through Beds of Broken Solids," U.S. Bur. Mines Bull. 307, (1929).

28. Gayler, R., and H. R. C. Pratt, "Holdup and Pressure Drop in Packed Columns," Trans. Instn. Chem. Eng. (London), 29, 110 (1951).

29. Gemmell, A. R., and N. Epstein, "Numerical Analysis of Stratified Laminar Flow of Two Immiscible Newtonian Liquids in a Circular Pipe," Can. J. Chem. Eng., 40, 215 (1962).

30. Govier, G. W., and M. M. Omer, "The Horizontal Pipeline Flow of Air-Water Mixtures," Can. J. Chem. Eng., 40, 93 (1962).

31. Govier, G. W., B. A. Radford, and J. S. C. Dunn, "The Upwards Vertical Flow of Air-Water Mixtures," Can. J. Chem. Eng., 35, 59 (1957).

32. Govier, G. W., and W. L. Short, "The Upward Vertical Flow of Air-Water Mixtures - III Effect of Tubing Diameter on Flow Pattern, Holdup and Pressure Drop," Can. J. Chem. Eng., 36, 195 (1958).

33. Govier, G. W., G. A. Sullivan, and R. K. Wood, "The Upward Vertical Flow of Oil Water Mixtures," Can. J. Chem. Eng., 39, 67 (1961).

34. Hassan, M. E., R. F. Nielsen, and J. C. Calhoun, "Effects of Pressure and Temperature on Oil-Water Interfacial Tensions for a Series of Hydrocarbons," J. Pet. Tech., 5, 299 (1953).

35. Hinze, J. O., "Fundamentals of the Hydrodynamic Mechanism of Splitting in Dispersion Processes," AIChE J., 1, 289 (1955).

36. Hodgman, C. D., Ed., "Handbook of Chemistry and Physics," 36th Ed., Cleveland, Chemical Rubber Publishing Co., 1954.

37. Hoogendoorn, C. J., "Gas-Liquid Flow in Horizontal Pipes," Chem. Eng. Sci., 9, 205 (1959).

38. Hughmark, G. A., and B. S. Pressburg, "Holdup and Pressure Drop with Gas-Liquid Flow in a Vertical Pipe," AIChE J., 7, 677 (1961).

39. "International Critical Tables," Vol. IV, New York, McGraw-Hill, 1926, p. 436.

40. Jesser, B. W., and J. C. Elgin, "Studies of Liquid Holdup in Packed Towers," Trans. AIChE, 39, 277 (1943).

41. Johnson, A. I., and E. A. L. Lavergne, "Holdup in Liquid-Liquid Extraction Columns," Can. J. Chem. Eng., 39, 37 (1961).

42. Kafarov, V. V., and B. M. Babanov, "Phase-Contact Area of Immiscible Liquids During Agitation by Mechanical Stirrers," J. Appl. Chem. (U.S.S.R.), 32, 810 (1959).

43. Lange, N. A., Ed., "Handbook of Chemistry," 9th Ed., Sandusky, Ohio, Handbook Publishers, Inc., 1956.

44. Larkins, R. P., "Two-Phase Cocurrent Flow in Packed Beds," Ph.D. Thesis, The University of Michigan, 1959.

45. Leacock, J., "Mass Transfer Between Isobutanol and Water in Co-current Flow Through a Packed Column," Ph.D. Thesis, The University of Michigan, 1960.

46. Leva, M., "Pressure Drop Through Packed Tubes," Chem. Eng. Prog., 43, 549 (1947).

47. Leva, M., M. Weintraub, M. Grummer, M. Pollchik, and H. H. Storch, "Fluid Flow Through Packed and Fluidized Systems," U.S. Bur. Mines Bull. 504, (1951).

48. Leverett, M. C., "Flow of Oil-Water Mixtures Through Unconsolidated Sands," Trans. AIME, 132, 149 (1939).

49. Levich, V. G., "Physicochemical Hydrodynamics," Englewood Cliffs, N. J., Prentice-Hall, 1962, pp. 454-464.

50. Lewis, J. B., I. Jones, and H. R. C. Pratt, "A Study of Droplet Behavior in Packed Columns," Trans. Instn. Chem. Eng. (London), 29, 126 (1951).

51. Lockhart, R. W., and R. C. Martinelli, "Proposed Correlation of Data for Isothermal Two-Phase, Two-Component Flow in Pipes," Chem. Eng. Prog., 45, 39 (1949).

52. Markas, S. E., and R. B. Beckman, "Radioisotope Technique for the Determination of Flow Characteristics in Liquid-Liquid Extraction Columns," AIChE J., 3, 223 (1957).

53. Martin, J. J., W. L. McCabe, and C. C. Monrad, "Pressure Drop Through Stacked Spheres, Effect of Orientation," Chem. Eng. Prog., 47, 91 (1951).

54. Martinelli, R. C., J. A. Putnam, and R. W. Lockhart, "Two-Phase, Two-Component Flow in the Viscous Region," Trans. AIChE, 42, 681 (1946).

55. Martinelli, R. C., L. M. K. Boelter, T. H. M. Taylor, E. G. Thomsen, and E. H. Morrin, "Isothermal Pressure Drop for Two-Phase, Two-Component Flow in a Horizontal Pipe," Trans. ASME, 66, 139 (1944).

56. Morcom, A. R., "Fluid Flow Through Granular Materials," Trans. Instn. Chem. Eng. (London), 24, 30 (1946).

57. Mugele, R. A., "Maximum Stable Droplets in Dispersoids," AIChE J., 6, 3 (1960).

58. Oman, A. O., and K. M. Watson, Nat. Pet. News Tech. Sect., No. 44, R795 (1944).

59. Perry, J. H., Ed., "Chemical Engineers' Handbook," 3rd. Ed., New York, McGraw-Hill, 1950, pp. 192-3.

60. Ranz, W. E., "Friction and Transfer Coefficients for Single Particles and Packed Beds," Chem. Eng. Prog., 48, 247 (1952).

61. Rodger, W. A., V. G. Trice, Jr., and J. H. Rushton, "Effect of Fluid Motion on Interfacial Area of Dispersions," Chem. Eng. Prog., 52, 515 (1956).

62. Rodriguez, F., L. C. Gratz, and D. L. Engle, "Interfacial Area in Liquid-Liquid Mixing," AIChE J., 7, 663 (1961).

63. Ros, N. C. J., "Simultaneous Flow of Gas and Liquid as Encountered in Oil Wells," paper presented at AIChE Meeting, Tulsa, September 25-28, 1960.

64. Russell, T. W. F., and M. E. Charles, "The Effect of the Less Viscous Liquid in the Laminar Flow of Two Immiscible Liquids," Can. J. Chem. Eng., 37, 18 (1959).

65. Russell, T. W. F., G. W. Hodgson, and G. W. Govier, "Horizontal Pipeline Flow of Mixtures of Oil and Water," Can. J. Chem. Eng., 37, 9 (1959).

66. Scheidegger, A. E., "The Physics of Flow Through Porous Media," University of Toronto Press, Toronto, (1960).

67. Scott, G. D., "Packing of Spheres," Nature, 188, 908 (1960).

68. Seidell, A., "Solubilities of Organic Compounds," 3rd Ed., Vol. II, New York, Van Nostrand, 1941, p. 268.

69. Shinnar, R., "On the Behavior of Liquid Dispersions in Mixing Vessels," J. Fluid Mech., 10, 259 (1961).

70. Shinnar, R., and J. M. Church, "Predicting Particle Size in Agitated Dispersions," Ind. Eng. Chem., 52, 253 (1960).

71. Sitaramayya, T., and G. S. Laddha, "Holdup in Packed Liquid-Liquid Extraction Columns," Chem. Eng. Sci., 13, 263 (1961).

72. Sleicher, C. A., Jr., "Maximum Stable Drop Size in Turbulent Flow," Shell Development Company, Emeryville, California.

73. Street, J. R., "A Study of Vertical Gas-Liquid Slug Flow," Ph.D. Thesis, The University of Michigan, 1962.

74. Trice, V. G., Jr., and W. A. Rodger, "Light Transmittance as a Measure of Interfacial Area in Liquid-Liquid Dispersions," AIChE J., 2, 205 (1956).

75. Vermuelen, T., G. M. Williams, and G. E. Langlois, "Interfacial Area in Liquid-Liquid and Gas Liquid Agitation," Chem. Eng. Prog., 51, 85 (1955).

76. Weaver, R. E. C., L. Lapidus, and J. C. Elgin, "The Mechanics of Vertical Moving Liquid-Liquid Fluidized Systems: I. Interphase Contacting of Droplets Passing Through a Second Quiescent Fluid," AIChE J., 5, 533 (1959).

77. White, A. M., "Pressure Drop and Loading Velocities in Packed Towers," Trans. AIChE, 31, 390 (1935).

78. Wicks, C. E., and R. B. Beckman, "Dispersed-Phase Holdup in Packed Countercurrent Liquid-Liquid Extraction Columns," AIChE J., 1, 426 (1955).

APPENDICES

APPENDIX A

DENSITY CORRECTION FACTOR FOR ROTAMETERS

A rotameter calibrated for a liquid of given density ordinarily must be recalibrated when the density of the liquid is changed. Correction factors based on the orifice equation have been computed by the Fischer & Porter Company and are presented in Instruction Bulletin 10A9020 Revision 1. The correction factor is a function of two dimensionless ratios -- the ratio of scale fluid density to metering fluid density and the ratio of float density to scale fluid density. The scale fluid is that originally used to calibrate the rotameter. The metering fluid is that for which a corrected flowrate is desired.

In the present investigation all floats were made of 316 stainless steel and all rotameters were calibrated with water. As a result the latter ratio mentioned above was a constant given by $R_2 = \frac{7.98}{0.998} = 8.00$. The correction factor is plotted in Figure A-1 for $R_2 = 8.00$. This curve was fitted by a quadratic equation by a least squares technique. The resulting equation, which was used in the computer processing of data, is

$$CF = 0.213 + 0.980\ R_1 - 0.1917\ R_1^2 \qquad (A\text{-}1)$$

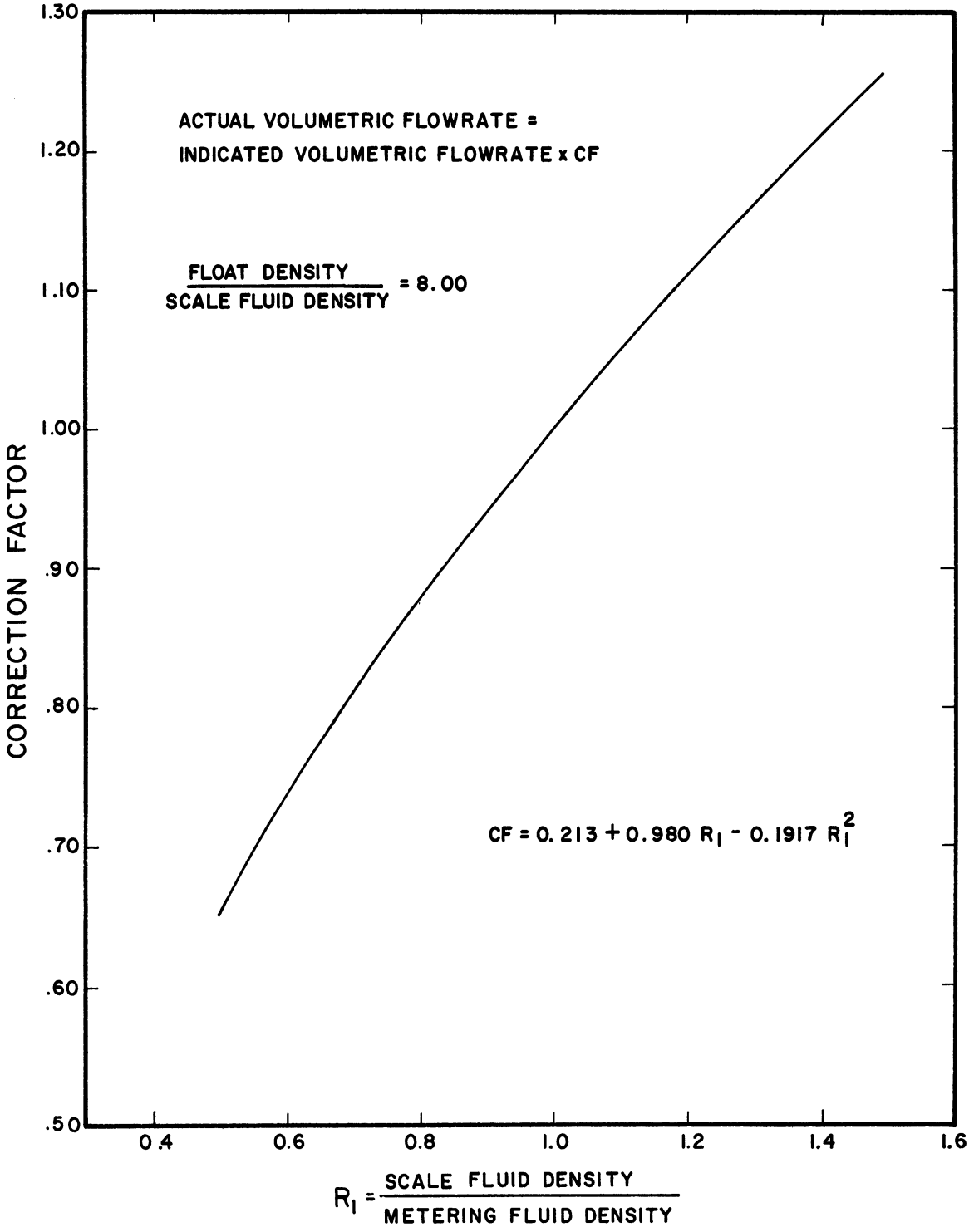

Figure A-1. Rotameter Correction Factor.

APPENDIX B

PHYSICAL PROPERTIES OF LIQUIDS

Some of the values of fluid properties extracted from the literature for use in this investigation were given in equation form. The following equations were used to compute the densities of saturated solutions of water and isobutanol at 75°F.[59]

$$\rho_I = 0.8055 + 0.00224\, p_w - 0.0000129\, p_w^2 \quad \text{(isobutanol phase)} \qquad \text{(B-1)}$$

$$\rho_w = 0.998 - 0.00169\, p_I + 0.000038\, p_I^2 \quad \text{(water phase)} \qquad \text{(B-2)}$$

where

ρ = density, gm/ml.

p_w = weight per cent water

p_I = weight per cent isobutanol

Seidell[68] gives the concentration of the saturated solutions as $p_w = 16.5$ and $p_I = 8.4$. Substitution in the above equations yields

$\rho_I = 0.832$ gm/ml

$\rho_w = 0.987$ gm/ml

These values were checked by means of precision hydrometers and found to be quite accurate.

Hassan, Nielsen, and Calhoun[34] present the following equation for the interfacial tension of water-isooctane at 1 atm:

$$\sigma = 49.5 - 0.07\,(t-25) \qquad \text{(B-3)}$$

where

σ = interfacial tension, dynes/cm.

t = temperature, °C

Viscosity as a function of temperature is presented in Figure B-1 for all liquids used in this investigation plus pure isobutanol and n-octane for comparison purposes. Data points represent measured values of viscosity. The viscosity curves for all liquids used here were fitted by a least squares technique to the equation

$$\log_{10}\mu = A + \frac{B}{T} \qquad (B\text{-}4)$$

where

μ = viscosity, cp

T = absolute temperature, °R

Values of A and B are given in Table I.

TABLE I

VALUES OF CONSTANTS FOR VISCOSITY CURVES

Liquid	A	B
Water	-3.043	1.608×10^3
Water saturated with isobutanol	-3.450	1.906×10^3
Isobutanol saturated with water	-3.512	2.142×10^3
Isooctane	-1.609	0.690×10^3

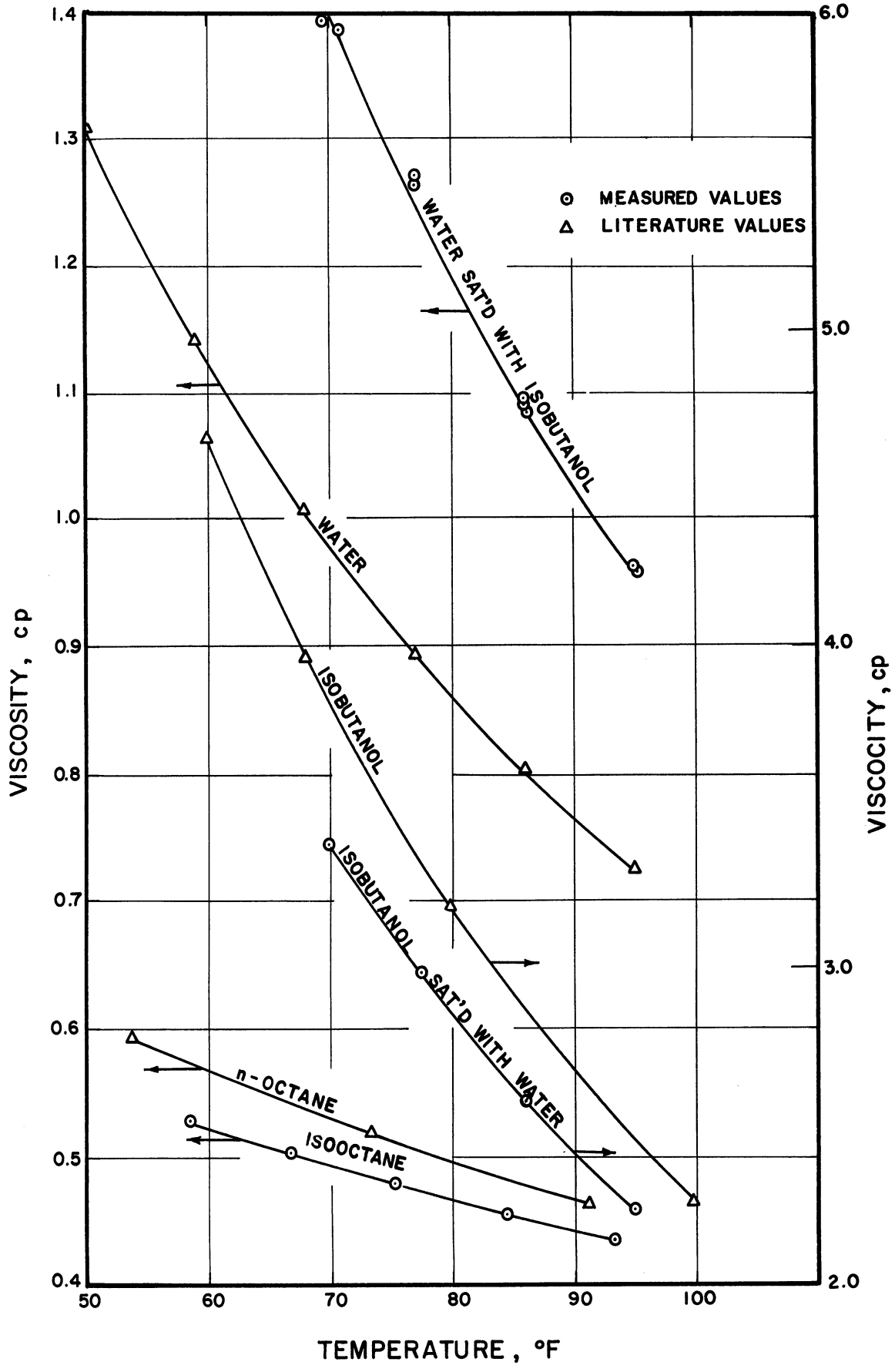

Figure B-1. Liquid Viscosity Data.

APPENDIX C

TABLES OF PROCESSED SINGLE-PHASE DATA

The following symbols are used in this Appendix:

A, B	= constants in liquid viscosity Equation (37)
CODE	= code number
D	= packing diameter, inches
DELFA	= average frictional pressure gradient in test section, psi/ft
DPDL(1)	= entrance total pressure gradient, psi/ft
DPDL(2)	= total pressure gradient in bottom section of column, psi/ft
DPDL(3)	= total pressure gradient in middle section of column, psi/ft
DPDL(4)	= total pressure gradient in top section of column, psi/ft
DPDLA	= average of DPDL(2), DPDL(3), and DPDL(4), psi/ft
E	= porosity
F	= dimensionless friction factor defined by Equation (39)
GPM	= liquid flowrate, gpm
NO	= number of runs in data set
REM	= modified Reymonds number, $\frac{D_p \rho U}{\mu(1-\epsilon)}$
RHO	= liquid specific gravity
T	= temperature, °F

(The number notation X.XXXE YY is equivalent to X.XXX$\cdot 10^{YY}$)

TABLE I

WATER FLOW THROUGH BED OF 0.501 INCH SPHERES

A= -.30430E 01 B= .16085E 04 RHO= .998 E= .400 D= .501 NO= 16

CODE	T	GPM	DPDL(1)	DPDL(2)	DPDL(3)	DPDL(4)	DPDLA	DELFA	REM	F
001WO	63.0	.651	.4398	.4351	.4351	.4351	.4351	.0027	101.47	317.35
002WO	63.0	1.522	.0000	.4438	.4438	.4438	.4438	.0114	237.27	569.98
003WO	64.0	2.354	.4462	.4533	.4538	.4543	.4538	.0214	371.83	701.40
004WO	66.5	3.165	.4559	.4681	.4686	.4683	.4683	.0359	517.05	905.48
005WO	68.5	3.926	.4618	.4844	.4853	.4867	.4855	.0530	658.71	1107.44
006WO	69.5	4.657	.4765	.5051	.5056	.5071	.5059	.0735	791.79	1310.56
007WO	71.0	5.409	.4839	.5248	.5256	.5283	.5262	.0938	937.85	1469.11
008WO	72.0	6.150	.4941	.5383	.5424	.5492	.5433	.1109	1080.44	1547.69
009WO	75.0	6.881	.5132	.5730	.5699	.5784	.5737	.1413	1257.02	1833.10
010WO	77.0	8.654	.5558	.6361	.6423	.6483	.6422	.2098	1622.17	2220.67
011WO	77.0	10.767	.6234	.7338	.7473	.7518	.7443	.3119	2018.33	2692.95
012WO	78.0	12.820	.6866	.8526	.8624	.8604	.8585	.4260	2434.22	3083.03
017WO	74.0	14.833	.0000	1.0235	1.0243	1.0212	1.0230	.5906	2674.92	3508.07
018WO	74.0	16.826	.0000	1.1713	1.1808	1.1599	1.1707	.7382	3034.34	3865.63
019WO	74.0	18.850	.0000	1.3418	1.3418	1.3259	1.3365	.9040	3399.19	4225.83
020WO	74.0	20.813	.0000	1.5237	1.5277	1.5055	1.5190	1.0865	3753.20	4599.74

TABLE II

ISOBUTANOL FLOW THROUGH BED OF 0.501 INCH SPHERES

A= -.35123E 01 B= .21422E 04 RHO= .832 E= .400 D= .501 NO= 7

CODE	T	GPM	DPDL(1)	DPDL(2)	DPDL(3)	DPDL(4)	DPDLA	DELFA	REM	F
046IO	73.0	4.341	.0000	.4459	.4458	.4459	.4458	.0853	189.19	502.15
051IO	74.0	4.341	.0000	.4446	.4446	.4446	.4446	.0841	192.49	503.51
045IO	76.0	5.788	.0000	.4832	.4847	.4858	.4846	.1241	265.66	576.62
050IO	74.0	5.788	.0000	.4807	.4813	.4821	.4813	.1208	256.66	542.67
047IO	73.0	7.235	.0000	.5661	.5692	.5675	.5676	.2071	315.31	731.22
048IO	73.0	9.794	.0000	.6577	.6633	.6646	.6619	.3014	426.88	786.00
049IO	73.0	12.633	.0000	.8148	.8179	.8230	.8186	.4581	550.58	926.23

TABLE III

WATER FLOW THROUGH BED OF 0.340 INCH SPHERES

A= -.34499E 01 B= .19057E 04 RHO= .987 E= .383 D= .340 NO= 13

CODE	T	GPM	DPDL(1)	DPDL(2)	DPDL(3)	DPDL(4)	DPDLA	DELFA	REM	F
088WO	78.0	.655	.0000	.4357	.4357	.4357	.4357	.0080	58.08	310.61
089WO	78.0	1.543	.0000	.4555	.4549	.4552	.4552	.0275	136.72	452.70
090WO	80.0	2.369	.4599	.4803	.4799	.4800	.4801	.0524	216.43	578.18
091WO	80.0	3.186	.4813	.5147	.5151	.5151	.5150	.0873	291.03	716.50
092WO	81.0	3.952	.5037	.5503	.5500	.5510	.5504	.1227	366.49	824.19
093WO	81.0	4.688	.5269	.5902	.5891	.5909	.5901	.1624	434.74	919.48
094WO	82.0	5.444	.5529	.6391	.6363	.6384	.6379	.2103	512.47	1040.51
095WO	82.0	6.190	.5758	.6905	.6892	.6915	.6904	.2627	582.70	1143.33
096WO	83.0	6.926	.6125	.7473	.7458	.7497	.7476	.3199	661.77	1263.07
097WO	83.0	8.701	.6969	.9079	.8979	.9006	.9021	.4744	831.30	1491.14
098WO	80.0	10.848	.8346	1.1922	1.1744	1.1945	1.1870	.7594	990.98	1830.16
099WO	79.0	12.905	1.0111	1.4516	1.4263	1.4561	1.4447	1.0170	1161.22	2029.62
100WO	80.0	14.942	1.1938	1.7474	1.7078	1.7428	1.7327	1.3050	1364.89	2283.52

TABLE IV

ISOBUTANOL FLOW THROUGH BED OF 0.340 INCH SPHERES

A= -.35123E 01 B= .21422E 04 RHO= .832 E= .383 D= .340 NO= 13

CODE	T	GPM	DPDL(1)	DPDL(2)	DPDL(3)	DPDL(4)	DPDLA	DELFA	REM	F
101IO	72.0	3.617	.0000	.5062	.5046	.5073	.5060	.1455	102.25	386.12
102IO	73.0	2.894	.0000	.4690	.4664	.4679	.4678	.1073	83.24	361.99
103IO	73.0	2.170	.0000	.4323	.4322	.4323	.4323	.0717	62.43	322.84
104IO	74.0	.723	.0000	.3836	.3837	.0000	.3836	.0231	21.17	317.77
105IO	76.0	1.447	.0000	.4056	.4057	.0000	.4057	.0451	43.83	325.94
106IO	73.5	4.341	.4649	.5544	.5520	.5541	.5535	.1930	125.94	438.04
107IO	74.0	5.053	.4918	.6088	.6049	.6102	.6080	.2475	147.88	486.66
108IO	74.0	5.788	.0000	.6722	.6633	.6736	.6697	.3092	169.38	530.84
109IO	74.0	6.500	.5663	.7390	.7265	.7445	.7367	.3762	190.23	575.07
110IO	75.0	7.390	.6080	.8171	.8017	.8175	.8121	.4516	220.05	617.78
111IO	78.0	9.794	.7639	1.1376	1.1199	1.1558	1.1378	.7773	307.02	844.62
112IO	79.0	12.187	.9255	1.3970	1.3696	1.4175	1.3947	1.0342	388.59	918.63
113IO	79.0	14.436	1.1238	1.6973	1.6533	1.7019	1.6842	1.3237	460.27	992.67

TABLE V

WATER FLOW THROUGH BED OF 0.164 INCH SPHERES

A= -.34499E 01 B= .19057E 04 RHO= .987 E= .337 D= .164 NO= 11

CODE	T	GPM	DPDL(1)	DPDL(2)	DPDL(3)	DPDL(4)	DPDLA	DELFA	REM	F
196WO	73.0	.655	.0000	.4690	.4675	.4717	.4694	.0418	24.15	205.51
197WO	77.0	1.543	.4918	.5461	.5431	.5558	.5483	.1207	69.45	268.28
198WO	78.0	2.369	.5454	.6439	.6356	.6636	.6477	.2200	94.26	323.40
199WO	81.0	3.186	.6086	.7624	.7465	.7879	.7656	.3379	132.62	386.42
200WO	81.0	3.952	.6811	.8960	.8852	.9222	.9012	.4735	164.51	436.48
201WO	84.0	4.688	.7630	1.0579	1.0405	1.0761	1.0582	.6305	204.07	512.40
202WO	85.0	5.444	.8435	1.2127	1.1880	1.2286	1.2098	.7821	240.52	555.46
203WO	85.0	6.190	.9300	1.3606	1.3355	1.3833	1.3598	.9321	273.48	582.24
204WO	85.0	6.926	1.0358	1.5426	1.5058	1.5745	1.5409	1.1133	306.00	621.49
205WO	86.0	8.701	1.3011	2.0204	1.9620	2.0546	2.0123	1.5847	390.10	714.69
206WO	86.0	10.848	1.7424	2.7030	2.6293	2.7372	2.6898	2.2622	486.39	818.28

TABLE VI

ISOBUTANOL FLOW THROUGH BED OF 0.164 INCH SPHERES

A= -.35123E 01 B= .21422E 04 RHO= .832 E= .337 D= .164 NO= 11

CODE	T	GPM	DPDL(1)	DPDL(2)	DPDL(3)	DPDL(4)	DPDLA	DELFA	REM	F
207IO	83.0	.723	.0000	.4855	.4799	.4869	.4841	.1236	11.08	271.58
208IO	75.0	1.447	.4783	.5992	.5939	.6040	.5990	.2385	19.34	228.78
209IO	75.0	2.170	.5633	.7431	.7396	.7569	.7465	.3860	29.01	246.83
210IO	76.0	2.894	.6334	.8933	.8859	.9243	.9012	.5407	39.35	263.77
211IO	76.0	3.617	.7243	1.0716	1.0632	1.1103	1.0817	.7212	49.19	281.48
212IO	76.0	4.341	.8093	1.2354	1.2107	1.2923	1.2461	.8856	59.02	288.06
213IO	76.0	5.053	.9046	1.4288	1.4036	1.4971	1.4432	1.0827	68.71	302.50
214IO	76.0	5.788	1.0179	1.6382	1.5966	1.7132	1.6493	1.2888	78.70	314.40
215IO	77.0	6.500	1.1551	1.8498	1.8031	1.9476	1.8668	1.5063	89.91	332.84
216IO	77.0	7.390	1.3190	2.1228	2.0550	2.2252	2.1344	1.7738	102.23	344.73
217IO	77.0	8.570	1.5996	2.5620	2.4817	2.6985	2.5807	2.2202	118.55	372.08

TABLE VII

WATER FLOW THROUGH BED OF 0.164 INCH SPHERES

A= -.30430E 01 B= .16085E 04 RHO= .998 E= .337 D= .164 NO= 12

CODE	T	GPM	DPDL(1)	DPDL(2)	DPDL(3)	DPDL(4)	DPDLA	DELFA	REM	F
286WO	71.0	.651	.0000	.4704	.4704	.4732	.4713	.0389	33.44	265.60
287WO	71.0	1.532	.0000	.5322	.5347	.5438	.5369	.1045	78.72	303.08
288WO	70.0	2.354	.5191	.6225	.6261	.6524	.6337	.2012	119.33	375.17
289WO	70.0	3.165	.5676	.7189	.7250	.7739	.7393	.3068	160.46	425.40
290WO	70.0	3.926	.6249	.8397	.8441	.9171	.8670	.4346	199.05	485.71
291WO	70.0	4.657	.6866	.9553	.9653	1.0917	1.0041	.5717	236.11	538.66
292WO	70.0	5.409	.7262	1.0917	1.1014	1.2281	1.1404	.7080	274.20	574.42
293WO	70.0	6.150	.7894	1.3191	1.3282	1.4555	1.3676	.9351	311.77	667.28
294WO	69.0	6.881	.8541	1.4827	1.4756	1.6146	1.5243	1.0919	344.26	687.20
295WO	70.0	8.654	1.0920	1.9442	1.9178	2.0124	1.9581	1.5257	438.71	773.69
296WO	70.0	10.767	1.4656	2.5921	2.5414	2.7058	2.6131	2.1807	545.85	888.77
297WO	70.0	9.715	1.3180	2.2966	2.2466	2.3421	2.2951	1.8627	492.54	841.33

TABLE VIII

ISOÖCTANE FLOW THROUGH BED OF 0.164 INCH SPHERES

A= -.16086E 01 B= .68994E 03 RHO= .692 E= .337 D= .164 NO= 8

CODE	T	GPM	DPDL(1)	DPDL(2)	DPDL(3)	DPDL(4)	DPDLA	DELFA	REM	F
29800	66.0	3.193	.0000	.5180	.5029	.5139	.5116	.2117	218.21	565.78
29900	67.0	3.991	.0000	.5899	.5828	.6035	.5921	.2922	274.32	628.27
30000	67.0	4.789	.0000	.7488	.7439	.7596	.7508	.4509	329.19	807.93
30100	68.0	5.575	.0000	.8438	.8401	.8696	.8512	.5513	385.40	853.40
30200	68.0	6.386	.0000	1.0008	.9994	1.0690	1.0230	.7232	441.43	977.37
30300	69.0	7.171	.0000	1.4782	1.3849	1.4782	1.4471	1.1472	498.59	1388.41
30400	64.0	9.455	.0000	2.1147	1.9972	2.0920	2.0680	1.7681	638.82	1577.07
30500	65.0	10.806	.0000	2.5921	2.5641	2.7513	2.6358	2.3360	734.31	1833.70

TABLE IX

WATER FLOW THROUGH BED OF 0.340 INCH SPHERES

A= -.30430E 01 B= .16085E 04 RHO= .998 E= .384 D= .340 NO= 14

CODE	T	GPM	DPDL(1)	DPDL(2)	DPDL(3)	DPDL(4)	DPDLA	DELFA	REM	F
351WO	64.0	1.532	.0000	.4596	.4595	.4596	.4596	.0271	160.02	528.28
352WO	63.5	2.354	.0000	.4800	.4798	.4806	.4801	.0477	244.13	600.71
353WO	63.0	3.165	.0000	.5098	.5083	.5139	.5107	.0782	326.06	727.63
354WO	62.5	3.926	.4941	.5478	.5448	.5506	.5477	.1153	401.75	858.73
355WO	63.0	4.657	.5294	.5859	.5834	.5872	.5855	.1531	479.81	967.50
356WO	62.5	5.409	.5529	.6293	.6234	.6279	.6269	.1944	553.43	1051.18
357WO	68.0	6.150	.5823	.6537	.6505	.6469	.6504	.2180	677.50	1115.68
358WO	68.0	6.881	.6087	.7013	.6938	.6985	.6979	.2654	758.05	1214.36
359WO	69.5	8.644	.6734	.8329	.8238	.8289	.8285	.3961	971.36	1471.60
360WO	71.0	10.777	.7615	1.0644	1.0402	1.0349	1.0465	.6141	1235.27	1866.22
361WO	72.0	12.820	.9025	1.2622	1.2375	1.2281	1.2426	.8102	1488.86	2097.10
362WO	73.0	14.823	1.0494	1.5237	1.5096	1.5009	1.5114	1.0790	1744.13	2447.20
363WO	73.5	16.826	1.2110	1.8192	1.7817	1.7737	1.7915	1.3591	1992.75	2733.39
364WO	74.0	18.850	1.4108	2.1261	2.0652	2.0693	2.0869	1.6544	2246.92	2989.53

TABLE X

ISOÖCTANE FLOW THROUGH BED OF 0.340 INCH SPHERES

A= -.16086E 01 B= .68994E 03 RHO= .692 E= .384 D= .340 NO= 7

CODE	T	GPM	DPDL(1)	DPDL(2)	DPDL(3)	DPDL(4)	DPDLA	DELFA	REM	F
36500	77.0	7.171	.0000	.5916	.5912	.5916	.5914	.2916	1163.43	2718.39
36600	77.0	6.386	.0000	.5451	.5448	.5451	.5450	.2452	1035.93	2567.04
36700	77.0	8.154	.0000	.6632	.6654	.6816	.6701	.3702	1322.81	3035.51
36800	77.5	10.806	.0000	.8452	.8455	.8587	.8498	.5500	1757.95	3411.83
36900	78.0	13.446	.0000	1.0462	1.0447	1.0462	1.0457	.7459	2193.47	3729.03
37000	78.0	15.927	.0000	1.3191	1.3168	1.3191	1.3183	1.0185	2598.11	4298.76
37100	78.0	18.420	.0000	1.5532	1.5504	1.5532	1.5523	1.2524	3004.75	4570.86

APPENDIX D

TABLES OF PROCESSED TWO-PHASE DATA

The following symbols are used in this Appendix:

CODE	= code number
DPDL(1)	= entrance total pressure gradient, psi/ft
DPDL(2)	= total pressure gradient in bottom section of column, psi/ft
DPDL(3)	= total pressure gradient in middle section of column, psi/ft
DPDL(4)	= total pressure gradient in top section of column, psi/ft
DPDLA	= average of DPDL(2), DPDL(3), and DPDL(4), psi/ft
GPM	= liquid flowrate, gpm
INT TENS	= interfacial tension, dynes/cm
LOG VIS	= logarithm to base 10 of viscosity; viscosity in cp
PACK DIA	= packing diameter, inches
RHO	= liquid specific gravity
RI	= organic phase holdup
RUNS	= number of runs in data set
T	= temperature, °F
VOIDAGE	= porosity

(The number notation X.XXXE YY is equivalent to $X.XXX \cdot 10^{YY}$)

TABLE I

ISOBUTANOL-WATER FLOW THROUGH BED OF 0.501 INCH SPHERES

SUBSCRIPT (W) = WATER PHASE
SUBSCRIPT (O) = ORGANIC PHASE

LOG VIS(W) = -.34499E 01 + .19057E 04/T RHO(W) = .987
LOG VIS(O) = -.35123E 01 + .21422E 04/T RHO(O) = .832

VOIDAGE = .400 PACK DIA = .501 INT TENS = 2.100 RUNS = 51

CODE	T	GPM(W)	GPM(O)	DPDL(1)	DPDL(2)	DPDL(3)	DPDL(4)	DPDLA	RI
021IB	74.0	.655	.723	.0000	.4316	.4316	.4316	.4316	.0000
022IB	76.0	.655	1.447	.0000	.4329	.4329	.4329	.4329	.0000
023IB	75.0	.655	2.170	.0000	.4334	.4334	.4334	.4334	.7179
024IB	79.0	1.543	1.447	.0000	.4401	.4414	.0000	.4407	.3917
025IB	77.5	1.543	2.894	.0000	.4662	.4696	.4697	.4685	.6116
026IB	77.5	1.543	4.341	.0000	.5089	.5170	.5213	.5158	.7234
027IB	70.0	1.543	5.788	.0000	.5820	.5816	.5847	.5827	.7673
028IH	72.5	1.543	9.794	.7273	.7349	.7341	.7355	.7348	.8906
029IH	74.0	1.543	12.187	.7079	.8313	.8976	.8809	.8699	.8001
030IH	75.0	3.186	1.447	.0000	.4910	.4874	.4869	.4885	.2355
031IB	74.5	3.186	2.894	.4709	.5241	.5266	.5275	.5261	.4383
032IB	76.0	3.186	4.341	.4933	.5723	.5816	.5820	.5786	.5589
033IB	76.0	3.186	5.788	.5260	.6577	.6654	.6701	.6644	.6357
034IS	77.0	3.186	9.794	.7466	.9015	.9168	.8974	.9053	.7070
035IH	77.0	3.186	12.633	.0000	1.0693	1.0859	1.0420	1.0657	.7344
036IB	66.0	4.688	1.447	.4843	.5392	.5390	.5379	.5387	.1752
037IB	69.0	4.688	2.894	.5007	.5778	.5843	.5875	.5832	.3342
038IH	70.0	4.688	4.341	.5499	.6439	.6407	.6453	.6433	.4630
039IH	74.0	4.688	5.788	.5976	.7321	.7416	.7473	.7403	.5370
040IH	75.0	4.688	7.034	.6483	.8382	.8578	.8526	.8495	.6138
041IH	75.0	4.688	9.794	.6840	1.0147	.9497	.9920	.9855	.6823
042IB	74.0	4.688	2.894	.0000	.5654	.5678	.5682	.5671	.3506
043IB	75.0	4.688	2.894	.0000	.5682	.5774	.5840	.5765	.3451
044IB	75.0	3.186	1.447	.0000	.4835	.4840	.4855	.4843	.2519
052IU	79.0	4.688	4.341	.5424	.6288	.6324	.6346	.6319	.4657
053IU	79.0	4.688	4.341	.5439	.6267	.6331	.6371	.6323	.4548
054IU	80.0	4.688	4.341	.5320	.6288	.6365	.6371	.6341	.4685
055IB	78.0	1.543	.723	.0000	.4391	.4391	.4391	.4391	.2410
056IB	78.0	1.543	.723	.0000	.4391	.4391	.4391	.4391	.2300
057IB	78.0	3.186	.723	.0000	.4717	.4716	.4724	.4719	.1423
058IB	75.0	3.186	1.447	.0000	.4902	.4910	.4917	.4910	.2574
059IB	75.0	4.688	4.341	.5529	.6384	.6401	.6409	.6398	.4712
060IB	76.0	6.190	1.447	.5216	.5533	.5534	.5527	.5531	.1642
061IB	77.5	6.190	.723	.5231	.5406	.5417	.5427	.5417	.0875
062IB	79.0	6.190	2.894	.5663	.6446	.6505	.6522	.6491	.2903
063IB	81.0	6.190	4.341	.6050	.7163	.7272	.7293	.7243	.3945
064IB	80.5	6.190	6.500	.6372	.8816	.8949	.8947	.8904	.5069
065IB	81.0	6.190	8.570	.6855	.9078	.9497	.9920	.9498	.5699
066IH	86.0	10.848	.723	.6527	.8189	.8234	.8210	.8211	.0000
067IH	87.0	10.848	1.447	.6647	.8650	.8701	.8664	.8672	.0930
068IH	88.0	10.848	2.894	.6647	.9373	.9338	.9191	.9301	.2026
069IH	89.5	10.848	4.341	.7481	1.0193	1.0178	1.0079	1.0150	.2656
070IH	90.0	10.848	6.500	.8212	1.2240	1.2221	1.1945	1.2135	.3616
071IS	87.0	15.930	1.447	.8838	1.2013	1.2039	1.1740	1.1931	.0930
072IH	80.5	15.930	2.894	.9702	1.3606	1.3696	1.3719	1.3674	.1478
073IH	84.0	15.930	4.341	1.0418	1.5016	1.5126	1.4971	1.5038	.2190
074IH	85.0	15.930	5.788	.0000	1.6109	1.6079	1.5949	1.6046	.2602
075IS	86.5	1.543	5.788	.0000	.5813	.5823	.5836	.5824	.7974
076IB	87.5	6.190	1.447	.6050	.5957	.5946	.5950	.5951	.1642
077IH	89.0	6.190	6.500	.6542	.8781	.8880	.8960	.8874	.5151
078IB	91.0	1.543	1.447	.0000	.4414	.4411	.4408	.4411	.4082

TABLE II

ISOBUTANOL-WATER FLOW THROUGH BED OF 0.340 INCH SPHERES

$SUBSCRIPT (W) = WATER PHASE
$SUBSCRIPT (O) = ORGANIC PHASE

LOG VIS(W) = -.34499E 01 + .19057E 04/T RHO(W) = .987
LOG VIS(O) = -.35123E 01 + .21422E 04/T RHO(O) = .832

VOIDAGE = .383 PACK DIA = .340 INT TENS = 2.100 RUNS = 50

CODE	T	GPM(W)	GPM(O)	DPDL(1)	DPDL(2)	DPDL(3)	DPDL(4)	DPDLA	RI
1141B	74.0	.655	.723	.0000	.4387	.4387	.4387	.4387	.4029
1151B	75.0	.655	1.447	.0000	.4629	.4624	.4628	.4627	.6190
1161B	74.0	.655	2.894	.4775	.5592	.5592	.5627	.5604	.8104
1171S	74.5	.655	4.341	.5260	.6379	.6273	.6329	.6327	.0000
1181H	76.0	.655	6.500	.6393	.8258	.8124	.8227	.8203	.0000
1191B	80.0	1.543	.723	.0000	.4767	.4762	.4759	.4763	.2389
1201B	79.5	1.543	1.447	.4664	.5007	.4991	.4994	.4997	.4111
1211H	79.0	4.688	4.341	.7094	.9624	.9452	.9328	.9468	.4658
1221B	80.0	1.543	2.894	.4977	.5771	.5757	.5758	.5762	.6299
1231B	80.0	1.543	4.341	.5404	.6887	.6853	.6866	.6869	.7119
1241S	73.5	1.543	6.500	.6885	.9277	.9141	.9401	.9273	.7229
1271B	78.5	3.186	.723	.4918	.5478	.5461	.5486	.5475	.1514
1281B	80.0	3.186	1.447	.5088	.5781	.5755	.5775	.5771	.2635
1291B	80.0	3.186	2.894	.5559	.6715	.6640	.6680	.6678	.4494
1301H	81.0	3.186	4.341	.6214	.8003	.7973	.8017	.7998	.5725
1311H	82.5	4.688	4.341	.6900	.9396	.9202	.9055	.9218	.4604
1341B	75.5	4.688	.723	.5445	.6402	.6363	.6397	.6387	.0994
1351B	77.0	4.688	1.447	.5445	.6853	.6812	.6849	.6838	.1978
1361H	78.5	4.688	2.894	.5931	.7913	.7877	.7930	.7907	.3564
1371H	76.0	4.688	4.341	.6870	.9578	.9406	.9328	.9437	.4713
1401B	79.0	6.190	.723	.6125	.7565	.7520	.7569	.7551	.0830
1411B	80.0	6.190	1.447	.6405	.8072	.8028	.8072	.8057	.1541
1421B	81.5	6.190	2.894	.7124	.9374	.9336	.9415	.9375	.2990
1461B	79.0	8.701	.723	.7347	1.0215	1.0019	1.0193	1.0142	.0447
1471B	80.0	8.701	1.447	.7735	1.0875	1.0632	1.0830	1.0779	.1213
1481B	81.0	8.701	2.894	.8659	1.2331	1.2084	1.2331	1.2249	.2416
1491H	73.0	8.701	4.341	.9687	1.4448	1.4263	1.4630	1.4447	.3291
1501H	74.5	8.701	6.500	1.1446	1.8065	1.7827	1.8384	1.8092	.4248
1511H	75.0	4.688	4.341	.6930	.9965	.9837	1.0079	.9960	.4686
1521H	77.0	12.905	.723	1.0343	1.5312	1.4944	1.5267	1.5174	.0447
1531H	77.5	12.905	1.447	1.0782	1.6268	1.6011	1.6336	1.6205	.0857
1541H	78.0	12.905	2.894	1.2147	1.8202	1.7736	1.8202	1.8047	.1732
1551B	79.0	.655	1.447	.0000	.4628	.4626	.4624	.4626	.6381
1561H	79.0	1.543	9.794	.8593	1.3037	1.2902	1.3151	1.3030	.8049
1571B	80.5	3.186	.723	.0000	.5550	.5506	.5530	.5529	.1404
1581B	79.5	4.688	6.500	.8122	1.2696	1.2675	1.2923	1.2764	.6025
1591S	80.0	6.190	6.500	.9210	1.4288	1.4195	1.4516	1.4333	.5205
1601B	80.5	8.701	1.447	.7630	1.0875	1.0632	1.0830	1.0779	.1158
1611S	81.0	6.190	9.794	1.2296	1.9977	1.9938	2.0318	2.0077	.6381
1621H	81.0	6.190	4.341	.7678	1.1171	1.1086	1.1194	1.1150	.4057
1631S	81.0	4.688	9.794	1.0984	1.8043	1.7895	1.8247	1.8062	.7037
1641S	74.0	3.186	6.500	.7502	1.1694	1.1812	1.1831	1.1779	.6983
1651S	74.0	3.186	9.794	.0000	1.6222	1.5625	1.5881	1.5910	.7283
1661B	75.0	4.688	1.447	.5642	.6949	.6901	.6922	.6924	.1978
1671H	76.0	1.543	12.187	1.0940	1.6518	1.6306	1.6655	1.6493	.8705
1681H	77.5	1.543	9.794	.9017	1.3219	1.3083	1.3264	1.3189	.7776
1691B	79.0	6.190	6.500	.9389	1.4357	1.4263	1.4539	1.4386	.5123
1701B	79.0	4.688	6.500	.8242	1.2673	1.2675	1.2923	1.2757	.5943
1711U	80.0	3.186	2.894	.5514	.6818	.6784	.6818	.6807	.4521
1721B	81.5	4.688	4.341	.6855	.9738	.9701	.9806	.9748	.4713

TABLE III

ISOBUTANOL-WATER FLOW THROUGH BED OF 0.164 INCH SPHERES

SUBSCRIPT (W) = WATER PHASE
SUBSCRIPT (O) = ORGANIC PHASE

LOG VIS(W) = -.34499E 01 + .19057E 04/T RHO(W) = .987
LOG VIS(O) = -.35123E 01 + .21422E 04/T RHO(O) = .832

VOIDAGE = .337 PACK DIA = .164 INT TENS = 2.100 RUNS = 63

CODE	T	GPM(W)	GPM(O)	DPDL(1)	DPDL(2)	DPDL(3)	DPDL(4)	DPDLA	RI
218IB	79.0	.655	.723	.5067	.5946	.5891	.6067	.5968	.4200
219IB	80.0	.655	1.447	.5886	.7789	.7781	.8189	.7920	.6452
220IB	80.0	.655	2.894	.7869	1.2923	1.2902	1.4061	1.3295	.8188
221IS	79.0	.655	4.341	.9464	1.7588	1.8349	2.0773	1.8903	.8297
222IH	76.0	.655	6.500	1.2803	2.1114	2.1299	2.4300	2.2238	.8623
223IH	80.0	.655	7.390	1.4913	2.4527	2.4023	2.6803	2.5118	.9165
224IB	82.0	1.543	.723	.5499	.6784	.6695	.6931	.6803	.2544
225IB	82.0	1.543	1.447	.6214	.8340	.8193	.8588	.8374	.3657
226IB	82.0	1.543	2.894	.8122	1.2696	1.2448	1.3378	1.2840	.6180
227IB	83.0	1.543	4.341	1.0090	1.7815	1.7554	1.8611	1.7994	.7130
228IS	70.0	1.543	5.788	1.4617	2.7258	2.7428	2.8168	2.7618	.7266
229IS	76.0	1.543	5.053	.0000	2.3390	2.3342	2.5210	2.3981	.7700
230IB	75.0	3.186	.723	.6796	.9510	.9383	.9851	.9582	.0000
231IB	75.0	3.186	1.447	.7601	1.0989	1.0791	1.1444	1.1075	.0000
232IH	76.0	3.186	2.894	.9419	1.4925	1.4763	1.5881	1.5190	.4010
233IH	77.0	3.186	4.341	1.2236	2.0614	2.0278	2.1683	2.0858	.5583
234IS	78.0	3.186	5.788	1.5848	2.7940	2.7428	2.9647	2.8338	.6615
235IH	79.0	4.688	.723	.8480	1.2354	1.1994	1.2696	1.2348	.0000
236IH	75.0	4.688	1.447	.9184	1.4061	1.3809	1.4516	1.4129	.0000
237IH	76.0	4.688	2.170	1.0299	1.5995	1.5512	1.6564	1.6023	.2002
238IH	76.0	4.688	2.894	1.1610	1.8338	1.7781	1.9180	1.8433	.2761
239IH	77.0	4.688	4.341	1.4427	2.3959	2.3569	2.5438	2.4322	.4281
240IB	79.0	2.369	.723	.0000	.7941	.7767	.8099	.7936	.0000
241IB	80.0	2.369	1.447	.6870	.9510	.9383	.9851	.9582	.2436
242IB	80.0	2.369	2.170	.7705	1.1103	1.0972	1.1444	1.1173	.3793
243IH	81.0	2.369	2.894	.8629	1.3151	1.3015	1.3606	1.3257	.4986
244IH	81.0	2.369	4.341	1.0880	1.8611	1.8235	1.9408	1.8752	.6343
245IS	82.0	2.369	5.788	1.4371	2.5665	2.5271	2.7030	2.5989	.7320
246IB	74.0	.655	.723	.5096	.6026	.5926	.5999	.5983	.3955
247IB	75.0	2.369	.723	.0000	.7982	.7836	.8106	.7975	.0000
248IH	75.0	4.688	.723	.0000	1.2422	1.2153	1.2696	1.2424	.0000
249IS	75.0	3.186	5.788	1.6095	2.7713	2.7655	2.9419	2.8262	.6723
250IS	75.0	1.543	5.053	.0000	2.3162	2.2888	2.4186	2.3412	.7863
256IU	75.0	.655	2.894	.0000	1.2923	1.2902	1.3833	1.3219	.0000
257IU	75.0	1.543	2.894	.0000	1.2923	1.2902	1.3378	1.3068	.0000
258IU	76.0	1.543	4.341	.0000	1.9294	1.9143	2.0204	1.9547	.0000
259IU	77.0	.655	4.341	.0000	1.6677	1.7781	1.9408	1.7956	.0000
260IH	71.0	2.369	5.053	.0000	2.4414	2.4023	2.5665	2.4771	.0000
261IS	71.0	2.369	5.788	.0000	2.7258	2.6747	2.9078	2.7694	.0000
262IS	72.0	1.543	4.686	.0000	2.1114	2.0845	2.2138	2.1366	.0000
263IS	75.0	1.543	5.788	.0000	2.7258	2.6974	2.8851	2.7694	.0000
264IB	77.0	.655	2.170	.0000	1.0761	1.0745	1.1103	1.0870	.0000
265IB	77.0	.655	3.617	.0000	1.7019	1.6646	1.7929	1.7198	.0000
266IS	77.0	.655	5.053	.0000	1.7701	1.7668	1.8953	1.8107	.0000
267IS	78.0	.655	5.788	.0000	1.7929	1.7441	1.8611	1.7994	.0000
268IB	78.0	1.109	.723	.0000	.6343	.6310	.6605	.6419	.0000
269IB	82.0	1.109	1.447	.0000	.8134	.8069	.8258	.8154	.0000
270IB	82.0	1.109	2.170	.0000	1.0306	1.0178	1.0648	1.0377	.0000
271IB	82.0	1.109	2.894	.0000	1.2923	1.2788	1.3424	1.3045	.0000
272IB	82.0	1.109	3.617	.0000	1.5767	1.5625	1.6564	1.5985	.0000
273IS	83.0	1.109	4.341	.0000	1.8725	1.8916	2.0204	1.9282	.0000
274IS	83.0	1.109	5.053	.0000	2.1228	2.1640	2.2821	2.1896	.0000
275IS	84.0	1.109	5.788	.0000	2.2252	2.3002	2.5096	2.3450	.0000
276IS	84.0	1.109	6.500	.0000	2.3162	2.4136	2.6575	2.4625	.0000
277IB	85.0	1.966	.723	.0000	.7417	.7300	.7562	.7426	.0000
278IB	85.0	1.966	1.447	.0000	.8878	.8660	.9029	.8856	.0000
279IB	85.5	1.966	2.170	.0000	1.0534	1.0291	1.0716	1.0514	.0000
280IB	86.0	1.966	2.894	.0000	1.2696	1.2448	1.3378	1.2840	.0000
281IB	86.0	1.966	3.617	.0000	1.5540	1.5171	1.6109	1.5607	.0000
282IS	86.0	1.966	4.341	.0000	1.8611	1.8349	1.9749	1.8903	.0000
283IS	86.0	1.966	5.053	.0000	2.2366	2.2094	2.3845	2.2768	.0000
284IS	87.0	1.966	5.788	.0000	2.6120	2.5839	2.8054	2.6671	.0000
285IS	87.0	1.966	6.500	.0000	2.8396	2.8449	3.0898	2.9248	.0000

ISOOCTANE-WATER FLOW THROUGH BED OF 0.164 INCH SPHERES

SUBSCRIPT (W) = WATER PHASE
SUBSCRIPT (O) = ORGANIC PHASE

LOG VIS(W) = -.30430E 01 + .16085E 04/T RHO(W) = .998
LOG VIS(O) = -.16086E 01 + .68994E 03/T RHO(O) = .692

VOIDAGE = .337 PACK DIA = .164 INT TENS = 49.500 RUNS = 45

CODE	T	GPM(W)	GPM(O)	DPDL(1)	DPDL(2)	DPDL(3)	DPDL(4)	DPDLA	RI
3060B	54.0	.651	.798	.7321	1.1144	1.0787	1.1144	1.1025	.0000
3070B	56.0	.651	1.596	.8350	1.4100	1.3395	1.4100	1.3865	.0000
3080B	56.0	.651	2.395	.9701	1.8419	1.7704	1.8419	1.8181	.0000
3090B	58.0	.651	3.193	1.0788	2.2057	2.1786	2.2284	2.2042	.0000
3100B	60.0	1.532	.798	.7380	1.1144	1.0334	1.0690	1.0723	.0000
3110B	61.0	1.532	1.596	.8497	1.3418	1.2488	1.3191	1.3032	.0000
3120B	62.0	1.532	2.395	.9642	1.6146	1.5209	1.5691	1.5682	.0000
3130B	62.0	1.532	3.193	1.1082	1.9329	1.7931	1.8874	1.8711	.0000
3140B	63.0	1.532	3.991	1.2434	2.2966	2.2012	2.2511	2.2497	.0000
3150B	73.0	1.532	3.991	.0000	2.2511	2.1332	2.2284	2.2043	.0000
3160B	75.0	1.532	4.789	.0000	2.6149	2.4507	2.5239	2.5298	.0000
3170B	76.0	2.354	.798	.7468	1.1372	1.0561	1.0803	1.0912	.0000
3180B	77.0	2.354	1.596	.8497	1.3191	1.2261	1.2509	1.2653	.0000
3190B	78.0	2.354	2.395	.9701	1.5464	1.4075	1.4555	1.4698	.0000
3200B	79.0	2.354	3.193	1.1023	1.8647	1.7024	1.7510	1.7727	.0000
3210B	79.0	2.354	3.991	1.2434	2.1375	2.0198	2.0693	2.0755	.0000
3220B	80.0	2.354	4.789	.0000	2.4785	2.3373	2.3875	2.4011	.0000
3230B	81.0	3.165	.798	.7703	1.1599	1.1127	1.1372	1.1366	.0000
3240B	81.0	3.165	1.596	.8673	1.3418	1.2715	1.2963	1.3032	.0000
3250B	69.0	3.165	2.395	.9966	1.6601	1.5436	1.5919	1.5985	.0000
3260B	73.0	3.165	3.193	1.1347	1.8874	1.7931	1.8647	1.8484	.0000
3270B	74.0	3.165	3.991	1.2698	2.1602	2.0879	2.1375	2.1285	.0000
3280B	75.0	3.165	4.789	.0000	2.4557	2.3827	2.4330	2.4238	.0000
3290B	77.0	3.926	.798	.8232	1.2281	1.2035	1.2281	1.2199	.0000
3300B	78.0	3.926	1.596	.9172	1.4100	1.3395	1.3873	1.3789	.0000
3310B	78.0	3.926	2.395	1.0171	1.6146	1.5436	1.5919	1.5834	.0000
3320B	78.5	3.926	3.193	1.1670	1.8647	1.7817	1.8306	1.8256	.0000
3330B	79.0	3.926	3.991	1.3109	2.1375	2.0765	2.1375	2.1172	.0000
3340B	80.0	3.926	4.789	.0000	2.4557	2.3600	2.4557	2.4238	.0000
3350B	80.5	4.657	.798	.8643	1.2850	1.2375	1.2963	1.2729	.0000
3360B	81.0	4.657	1.596	.9495	1.4668	1.4075	1.4555	1.4433	.0000
3370B	81.0	4.657	2.395	1.0788	1.6714	1.6116	1.6487	1.6439	.0000
3380B	82.0	4.657	3.193	1.1934	1.9215	1.8498	1.9101	1.8938	.0000
3390B	82.0	4.657	3.991	.0000	2.2057	2.1105	2.1829	2.1664	.0000
3400B	82.0	6.150	.798	.9642	1.5237	1.4756	1.5350	1.5114	.0000
3410B	83.0	6.150	1.596	1.0759	1.7169	1.6570	1.7283	1.7007	.0000
3420B	83.5	6.150	2.395	1.1993	1.9215	1.8611	1.9215	1.9014	.0000
3430B	84.0	6.150	3.193	1.3462	2.1716	2.0879	2.1602	2.1399	.0000
3440B	83.0	.651	2.395	.0000	1.7737	1.7024	1.7283	1.7348	.0000
3450B	84.5	1.532	3.991	.0000	2.2739	2.2466	2.2511	2.2572	.0000
3460B	85.0	2.354	.798	.0000	1.1599	1.1127	1.1372	1.1366	.0000
3470B	85.0	3.165	2.395	.0000	1.5464	1.4983	1.5237	1.5228	.0000
3480B	86.0	3.926	3.991	.0000	2.1375	2.0425	2.0693	2.0831	.0000
3490B	86.0	4.657	.798	.0000	1.2622	1.2148	1.2622	1.2464	.0000
3500B	86.0	6.150	1.596	.0000	1.7055	1.6343	1.6828	1.6742	.0000

TABLE V

ISOOCTANE-WATER FLOW THROUGH BED OF 0.340 INCH SPHERES

SUBSCRIPT (W) = WATER PHASE
SUBSCRIPT (O) = ORGANIC PHASE

LOG VIS(W) = -.30430E 01 + .16085E 04/T RHO(W) = .998
LOG VIS(O) = -.16086E 01 + .68994E 03/T RHO(O) = .692

VOIDAGE = .384 PACK DIA = .340 INT TENS = 49.500 RUNS = 59

CODE	T	GPM(W)	GPM(O)	DPDL(1)	DPDL(2)	DPDL(3)	DPDL(4)	DPDLA	RI
3720B	69.5	.651	.798	.0000	.5234	.5205	.5193	.5211	.4834
3730B	73.0	.651	1.596	.0000	.5818	.5773	.5763	.5785	.6627
3740B	74.0	.651	3.193	.0000	.7664	.7751	.7719	.7711	.6923
3750B	75.5	.651	4.789	.6293	.8644	.8633	.8871	.8716	.7883
3760S	76.0	.651	6.386	.6440	.8871	.9313	.9439	.9208	.8083
3770S	77.0	.651	8.154	.6822	.9439	.9767	1.0008	.9738	.0000
3780B	78.0	.651	10.806	.7850	1.1599	1.1127	1.1372	1.1366	.0000
3790B	79.0	.651	13.446	.9349	1.4100	1.3622	1.3645	1.3789	.0000
3800B	81.0	1.532	.798	.0000	.5302	.5178	.5207	.5229	.3239
3810B	82.0	1.532	1.596	.0000	.5580	.5530	.5573	.5561	.4171
3820B	82.0	1.532	3.193	.0000	.6850	.6897	.6768	.6838	.5102
3830B	83.0	1.532	4.789	.6175	.8397	.8496	.8479	.8457	.6838
3840S	84.0	1.532	6.386	.6675	.9553	.9767	1.0008	.9776	.7473
3850S	84.0	1.532	8.154	.7380	1.0235	1.0561	1.0690	1.0495	.0000
3860S	84.0	1.532	10.806	.8614	1.2395	1.2035	1.2281	1.2237	.0000
3870S	85.0	1.532	13.446	.9966	1.5237	1.3962	1.4441	1.4547	.0000
3880B	86.0	2.354	.798	.0000	.5329	.5245	.5261	.5278	.0000
3890B	86.0	2.354	1.596	.0000	.5465	.5367	.5356	.5396	.0000
3900B	87.0	2.354	3.193	.0000	.6605	.6518	.6524	.6549	.0000
3910B	87.0	2.354	4.789	.0000	.8099	.8116	.8085	.8100	.0000
3920S	68.0	2.354	6.386	.7174	1.0235	1.0334	1.0576	1.0382	.0000
3930S	70.0	2.354	8.154	.7938	1.1713	1.2035	1.2395	1.2047	.0000
3940S	71.0	2.354	10.806	.9437	1.3532	1.3509	1.3645	1.3562	.0000
3950S	71.0	2.354	13.446	1.1082	1.6260	1.5890	1.6032	1.6060	.0000
3960B	73.0	3.165	.798	.0000	.5546	.5503	.5465	.5505	.1532
3970B	73.0	3.165	1.596	.0000	.5967	.5909	.5859	.5911	.2463
3980B	74.0	3.165	3.193	.0000	.7108	.6884	.6917	.6970	.3888
3990B	75.0	3.165	4.789	.6616	.8370	.8347	.8316	.8344	.4820
4000B	76.0	3.165	6.386	.7409	1.0235	.9880	1.0008	1.0041	.6245
4010S	77.0	3.165	8.154	.8291	1.1599	1.1808	1.1826	1.1744	.0000
4020S	77.0	3.165	10.806	.9731	1.4100	1.4075	1.4441	1.4205	.0000
4030S	78.0	3.165	13.446	1.1435	1.6828	1.6457	1.6714	1.6666	.0000
4040B	78.5	4.657	.798	.0000	.6049	.6017	.6008	.6025	.0000
4050B	79.0	4.657	1.596	.0000	.6483	.6383	.6368	.6411	.0000
4060B	77.0	4.657	3.193	.6381	.7610	.7493	.7474	.7526	.0000
4070B	80.0	4.657	4.789	.0000	.9103	.8753	.8778	.8878	.0000
4080B	80.0	4.657	6.386	.8085	1.0690	1.0447	1.0349	1.0495	.0000
4090S	81.0	4.657	8.154	.9055	1.2281	1.2035	1.2054	1.2123	.0000
4100S	81.0	4.657	10.806	1.0994	1.5123	1.5209	1.5464	1.5265	.0000
4110S	82.0	4.657	13.446	1.2874	1.8419	1.8384	1.8419	1.8408	.0000
4120B	82.0	6.150	.798	.0000	.6945	.6816	.6795	.6852	.3840
4130B	82.5	6.150	1.596	.0000	.7406	.7277	.7284	.7322	.1489
4140B	83.0	6.150	3.193	.0000	.8601	.8319	.8329	.8417	.2632
4150B	83.0	6.150	4.789	.0000	1.0121	.9767	.9780	.9893	.3437
4160B	83.5	6.150	6.386	.0000	1.1713	1.1354	1.1372	1.1480	.4411
4170B	83.5	6.150	8.154	.0000	1.3304	1.3055	1.2963	1.3107	.0000
4180S	74.0	6.150	10.806	.0000	1.6828	1.6343	1.6714	1.6628	.0000
4190S	74.0	6.150	13.446	.0000	2.0238	2.0085	2.0465	2.0263	.0000
4200B	74.0	8.644	.798	.0000	.8985	.8860	.8871	.8905	.0000
4210B	75.0	8.644	1.596	.0000	.9667	.9427	.9553	.9549	.0000
4220B	75.0	8.644	3.193	.0000	1.1031	1.0674	1.0690	1.0798	.0000
4230B	75.0	8.644	4.789	.0000	1.2622	1.2261	1.2281	1.2388	.0000
4240B	75.0	8.644	6.386	.0000	1.4555	1.3962	1.4327	1.4281	.0000
4250B	75.0	8.644	8.154	.0000	1.6601	1.5436	1.5919	1.5985	.0000
4260S	75.0	8.644	10.806	.0000	1.9783	1.9064	1.9556	1.9468	.0000
4270B	75.5	12.820	.798	.0000	1.3418	1.3055	1.3191	1.3221	.0000
4280B	75.5	12.820	1.596	.0000	1.4100	1.3622	1.3873	1.3865	.0000
4290B	76.0	12.820	3.193	.0000	1.5919	1.5436	1.5691	1.5682	.0000
4300B	76.0	12.820	4.789	.0000	1.7965	1.7250	1.7624	1.7613	.0000

TABLE VI

ISOOCTANE-ALKATERGE "C" - WATER FLOW THROUGH BED OF 0.340 INCH SPHERES

SUBSCRIPT (W) = WATER PHASE
SUBSCRIPT (O) = ORGANIC PHASE

LOG VIS(W) = -.30430E 01 + .16085E 04/T RHO(W) = .998
LOG VIS(O) = -.16086E 01 + .68994E 03/T RHO(O) = .692

VOIDAGE = .384 PACK DIA = .340 INT TENS = 16.000 RUNS = 40

CODE	T	GPM(W)	GPM(O)	DPDL(1)	DPDL(2)	DPDL(3)	DPDL(4)	DPDLA	RI
43108	77.0	.651	.798	.0000	.4677	.4676	.4677	.4677	.4679
43208	78.0	.651	1.596	.0000	.5234	.5259	.5248	.5247	.5893
43308	78.5	.651	3.193	.0000	.7515	.7575	.7488	.7526	.7248
43408	80.0	.651	4.789	.0000	1.0235	1.0674	1.1144	1.0685	.8673
43508	80.5	.651	6.386	.0000	1.4327	1.4529	1.4782	1.4546	.0000
43608	80.5	.651	8.154	.0000	1.7510	1.8838	1.9556	1.8635	.0000
43708	80.0	1.532	.798	.0000	.4800	.4798	.4800	.4799	.2470
43808	80.0	1.532	1.596	.0000	.5193	.5191	.5193	.5193	.4016
43908	80.0	1.532	3.193	.0000	.6578	.6491	.6592	.6554	.5554
44008	81.0	1.532	4.789	.0000	.8628	.8753	.8778	.8720	.7177
44108	81.0	1.532	6.386	.0000	1.1144	1.1127	1.1372	1.1215	.7883
44208	82.0	1.532	8.154	.0000	1.4100	1.4529	1.4555	1.4394	.0000
44308	82.0	2.354	.798	.0000	.4962	.4974	.4976	.4971	.0000
44408	83.0	2.354	1.596	.0000	.5343	.5340	.5343	.5342	.0000
44508	83.0	2.354	3.193	.0000	.6469	.6369	.6388	.6409	.0000
44608	83.5	2.354	4.789	.0000	.8085	.7994	.8044	.8041	.0000
44708	83.5	2.354	6.386	.0000	1.0462	1.0447	1.0235	1.0382	.0000
44808	84.0	2.354	8.154	.0000	1.2509	1.2715	1.2850	1.2691	.0000
44908	84.5	2.354	10.806	.0000	1.6601	1.7250	1.7283	1.7044	.0000
45008	85.0	3.165	.798	.0000	.5234	.5232	.5234	.5233	.1292
45108	85.0	3.165	1.596	.0000	.5587	.5530	.5573	.5563	.2322
45208	85.0	3.165	3.193	.0000	.6673	.6532	.6578	.6594	.3790
45308	85.0	3.165	4.789	.0000	.8099	.7981	.8017	.8032	.5215
45408	85.0	3.165	6.386	.0000	1.0008	.9767	1.0008	.9927	.6274
45508	85.5	3.165	8.154	.0000	1.2167	1.2035	1.2281	1.2161	.0000
45608	85.5	3.165	10.806	.0000	1.5919	1.6116	1.6373	1.6136	.0000
45708	86.0	4.657	.798	.0000	.5845	.5760	.5804	.5803	.0000
45808	86.0	4.657	1.596	.0000	.6307	.6166	.6171	.6214	.0000
45908	86.5	4.657	3.193	.0000	.7298	.7141	.7175	.7205	.0000
46008	87.0	4.657	4.789	.0000	.8871	.8520	.8644	.8678	.0000
46108	87.0	4.657	6.386	.0000	1.0576	1.0107	1.0235	1.0306	.0000
46208	87.0	4.657	8.154	.0000	1.2281	1.2035	1.2167	1.2161	.0000
46308	87.0	4.657	10.806	.0000	1.5691	1.5890	1.6146	1.5909	.0000
46408	87.5	6.150	.798	.0000	.6809	.6721	.6673	.6734	.0755
46508	88.0	6.150	1.596	.0000	.7393	.7209	.7243	.7282	.1454
46608	86.0	6.150	3.193	.0000	.8506	.8333	.8343	.8394	.2618
46708	86.5	6.150	4.789	.0000	1.0008	.9653	.9780	.9814	.3493
46808	86.5	6.150	6.386	.0000	1.1599	1.1241	1.1372	1.1404	.4425
46908	86.5	6.150	8.154	.0000	1.3532	1.3168	1.3418	1.3373	.0000
47008	86.0	6.150	10.806	.0000	1.6942	1.6570	1.6828	1.6780	.0000

APPENDIX E

TABLES OF PROCESSED DROP SIZE DATA

The following symbols are used in this Appendix:

CLASSES	= the number of different size classifications used in analyzing the photographs
CODE	= photograph number
DSAUT IN	= Sauter mean diameter, inches
DSAUT MIC	= Sauter mean diameter, microns
FPS	= superficial liquid velocity, ft/sec
FPSTOT	= sum of superficial velocities, ft/sec
GPM	= liquid flowrate, gpm
INT TENS	= interfacial tension, dynes/cm
LOG VIS	= logarithm to base 10 of liquid viscosity; viscosity in cp
N	= number of drops counted in photograph
PACK DIA	= packing diameter, inches
PHOTOS	= number of photographs in data set
RHO	= liquid specific gravity
VOIDAGE	= porosity

(The number notation X.XXXE YY is equivalent to $X.XXX \cdot 10^{YY}$)

TABLE I

ISOBUTANOL-WATER FLOW THROUGH BED OF 0.501 INCH SPHERES

SUBSCRIPT (W) = WATER PHASE
SUBSCRIPT (O) = ORGANIC PHASE

LOG VIS(W) = -.34499E 01 + .19057E 04/T RHO(W) = .987
LOG VIS(O) = -.35123E 01 + .21422E 04/T RHO(O) = .832

VOIDAGE = .400 PACK DIA = .501 INT TENS = 2.100 PHOTOS = 21 CLASSES = 2

CODE	GPM(W)	GPM(O)	FPS(W)	FPS(O)	FPSTOT	DSAUT IN	DSAUT MIC	N
007	1.543	1.447	.04019	.03769	.07788	.03444	874.79	102
008	1.543	1.447	.04019	.03769	.07788	.03627	921.25	85
009	1.543	1.447	.04019	.03769	.07788	.03419	868.32	114
010	1.543	1.447	.04019	.03769	.07788	.03666	931.14	99
017	1.543	1.447	.04019	.03769	.07788	.03482	884.38	107
018	1.543	1.447	.04019	.03769	.07788	.03667	931.53	141
081	1.543	1.447	.04019	.03769	.07788	.03792	963.14	45
078	3.186	1.447	.08300	.03769	.12069	.02724	691.83	38
082	3.186	1.447	.08300	.03769	.12069	.02782	706.65	49
079	4.688	1.447	.12213	.03769	.15983	.02053	521.35	13
083	4.688	1.447	.12213	.03769	.15983	.02155	547.33	48
084	6.190	1.447	.16127	.03769	.19896	.01659	421.29	32
080	6.190	1.447	.16127	.03769	.19896	.01294	328.73	18
085	8.701	1.447	.22667	.03769	.26436	.00836	212.33	11
086	1.543	2.894	.04019	.07539	.11557	.02860	726.38	41
096	1.543	2.894	.04019	.07539	.11557	.02767	702.94	79
087	1.543	4.341	.04019	.11308	.15327	.03041	772.29	33
097	1.543	4.341	.04019	.11308	.15327	.02170	551.28	24
089	3.186	2.894	.08300	.07539	.15838	.02290	581.54	66
090	4.688	2.894	.12213	.07539	.19752	.01906	484.14	56
093	3.186	4.341	.08300	.11308	.19608	.01859	472.12	27

TABLE II

ISOBUTANOL-WATER FLOW THROUGH BED OF 0.340 INCH SPHERES

SUBSCRIPT (W) = WATER PHASE
SUBSCRIPT (O) = ORGANIC PHASE

LOG VIS(W) = -.34499E 01 + .19057E 04/T RHO(W) = .987
LOG VIS(O) = -.35123E 01 + .21422E 04/T RHO(O) = .832

VOIDAGE = .383 PACK DIA = .340 INT TENS = 2.100 PHOTOS = 30 CLASSES = 2

CODE	GPM(W)	GPM(O)	FPS(W)	FPS(O)	FPSTOT	DSAUT IN	DSAUT MIC	N
099	.655	.723	.01707	.01885	.03592	.04079	1035.97	232
101	.655	.723	.01707	.01885	.03592	.04115	1045.15	215
100	1.543	1.447	.04019	.03769	.07788	.02688	682.85	195
118	1.543	1.447	.04019	.03769	.07788	.02784	707.08	162
102	1.543	.723	.04019	.01885	.05903	.02980	756.87	242
103	1.543	.723	.04019	.01885	.05903	.02911	739.32	205
110	.655	1.447	.01707	.03769	.05477	.03344	849.30	91
111	.655	1.447	.01707	.03769	.05477	.03607	916.28	76
123	.655	2.894	.01707	.07539	.09246	.02602	660.96	116
124	.655	2.894	.01707	.07539	.09246	.02714	689.44	105
104	3.186	.723	.08300	.01885	.10184	.01992	505.91	154
105	3.186	.723	.08300	.01885	.10184	.01999	507.78	169
106	4.688	.723	.12213	.01885	.14098	.01348	342.40	94
107	4.688	.723	.12213	.01885	.14098	.01392	353.50	139
108	6.190	.723	.16127	.01885	.18011	.01180	299.72	98
109	6.190	.723	.16127	.01885	.18011	.01135	288.19	130
112	3.186	1.447	.08300	.03769	.12069	.01872	475.53	122
113	3.186	1.447	.08300	.03769	.12069	.01883	478.22	128
114	4.688	1.447	.12213	.03769	.15983	.01298	329.82	77
115	4.688	1.447	.12213	.03769	.15983	.01365	346.73	143
116	6.190	1.447	.16127	.03769	.19896	.00998	253.58	108
117	6.190	1.447	.16127	.03769	.19896	.00948	240.88	112
119	3.186	2.894	.08300	.07539	.15838	.01380	350.56	169
120	3.186	2.894	.08300	.07539	.15838	.01385	351.71	128
121	1.543	2.894	.04019	.07539	.11557	.01907	484.38	149
122	1.543	2.894	.04019	.07539	.11557	.01858	471.96	138
125	1.543	4.341	.04019	.11308	.15327	.01284	326.19	124
126	1.543	4.341	.04019	.11308	.15327	.01183	300.58	75
127	.655	4.341	.01707	.11308	.13015	.01419	360.36	150
128	.655	4.341	.01707	.11308	.13015	.01654	420.11	122

TABLE III

ISOBUTANOL-WATER FLOW THROUGH BED OF 0.164 INCH SPHERES

SUBSCRIPT (W) = WATER PHASE
SUBSCRIPT (O) = ORGANIC PHASE

LOG VIS(W) = -.34499E 01 + .19057E 04/T RHO(W) = .987
LOG VIS(O) = -.35123E 01 + .21422E 04/T RHO(O) = .832

VOIDAGE = .337 PACK DIA = .164 INT TENS = 2.100 PHOTOS = 26 CLASSES = 2

CODE	GPM(W)	GPM(O)	FPS(W)	FPS(O)	FPSTOT	DSAUT IN	DSAUT MIC	N
131	.655	.723	.01707	.01885	.03592	.01858	472.01	45
132	.655	.723	.01707	.01885	.03592	.01873	475.84	53
133	1.543	.723	.04019	.01885	.05903	.01579	400.98	64
134	1.543	.723	.04019	.01885	.05903	.01511	383.75	54
144	1.543	1.447	.04019	.03769	.07788	.01276	324.15	75
145	.655	1.447	.01707	.03769	.05477	.01605	407.74	110
146	.655	1.447	.01707	.03769	.05477	.01808	459.22	95
135	3.186	.723	.08300	.01885	.10184	.01041	264.53	72
136	3.186	.723	.08300	.01885	.10184	.01082	274.88	92
137	4.688	.723	.12213	.01885	.14098	.00884	224.65	108
138	4.688	.723	.12213	.01885	.14098	.00780	198.06	82
139	4.688	1.447	.12213	.03769	.15983	.00728	185.01	72
140	4.688	1.447	.12213	.03769	.15983	.00681	172.85	57
141	3.186	1.447	.08300	.03769	.12069	.00898	228.21	121
142	3.186	1.447	.08300	.03769	.12069	.00920	233.75	70
143	1.543	1.447	.04019	.03769	.07788	.01140	289.53	116
147	.655	2.894	.01707	.07539	.09246	.00835	212.20	85
148	.655	2.894	.01707	.07539	.09246	.00777	197.35	83
149	1.543	2.894	.04019	.07539	.11557	.00726	184.30	116
150	1.543	2.894	.04019	.07539	.11557	.00698	177.42	139
151	3.186	2.894	.08300	.07539	.15838	.00682	173.28	162
152	3.186	2.894	.08300	.07539	.15838	.00658	167.06	130
153	1.543	4.341	.04019	.11308	.15327	.00568	144.28	148
154	1.543	4.341	.04019	.11308	.15327	.00584	148.36	126
155	.655	4.341	.01707	.11308	.13015	.00581	147.61	137
156	.655	4.341	.01707	.11308	.13015	.00622	157.93	101

TABLE IV

ISOÖCTANE-WATER FLOW THROUGH BED OF 0.164 INCH SPHERES

SUBSCRIPT (W) = WATER PHASE
SUBSCRIPT (O) = ORGANIC PHASE

LOG VIS(W) = -.30430E 01 + .16085E 04/T RHO(W) = .998
LOG VIS(O) = -.16086E 01 + .68994E 03/T RHO(O) = .692

VOIDAGE = .337 PACK DIA = .164 INT TENS = 49.500 PHOTOS = 24 CLASSES = 1

CODE	GPM(W)	GPM(O)	FPS(W)	FPS(O)	FPSTOT	DSAUT IN	DSAUT MIC	N
183	.651	.798	.01696	.02079	.03775	.03861	980.63	90
184	.651	.798	.01696	.02079	.03775	.04021	1021.24	147
157	.651	.798	.01696	.02079	.03775	.04161	1056.86	283
158	.651	.798	.01696	.02079	.03775	.04175	1060.45	165
159	.651	1.596	.01696	.04159	.05855	.03353	851.77	155
160	.651	1.596	.01696	.04159	.05855	.03440	873.82	163
161	.651	3.193	.01696	.08318	.10014	.02264	575.02	168
162	.651	3.193	.01696	.08318	.10014	.02515	638.88	160
163	1.532	.798	.03992	.02079	.06071	.03699	939.42	158
164	1.532	.798	.03992	.02079	.06071	.03807	966.90	131
166	1.532	1.596	.03992	.04159	.08151	.03293	836.40	160
167	1.532	3.193	.03992	.08318	.12310	.02387	606.22	190
168	1.532	3.193	.03992	.08318	.12310	.02508	637.04	172
169	1.532	3.979	.03992	.10365	.14357	.02063	524.11	166
170	1.532	3.979	.03992	.10365	.14357	.01970	500.31	137
171	3.165	.798	.08245	.02079	.10325	.03274	831.70	134
172	3.165	.798	.08245	.02079	.10325	.03217	817.00	131
173	3.165	1.596	.08245	.04159	.12404	.02775	704.91	126
174	3.165	1.596	.08245	.04159	.12404	.02713	689.12	119
175	3.165	3.193	.08245	.08318	.16563	.02071	526.14	101
176	3.165	3.193	.08245	.08318	.16563	.02072	526.21	122
177	4.657	.798	.12133	.02079	.14212	.02667	677.33	91
178	4.657	.798	.12133	.02079	.14212	.02243	569.80	108
179	4.657	1.596	.12133	.04159	.16292	.02194	557.31	66

TABLE V

ISOOCTANE-WATER FLOW THROUGH BED OF 0.340 INCH SPHERES

SUBSCRIPT (W) = WATER PHASE
SUBSCRIPT (O) = ORGANIC PHASE

LOG VIS(W) = -.30430E 01 + .16085E 04/T RHO(W) = .998
LOG VIS(O) = -.16086E 01 + .68994E 03/T RHO(O) = .692

VOIDAGE = .384 PACK DIA = .340 INT TENS = 49.500 PHOTOS = 2 CLASSES = 1

CODE	GPM(W)	GPM(O)	FPS(W)	FPS(O)	FPSTOT	DSAUT IN	DSAUT MIC	N
185	.651	.798	.01696	.02079	.03775	.09236	2346.01	39
186	.651	.798	.01696	.02079	.03775	.06959	1767.64	16

TABLE VI

ISOÖCTANE-ALKATERGE "C"-WATER FLOW THROUGH BED OF 0.340 INCH SPHERES

SUBSCRIPT (W) = WATER PHASE
SUBSCRIPT (O) = ORGANIC PHASE

LOG VIS(W) = -.30430E 01 + .16085E 04/T RHO(W) = .998
LOG VIS(O) = -.16086E 01 + .68994E 03/T RHO(O) = .692

VOIDAGE = .384 PACK DIA = .340 INT TENS = 16.000 PHOTOS = 2 CLASSES = 1

CODE	GPM(W)	GPM(O)	FPS(W)	FPS(O)	FPSTOT	DSAUT IN	DSAUT MIC	N
209	.651	.798	.01696	.02079	.03775	.06067	1540.91	42
210	.651	.798	.01696	.02079	.03775	.05750	1460.52	30

APPENDIX F

ESTIMATION OF INTERFACIAL TENSION EFFECT

In order to decide whether interfacial tension can be neglected as a contributor to pressure drop, a comparison was made between the energy required to generate the interfacial area and the energy loss due to friction.

Run 311 is used as an example. The conditions for this run were:

Packing diameter = 0.164 inches

Porosity = 0.337

Water flowrate = 1.53 gpm

Isooctane flowrate = 1.60 gpm

Interfacial tension = 49.5 dynes/cm

The frictional pressure drop based on the "single-phase" assumption (i.e. the mixture can be treated as a single-phase fluid with averaged physical properties) is 0.228 psi/ft of column length (Refer to Table I, Appendix G). At a total flowrate of 3.13 gpm, this pressure loss amounts to an energy loss of

$$0.228 \frac{\text{psi}}{\text{ft}} \times 3.13 \frac{\text{gal}}{\text{min}} \times \frac{1}{7.48} \frac{\text{ft}^3}{\text{gal}} \times 60 \frac{\text{min}}{\text{hr}} \times 144 \frac{\text{in}^2}{\text{ft}^2}$$

$$= 825 \frac{\text{ft-lb}}{\text{hr}}/\text{ft of column length}$$

The most conservative estimate that can be made concerning droplet formation is that the dispersed phase droplets are formed only once in one foot of packing and that no coalescence or redispersion

occurs. Based on this assumption the energy required to generate interfacial area can be computed as follows:

drop size (Sauter mean diameter) = 0.033 in. (Table IV, Appendix E)

surface area per 1.60 gal. of dispersed phase =

$$1.60 \text{ gal} \times \frac{1}{7.48} \frac{\text{ft}^3}{\text{gal}} \times \left[\frac{6}{0.033 \text{ in.}}\right] \times 12 \frac{\text{in.}}{\text{ft}} = 511 \text{ ft}^2$$

The term in brackets represents the ratio of surface area to volume for the dispersed phase.

$$\text{surface energy} = 511 \text{ ft}^2 \times 49.5 \frac{\text{dynes}}{\text{cm}} \times 7.38 \times 10^{-8} \frac{\text{ft-lb}}{\text{dyne-cm}}$$

$$\times (30.5)^2 \frac{\text{cm}^2}{\text{ft}^2}$$

$$= 1.7 \text{ ft-lb}/1.60 \text{ gal of dispersed phase}$$

rate of surface energy dissipation =

$$\frac{1.74}{1.60} \frac{\text{ft-lb}}{\text{gal}} \times 1.60 \frac{\text{gal}}{\text{min}} \times 60 \frac{\text{min}}{\text{hr}}$$

$$= 104 \text{ ft-lb/hr}$$

It should be noted that the surface energy dissipation rate amounts to approximately 12% of the frictional dissipation rate even with the conservative estimate of no coalescence and redispersion in one foot of packing. It should also be remembered that a certain amount of energy input is required to keep the dispersion from coalescing. It is obvious, therefore, that interfacial tension cannot be neglected in any correlation of two-phase pressure drop in packed beds.

APPENDIX G

TABLE OF TWO-PHASE PRESSURE DROP CORRELATION PARAMETERS

The following symbols are used in this Appendix:

CODE = code number

DELFA = δ_f, average frictional pressure gradient, psi/ft

DELFP = δ_{fp}, predicted frictional pressure gradient, psi/ft

DPDLA = $\frac{P_1-P_2}{Z_1-Z_2}$, average total pressure gradient, psi/ft

PRAT = $P_{RATIO} = \frac{\delta_f}{\delta_{fp}}$, ratio of frictional pressure gradient to predicted frictional pressure gradient

PRATP = value of P_{RATIO} predicted by Equation (80)

RHOM = ρ_m, mean density

RI = organic phase holdup

WE = $\frac{D_p \rho_m U_m^2}{\sigma g_c}$, Weber number

(The number notation X.XXXE YY is equivalent to $X.XXX \cdot 10^{YY}$)

CODE	DPDLA	RHOM	DELFA	DELFP	PRAT	WE	RI	PRATP
021IB	.4316	.9057	.0391	.0162	2.4222	.65693E 00	.4974	1.6578
022IB	.4329	.8803	.0515	.0294	1.7527	.14844E 01	.6673	1.5438
023IB	.4334	.8679	.0573	.0456	1.2581	.26442E 01	.7179	1.3919
024IB	.4407	.9120	.0456	.0427	1.0680	.31098E 01	.3917	1.1738
025IB	.4685	.8859	.0846	.0818	1.0341	.66526E 01	.6110	1.1989
026IB	.5158	.8726	.1376	.1287	1.0692	.11525E 02	.7234	1.1567
027IB	.5827	.8646	.2081	.1939	1.0730	.17726E 02	.7673	1.1200
028IH	.7348	.8531	.3652	.3906	.9350	.41836E 02	.8906	1.0630
029IH	.8699	.8494	.5019	.5364	.9357	.61096E 02	.8001	1.0548
030IH	.4885	.9386	.0818	.0810	1.0098	.76865E 01	.2355	1.0461
031IB	.5261	.9132	.1304	.1310	.9953	.12880E 02	.4383	1.0853
032IB	.5786	.8976	.1897	.1874	1.0124	.19402E 02	.5589	1.0927
033IB	.6644	.8870	.2801	.2532	1.1059	.27254E 02	.6357	1.0854
034IS	.9053	.8700	.5283	.4768	1.1079	.55933E 02	.7070	1.0581
035IH	1.0657	.8632	.6917	.6746	1.0253	.82416E 02	.7344	1.0460
036IB	.5387	.9504	.1269	.1321	.9606	.13650E 02	.1752	1.0223
037IB	.5832	.9278	.1812	.1907	.9500	.20351E 02	.3342	1.0420
038IH	.6433	.9125	.2479	.2585	.9591	.28382E 02	.4630	1.0566
039IH	.7403	.9014	.3498	.3291	1.0628	.37742E 02	.5370	1.0582
040IH	.8495	.8940	.4622	.3993	1.1574	.46872E 02	.6138	1.0591
041IH	.9855	.8822	.6032	.5802	1.0397	.70600E 02	.6823	1.0495
042IB	.5671	.9278	.1651	.1856	.8896	.20351E 02	.3506	1.0452
043IB	.5765	.9278	.1745	.1846	.9452	.20351E 02	.3451	1.0441
044IB	.4843	.9386	.0776	.0810	.9588	.76865E 01	.2519	1.0506
052IU	.6319	.9125	.2365	.2472	.9571	.28382E 02	.4657	1.0571
053IU	.6323	.9125	.2369	.2472	.9585	.28382E 02	.4548	1.0551
054IU	.6341	.9125	.2387	.2460	.9704	.28382E 02	.4685	1.0575
055IB	.4391	.9375	.0329	.0269	1.2212	.18368E 01	.2410	1.1162
056IB	.4391	.9375	.0329	.0269	1.2212	.18368E 01	.2300	1.1091
057IB	.4719	.9583	.0567	.0581	.9753	.55883E 01	.1423	1.0314
058IB	.4910	.9386	.0843	.0810	1.0410	.76865E 01	.2574	1.0522
059IB	.6398	.9125	.2444	.2519	.9702	.28382E 02	.4712	1.0580
060IB	.5531	.9576	.1382	.1801	.7673	.21312E 02	.1642	1.0157
061IB	.5417	.9708	.1210	.1483	.8164	.17706E 02	.0875	1.0103
062IB	.6491	.9376	.2429	.2452	.9904	.29523E 02	.2903	1.0268
063IB	.7243	.9231	.3243	.3183	1.0187	.39062E 02	.3945	1.0362
064IB	.8904	.9076	.4971	.4465	1.1132	.55770E 02	.5069	1.0423
065IB	.9498	.8970	.5611	.5852	.9588	.74568E 02	.5699	1.0409
066IH	.8211	.9773	.3976	.3643	1.0916	.49933E 02	.0497	1.0041
067IH	.8672	.9688	.4474	.4076	1.0978	.55878E 02	.0930	1.0053
068IH	.9301	.9544	.5166	.5009	1.0313	.68766E 02	.2026	1.0097
069IH	1.0150	.9427	.6065	.6015	1.0084	.82983E 02	.2656	1.0124
070IH	1.2135	.9289	.8110	.7686	1.0552	.10667E 03	.3616	1.0169
071IS	1.1931	.9741	.7710	.7801	.9883	.11222E 03	.0930	1.0034
072IH	1.3674	.9632	.9500	.9163	1.0368	.13021E 03	.1478	1.0046
073IH	1.5038	.9538	1.0905	1.0461	1.0424	.14953E 03	.2190	1.0066
074IH	1.6046	.9457	1.1948	1.1877	1.0060	.17018E 03	.2602	1.0077
075IS	.5824	.8646	.2077	.1737	1.1958	.17726E 02	.7974	1.1187
076IB	.5951	.9576	.1802	.1724	1.0454	.21312E 02	.1642	1.0157
077IH	.8874	.9076	.4941	.4339	1.1387	.55770E 02	.5151	1.0432
078IB	.4411	.9120	.0459	.0386	1.1904	.31098E 01	.4082	1.1854
114IB	.4367	.9057	.0463	.0347	1.3327	.44582E 00	.4029	1.6104
115IB	.4627	.8803	.0813	.0641	1.2676	.10074E 01	.6190	1.6538
116IB	.5604	.8606	.1874	.1392	1.3462	.28071E 01	.8104	1.3720
117IS	.6327	.8523	.2634	.2314	1.1382	.55088E 01	.8565	1.2340
118IH	.8203	.8462	.4537	.4005	1.1326	.11218E 02	.8996	1.1411
119IB	.4763	.9375	.0700	.0576	1.2164	.12465E 01	.2389	1.1463
120IB	.4997	.9120	.1046	.0926	1.1293	.21104E 01	.4111	1.2388

CODE	DPDIA	RHOM	DELFA	DELFP	PRAT	WE	RI	PRATP
1211H	.9468	.9125	.5514	.5488	1.0047	.19261E 02	.4658	1.0727
1221B	.5762	.8859	.1923	.1756	1.0953	.45148E 01	.6299	1.2604
1231B	.6869	.8726	.3088	.2777	1.1117	.78211E 01	.7119	1.1987
1241S	.9273	.8617	.5539	.4843	1.1438	.14433E 02	.7229	1.1361
1271B	.5475	.9583	.1323	.1276	1.0362	.37925E 01	.1514	1.0424
1281B	.5771	.9386	.1704	.1728	.9858	.52164E 01	.2635	1.0687
1291B	.6678	.9132	.2721	.2795	.9737	.87407E 01	.4494	1.1128
1301H	.7998	.8976	.4108	.4028	1.0198	.13167E 02	.5725	1.1214
1311H	.9218	.9125	.5264	.5406	.9737	.19261E 02	.4604	1.0714
1341B	.6387	.9663	.2200	.2192	1.0037	.73274E 01	.0994	1.0196
1351B	.6838	.9504	.2719	.2755	.9871	.92632E 01	.1978	1.0328
1361H	.7907	.9278	.3886	.4024	.9658	.13811E 02	.3564	1.0591
1371H	.9437	.9125	.5484	.5563	.9857	.19261E 02	.4713	1.0739
1401B	.7551	.9708	.3345	.3280	1.0196	.12016E 02	.0830	1.0127
1411B	.8057	.9576	.3908	.3945	.9906	.14464E 02	.1541	1.0188
1421B	.9375	.9376	.5312	.5408	.9823	.20035E 02	.2990	1.0357
1461B	1.0142	.9751	.5917	.5695	1.0391	.22425E 02	.0447	1.0064
1471B	1.0779	.9649	.6598	.6533	1.0099	.25729E 02	.1213	1.0105
1481B	1.2249	.9483	.8140	.8359	.9738	.33011E 02	.2416	1.0192
1491H	1.4447	.9354	1.0394	1.0642	.9766	.41196E 02	.3291	1.0264
1501H	1.8092	.9207	1.4103	1.4030	1.0052	.55088E 02	.4248	1.0328
1511H	.9960	.9125	.6007	.5589	1.0747	.19261E 02	.4686	1.0733
1521H	1.5174	.9788	1.0933	1.1285	.9688	.47073E 02	.0447	1.0041
1531H	1.6205	.9714	1.1996	1.2433	.9648	.51809E 02	.0857	1.0052
1541H	1.8047	.9586	1.3893	1.4878	.9338	.61957E 02	.1732	1.0086
1551B	.4626	.8803	.0811	.0613	1.3234	.10074E 01	.6381	1.6710
1561H	1.3030	.8531	.9333	.8357	1.1169	.28391E 02	.8049	1.0881
1571B	.5529	.9583	.1376	.1261	1.0912	.37925E 01	.1404	1.0394
1581B	1.2764	.8969	.8878	.8020	1.1070	.29072E 02	.6025	1.0782
1591S	1.4333	.9076	1.0400	.9977	1.0425	.37848E 02	.5205	1.0558
1601B	1.0779	.9649	.6598	.6524	1.0113	.25729E 02	.1158	1.0101
1611S	2.0077	.8920	1.6212	1.5096	1.0739	.59019E 02	.6381	1.0529
1621H	1.1150	.9231	.7150	.7093	1.0081	.26509E 02	.4057	1.0482
1631S	1.8062	.8822	1.4239	1.2640	1.1265	.47912E 02	.7037	1.0639
1641S	1.1779	.8830	.7953	.6463	1.2306	.21450E 02	.6983	1.1052
1651S	1.5910	.8700	1.2140	1.0740	1.1303	.37959E 02	.7283	1.0746
1661B	.6924	.9504	.2806	.2782	1.0086	.92632E 01	.1978	1.0328
1671H	1.6493	.8494	1.2812	1.1795	1.0862	.41462E 02	.8705	1.0652
1681H	1.3189	.8531	.9492	.8419	1.1274	.28391E 02	.7776	1.0892
1691B	1.4386	.9076	1.0453	1.0011	1.0442	.37848E 02	.5123	1.0546
1701B	1.2757	.8969	.8870	.8036	1.1038	.29072E 02	.5943	1.0771
1711U	.6807	.9132	.2850	.2795	1.0197	.87407E 01	.4521	1.1138
1721B	.9748	.9125	.5794	.5429	1.0673	.19261E 02	.4713	1.0739
2181B	.5968	.9057	.2044	.1667	1.2261	.21504E 00	.4200	2.0261
2191B	.7920	.8803	.4105	.2971	1.3817	.48592E 00	.6452	2.0667
2201B	1.3295	.8606	.9566	.6013	1.5909	.13540E 01	.8188	1.5828
2211S	1.8903	.8523	1.5210	1.0140	1.5001	.26572E 01	.8297	1.3792
2221H	2.2238	.8462	1.8571	1.6505	1.1252	.54111E 01	.8623	1.2349
2231H	2.5118	.8446	2.1458	1.8766	1.1434	.68289E 01	.9165	1.1867
2241B	.6803	.9375	.2741	.2562	1.0698	.60126E 00	.2544	1.2516
2251B	.8374	.9120	.4422	.4029	1.0975	.10180E 01	.3657	1.3131
2261B	1.2840	.8859	.9002	.7351	1.2246	.21777E 01	.6180	1.4036
2271B	1.7994	.8726	1.4213	1.1080	1.2827	.37726E 01	.7130	1.3133
2281S	2.7618	.8646	2.3871	1.7501	1.3640	.58025E 01	.7266	1.2406
2291S	2.3981	.8683	2.0218	1.4081	1.4359	.47175E 01	.7700	1.2740
2301B	.9582	.9583	.5429	.5280	1.0283	.18293E 01	.1175	1.0530
2311B	1.1075	.9386	.7008	.7191	.9746	.25161E 01	.2283	1.0888
2321H	1.5190	.9132	1.1233	1.1295	.9945	.42161E 01	.4010	1.1491
2331H	2.0858	.8976	1.6969	1.5844	1.0710	.63512E 01	.5583	1.1858
2341S	2.8338	.8870	2.4495	2.0841	1.1753	.89213E 01	.6615	1.1766

CODE	LPDLA	RHOM	DELTA	DELFP	PRAT	WE	RI	PRATP
235IH	1.2348	.9663	.8161	.8007	1.0192	.35344E 01	.0778	1.0263
236IH	1.4129	.9504	1.0010	1.0458	.9572	.44681E 01	.1599	1.0406
237IH	1.6023	.9380	1.1959	1.2691	.9423	.55106E 01	.2002	1.0460
238IH	1.8433	.9278	1.4413	1.5135	.9523	.66619E 01	.2761	1.0631
239IH	2.4322	.9125	2.0368	2.0257	1.0055	.92908E 01	.4281	1.1008
240IB	.7936	.9507	.3816	.3779	1.0097	.11358E 01	.1582	1.0943
241IB	.9582	.9282	.5560	.5403	1.0290	.16884E 01	.2436	1.1243
242IB	1.1173	.9129	.7217	.7194	1.0033	.23498E 01	.3793	1.1968
243IH	1.3257	.9018	.9350	.9026	1.0358	.31199E 01	.4986	1.2497
244IH	1.8752	.8867	1.4909	1.3221	1.1277	.49865E 01	.6343	1.2462
245IS	2.5989	.8770	2.2189	1.7780	1.2479	.72883E 01	.7320	1.2090
246IB	.5983	.9057	.2059	.1789	1.1507	.21504E 00	.3955	1.9346
247IB	.7975	.9507	.3855	.3940	.9784	.11358E 01	.1582	1.0943
248IH	1.2424	.9663	.8237	.8254	.9979	.35344E 01	.0778	1.0263
249IS	2.8262	.8870	2.4419	2.1370	1.1427	.89213E 01	.6723	1.1784
250IS	2.3412	.8683	1.9650	1.4226	1.3813	.47175E 01	.7863	1.2726
256IU	1.3219	.8606	.9490	.6402	1.4825	.13540E 01	.7718	1.5968
257IU	1.3068	.8859	.9229	.7940	1.1623	.21777E 01	.5815	1.3795
258IU	1.9547	.8726	1.5766	1.1898	1.3251	.37726E 01	.6798	1.3072
259IU	1.7956	.8523	1.4262	.9905	1.4399	.26572E 01	.8366	1.3768
260IH	2.4701	.8815	2.0881	1.6994	1.2287	.60653E 01	.6139	1.2117
261IS	2.7694	.8770	2.3894	1.9639	1.2167	.72883E 01	.6470	1.1973
262IS	2.1366	.8704	1.7595	1.3500	1.3033	.42171E 01	.6969	1.2899
263IS	2.7694	.8646	2.3948	1.6627	1.4403	.58025E 01	.7409	1.2412
264IB	1.0870	.8679	.7109	.4603	1.5444	.86558E 00	.7154	1.7859
265IB	1.7198	.8558	1.3490	.8009	1.6844	.19512E 01	.8095	1.4671
266IS	1.8107	.8498	1.4425	1.1899	1.2123	.34586E 01	.8566	1.3128
267IS	1.7994	.8478	1.4320	1.3937	1.0275	.43955E 01	.8727	1.2638
268IB	.6419	.9258	.2408	.2170	1.1095	.38829E 00	.3074	1.4365
269IB	.8154	.8993	.4257	.3445	1.2356	.73374E 00	.4857	1.5936
270IB	1.0377	.8844	.6545	.4957	1.3204	.11880E 01	.5922	1.5650
271IB	1.3045	.8749	.9254	.6598	1.4026	.17510E 01	.6625	1.4884
272IB	1.5985	.8684	1.2223	.8368	1.4607	.24228E 01	.7122	1.4129
273IS	1.9282	.8635	1.5540	1.0161	1.5294	.32033E 01	.7492	1.3497
274IS	2.1896	.8599	1.8170	1.2141	1.4966	.40781E 01	.7774	1.2995
275IS	2.3450	.8569	1.9737	1.4179	1.3920	.50907E 01	.8005	1.2582
276IS	2.4625	.8546	2.0922	1.6399	1.2758	.61798E 01	.8188	1.2260
277IB	.7426	.9453	.3330	.3007	1.1076	.85401E 00	.1889	1.1373
278IB	.8856	.9213	.4864	.4509	1.0786	.13403E 01	.3365	1.2316
279IB	1.0514	.9057	.6589	.6110	1.0785	.19354E 01	.4411	1.2809
280IB	1.2840	.8947	.8964	.7825	1.1455	.26393E 01	.5179	1.2920
281IB	1.5607	.8866	1.1765	.9700	1.2129	.34519E 01	.5765	1.2820
282IS	1.8903	.8803	1.5089	1.1704	1.2892	.43733E 01	.6224	1.2629
283IS	2.2768	.8754	1.8975	1.3803	1.3747	.53868E 01	.6590	1.2414
284IS	2.6671	.8713	2.2896	1.5965	1.4341	.65425E 01	.6900	1.2195
285IS	2.9248	.8680	2.5487	1.8304	1.3924	.77702E 01	.7151	1.1998
3060B	1.1025	.8295	.7431	.0857	8.6752	.92308E-02	.4745	9.8011
3070B	1.3865	.7806	1.0482	.1378	7.6049	.20893E-01	.6521	8.6595
3080B	1.8181	.7574	1.4899	.2044	7.2884	.37227E-01	.7404	6.6325
3090B	2.2042	.7438	1.8819	.2821	6.6718	.58233E-01	.7930	5.2188
3100B	1.0723	.8932	.6852	.1762	3.8884	.25708E-01	.2620	2.8755
3110B	1.3032	.8419	.9384	.2455	3.8225	.43670E-01	.4312	3.8904
3120B	1.5682	.8114	1.2166	.3277	3.7132	.66304E-01	.5388	4.0637
3130B	1.8711	.7912	1.5283	.4242	3.6024	.93610E-01	.6126	3.8524
3140B	2.2497	.7769	1.9130	.5322	3.5944	.12559E 00	.6662	3.5371
3150B	2.2043	.7769	1.8676	.5167	3.6147	.12559E 00	.6662	3.5371
3160B	2.5298	.7662	2.1979	.6351	3.4604	.16224E 00	.7068	3.2257
317CB	1.0912	.9205	.6923	.2585	2.6788	.48456E-01	.1796	1.7758
318CB	1.2653	.8743	.8865	.3422	2.5903	.72288E-01	.3222	2.3392
3190B	1.4698	.8437	1.1042	.4389	2.5157	.10079E 00	.4250	2.6770

CODE	DPDLA	RHOM	DELFA	DELFP	PRAT	WE	RI	PRATP
32008	1.7727	.8219	1.4166	.5485	2.5825	.13397E 00	.5014	2.7941
32108	2.0755	.8055	1.7265	.6728	2.5661	.17182E 00	.5602	2.7741
32208	2.4011	.7928	2.0576	.8083	2.5456	.21434E 00	.6067	2.6853
32308	1.1366	.9364	.7309	.3677	1.9875	.77931E-01	.1349	1.4288
32408	1.3032	.8954	.9152	.4688	1.9522	.10756E 00	.2551	1.7393
32508	1.5985	.8662	1.2232	.6088	2.0093	.14187E 00	.3489	1.9951
32608	1.8484	.8443	1.4825	.7277	2.0374	.18084E 00	.4227	2.1550
32708	2.1285	.8273	1.7700	.8664	2.0430	.22449E 00	.4820	2.2291
32808	2.4238	.8138	2.0712	1.0180	2.0345	.27281E 00	.5304	2.2418
32908	1.2199	.9463	.8099	.5035	1.6086	.11192E 00	.1083	1.2838
33008	1.3789	.9095	.9848	.6178	1.5941	.14699E 00	.2120	1.4742
33108	1.5834	.8821	1.2012	.7475	1.6070	.18673E 00	.2972	1.6549
33208	1.8256	.8608	1.4527	.8889	1.6342	.23115E 00	.3670	1.7943
33308	2.1172	.8437	1.7516	1.0434	1.6786	.28024E 00	.4248	1.8852
33408	2.4238	.8299	2.0642	1.2096	1.7066	.33400E 00	.4731	1.9337
33508	1.2729	.9532	.8599	.6338	1.3568	.15033E 00	.0905	1.2074
33608	1.4433	.9199	1.0447	.7634	1.3684	.19063E 00	.1814	1.3338
33708	1.6439	.8941	1.2565	.9074	1.3847	.23560E 00	.2592	1.4636
33808	1.8938	.8735	1.5153	1.0617	1.4272	.28524E 00	.3248	1.5757
33908	2.1664	.8568	1.7951	1.2318	1.4573	.33956E 00	.3803	1.6609
34008	1.5114	.9628	1.0942	.9599	1.1399	.24629E 00	.0669	1.1276
34108	1.7007	.9349	1.2956	1.1173	1.1596	.29725E 00	.1389	1.1911
34208	1.9014	.9122	1.5061	1.2893	1.1682	.35289E 00	.2039	1.2615
34308	2.1399	.8934	1.7528	1.4743	1.1889	.41320E 00	.2613	1.3303
34408	1.7348	.7574	1.4066	.1842	7.6344	.37227E-01	.7404	6.6325
34508	2.2572	.7769	1.9206	.5013	3.8313	.12559E 00	.6662	3.5371
34608	1.1366	.9205	.7378	.2463	2.9950	.48456E-01	.1796	1.7758
34708	1.5228	.8662	1.1474	.5754	1.9943	.14187E 00	.3489	1.9951
34808	2.0831	.8437	1.7175	1.0259	1.6740	.28024E 00	.4248	1.8852
34908	1.2464	.9532	.8334	.6203	1.3436	.15033E 00	.0905	1.2074
35008	1.6742	.9349	1.2691	1.1075	1.1459	.29725E 00	.1389	1.1911
37208	.5211	.8295	.1617	.0187	8.6543	.19137E-01	.4834	6.7373
37308	.5785	.7806	.2402	.0317	7.5762	.43314E-01	.6627	5.9131
37408	.7711	.7438	.4488	.0694	6.4653	.12073E 00	.6923	3.6547
37508	.8716	.7286	.5559	.1216	4.5705	.23689E 00	.7883	2.7615
37608	.9208	.7203	.6087	.1887	3.2263	.39179E 00	.8080	2.2732
37708	.9738	.7146	.6642	.2799	2.3729	.60861E 00	.9117	1.8517
37808	1.1366	.7094	.8292	.4506	1.8404	.10230E 01	.9320	1.5923
37908	1.3789	.7061	1.0729	.6606	1.6242	.15416E 01	.9447	1.4465
38008	.5229	.8932	.1359	.0386	3.5150	.53297E-01	.3239	2.6329
38108	.5561	.8419	.1913	.0566	3.3786	.90534E-01	.4171	2.7418
38208	.6838	.7912	.3410	.1040	3.2782	.19407E 00	.5102	2.4584
38308	.8457	.7662	.5137	.1658	3.0985	.33635E 00	.6838	2.3925
38408	.9776	.7512	.6521	.2422	2.6923	.51738E 00	.7473	2.0907
38508	1.0495	.7404	.7287	.3443	2.1162	.76313E 00	.8127	1.8372
38608	1.2237	.7300	.9074	.5314	1.7077	.12209E 01	.8524	1.6020
38708	1.4547	.7233	1.1412	.7573	1.5070	.17828E 01	.8782	1.4598
38808	.5278	.9205	.1290	.0628	2.0544	.10046E 00	.1914	1.5301
38908	.5396	.8743	.1608	.0855	1.8801	.14987E 00	.3360	1.9064
39008	.6549	.8219	.2988	.1416	2.1099	.27774E 00	.5143	2.1789
39108	.8100	.7928	.4665	.2127	2.1928	.44436E 00	.6180	2.0880
39208	1.0382	.7744	.7026	.3077	2.2837	.64973E 00	.6854	1.9244
39308	1.2047	.7605	.8752	.4197	2.0855	.92244E 00	.7369	1.7596
39408	1.3562	.7467	1.0326	.6224	1.6590	.14206E 01	.7888	1.5759
39508	1.6060	.7376	1.2865	.8651	1.4870	.20228E 01	.8235	1.4520
39608	.5505	.9364	.1447	.0984	1.4706	.16157E 00	.1532	1.3078
39708	.5911	.8954	.2032	.1260	1.6128	.22300E 00	.2463	1.4465
39808	.6970	.8443	.3311	.1916	1.7280	.37491E 00	.3888	1.6432
39908	.8344	.8138	.4818	.2719	1.7722	.56558E 00	.4820	1.6906
40008	1.0041	.7934	.6603	.3667	1.8005	.79499E 00	.6245	1.7640

CODE	DPDIA	RHOM	DELPA	DELPP	PRAT	WE	RI	PRATP
4010S	1.1744	.7776	.8375	.4890	1.7129	.10943E 01	.6738	1.6616
4020S	1.4205	.7613	1.0907	.7070	1.5427	.16325E 01	.7340	1.5317
4030S	1.6666	.7503	1.3415	.9636	1.3923	.22744E 01	.7753	1.4314
4040B	.6025	.9532	.1894	.1674	1.1315	.31166E 00	.0989	1.1399
4050B	.6411	.9199	.2425	.2029	1.1951	.39521E 00	.1932	1.2281
4060B	.7526	.8735	.3741	.2869	1.3037	.59136E 00	.3385	1.3895
4070B	.8878	.8429	.5226	.3823	1.3671	.82625E 00	.4414	1.4783
4080B	1.0495	.8211	.6938	.4943	1.4036	.10999E 01	.5171	1.5031
4090S	1.2123	.8032	.8643	.6347	1.3616	.14482E 01	.5804	1.4886
4100S	1.5265	.7842	1.1868	.8804	1.3480	.20599E 01	.6496	1.4353
4110S	1.8408	.7707	1.5068	1.1642	1.2942	.27749E 01	.6990	1.3769
4120B	.6852	.9628	.2680	.2547	1.0524	.51059E 00	.0840	1.0921
4130B	.7322	.9349	.3271	.2984	1.0962	.61625E 00	.1489	1.1298
4140B	.8417	.8934	.4545	.3973	1.1440	.85663E 00	.2632	1.2118
4150B	.9890	.8640	.6146	.5113	1.2020	.11358E 01	.3437	1.2654
4160B	1.1480	.8421	.7831	.6395	1.2245	.14536E 01	.4411	1.3358
4170B	1.3107	.8236	.9539	.7992	1.1936	.18510E 01	.5083	1.3552
4180S	1.6628	.8030	1.3149	1.0826	1.2146	.25361E 01	.5814	1.3451
4190S	2.0263	.7880	1.6848	1.3957	1.2072	.33243E 01	.6355	1.3175
4200B	.8905	.9721	.4693	.4540	1.0337	.95202E 00	.0511	1.0486
4210B	.9549	.9503	.5431	.5112	1.0625	.10946E 01	.1067	1.0676
4220B	1.0798	.9155	.6831	.6388	1.0694	.14089E 01	.2065	1.1120
4230B	1.2388	.8889	.8537	.7812	1.0927	.17620E 01	.2889	1.1547
4240B	1.4281	.8680	1.0520	.9383	1.1212	.21537E 01	.3568	1.1888
4250B	1.5985	.8495	1.2304	1.1294	1.0894	.26330E 01	.4189	1.2141
4260S	1.9468	.8280	1.5880	1.4500	1.0952	.34409E 01	.4928	1.2311
4270B	1.3221	.9801	.8975	.8906	1.0077	.19967E 01	.0329	1.0265
4280B	1.3865	.9641	.9687	.9724	.9962	.22012E 01	.0707	1.0335
4290B	1.5682	.9370	1.1622	1.1462	1.0140	.26393E 01	.1435	1.0505
4300B	1.7613	.9148	1.3649	1.3355	1.0221	.31161E 01	.2085	1.0691
4310B	.4677	.8295	.1083	.0178	6.0696	.59205E-01	.4679	3.7037
4320B	.5247	.7806	.1864	.0311	6.0032	.13400E 00	.5893	3.1933
4330B	.7526	.7438	.4303	.0686	6.2697	.37350E 00	.7248	2.3319
4340B	1.0685	.7286	.7527	.1206	6.2394	.73286E 00	.8673	1.8128
4350B	1.4546	.7203	1.1425	.1875	6.0938	.12121E 01	.8852	1.5789
4360B	1.8635	.7146	1.5538	.2788	5.5731	.18829E 01	.9080	1.4237
4370B	.4799	.8932	.0929	.0389	2.3907	.16489E 00	.2470	1.5413
4380B	.5193	.8419	.1545	.0571	2.7062	.28009E 00	.4016	1.8114
4390B	.6554	.7912	.3125	.1046	2.9889	.60040E 00	.5554	1.8044
4400B	.8720	.7662	.5400	.1664	3.2445	.10406E 01	.7177	1.7012
4410B	1.1215	.7512	.7960	.2433	3.2720	.16006E 01	.7883	1.5347
4420B	1.4394	.7404	1.1186	.3451	3.2412	.23609E 01	.8055	1.4158
4430B	.4971	.9205	.0982	.0639	1.5365	.31079E 00	.1782	1.2410
4440B	.5342	.8743	.1553	.0864	1.7973	.46365E 00	.3205	1.4165
4450B	.6409	.8219	.2848	.1430	1.9914	.85926E 00	.4998	1.5601
4460B	.8041	.7928	.4606	.2141	2.1514	.13747E 01	.6053	1.5273
4470B	1.0382	.7744	.7026	.3001	2.3416	.20101E 01	.6743	1.4529
4480B	1.2691	.7605	.9396	.4122	2.2794	.28538E 01	.7272	1.3747
4490B	1.7044	.7467	1.3809	.6143	2.2480	.43951E 01	.7808	1.2855
4500B	.5233	.9364	.1176	.0935	1.2580	.49984E 00	.1292	1.1292
4510B	.5563	.8954	.1684	.1208	1.3940	.68989E 00	.2322	1.2036
4520B	.6594	.8443	.2936	.1864	1.5751	.11599E 01	.3790	1.3053
4530B	.8032	.8138	.4506	.2667	1.6895	.17498E 01	.5215	1.3809
4540B	.9927	.7934	.6490	.3617	1.7940	.24595E 01	.6274	1.3791
4550B	1.2161	.7776	.8792	.4839	1.8170	.33856E 01	.6624	1.3236
4560B	1.6136	.7613	1.2837	.7013	1.8305	.50505E 01	.7243	1.2622
4570B	.5803	.9532	.1673	.1632	1.0250	.96420E 00	.0895	1.0645
4580B	.6214	.9199	.2229	.1989	1.1207	.12227E 01	.1800	1.1037
4590B	.7205	.8735	.3420	.2809	1.2173	.18295E 01	.3231	1.1790
4610B	1.0306	.8211	.6748	.4894	1.3790	.34028E 01	.5026	1.2392
4620B	1.2161	.8032	.8681	.6303	1.3773	.44805E 01	.5670	1.2352
4630B	1.5905	.7842	1.2511	.8755	1.4291	.63727E 01	.6376	1.2121
4640B	.6734	.9628	.2562	.2508	1.0219	.15796E 01	.0755	1.0427
4650B	.7282	.9349	.3231	.2944	1.0972	.19065E 01	.1454	1.0626
4660B	.8394	.8934	.4523	.3950	1.1450	.26502E 01	.2618	1.1039
4670B	.9814	.8640	.6070	.5084	1.1939	.35137E 01	.3493	1.1345
4680B	1.1404	.8421	.7755	.6370	1.2175	.44971E 01	.4425	1.1668
4690B	1.3373	.8236	.9804	.7965	1.2309	.57264E 01	.4937	1.1686
4700B	1.6780	.8030	1.3301	1.0701	1.2430	.78460E 01	.5679	1.1661

APPENDIX H

SUPPLEMENTARY BIBLIOGRAPHY

In addition to the works listed in the reference list, a number of recent articles of general interest to the worker in the field of liquid-liquid and gas-liquid two-phase flow have appeared in the literature. Although these articles are not directly applicable to the present problem they may be of assistance in attacking related problems. For this reason this appendix lists these references without comment for the benefit of workers in the field. This list is by no means complete but should serve as a starting point for future work.

Drop Behavior in Liquid-Liquid Systems

1. Elzinga, E. R., Jr., and J. T. Banchero, "Some Observations on the Mechanics of Drops in Liquid-Liquid Systems," AIChE J., 7, 394 (1961).

2. Garner, F. H., and A. H. P. Skelland, "Some Factors Affecting Droplet Behavior in Liquid-Liquid System," Chem. Eng. Sci., 4, 149 (1955).

3. Gibbons, J. H., G. Houghton, and J. Coull, "Effect of a Surface Active Agent on the Velocity of Rise of Benzene Drops in Water," AIChE J., 8, 274 (1962).

4. Hughes, R. R., and E. R. Gilliland, "The Mechanics of Drops," Heat Transfer and Fluid Mechanics Institute, 1951, 53 (1951).

5. Johnson, A. I., and L. Braida, "The Velocity of Fall of Circulating and Oscillating Liquid Drops Through Quiescent Liquid Phases," Can. J. Chem. Eng., 35, 165 (1957).

6. Klee, A. J., and R. E. Treybal, "Rate of Rise or Fall of Liquid Drops," AIChE J., 2, 444 (1956).

7. Krishna, P. M., D. Venkateswarlu, and G. S. R. Narasimhamurty, "Fall of Liquid Drops in Water. Terminal Velocities," J. Chem. Eng. Data, 4, 336 (1959).

8. Krishna, P. M., D. Venkateswarlu, and G. S. R. Narasimhamurty, "Fall of Liquid Drops in Water. Drag Coefficients, Peak Velocities, and Maximum Drop Sizes," J. Chem. Eng. Data, 4, 340 (1959).

9. Licht, W., and G. S. R. Narasimhamurty, "Rate of Fall of Single Liquid Droplets," AIChE J., 1, 366 (1955).

10. Madden, A. J., and G. L. Damerell, "Coalescence Frequencies in Agitated Liquid-Liquid Systems," AIChE J., 8, 233 (1962).

11. Satapathy, R., and W. Smith, "The Motion of Single Immiscible Drops Through a Liquid," J. Fluid Mech., 10, 561 (1961).

12. Warshay, M., E. Bogusz, M. Johnson, and R. C. Kintner, "Ultimate Velocity of Drops in Stationary Liquid Media," Can. J. Chem. Eng., 37, 29 (1959).

Slip Velocities in Vertical Moving Systems

1. Beyaert, B. O., L. Lapidus, and J. C. Elgin, "The Mechanics of Vertical Moving Liquid-Liquid Fluidized Systems: II. Countercurrent Flow," AIChE J., 7, 46 (1961).

2. Lapidus, L., and J. C. Elgin, "Mechanics of Vertical-Moving Fluidized Systems," AIChE J., 3, 63 (1957).

3. Price, B. G., L. Lapidus, and J. C. Elgin, "Mechanics of Vertical-Moving Fluidized Systems," AIChE J., 5, 93 (1959).

4. Quinn, J. A., L. Lapidus, and J. C. Elgin, "The Mechanics of Moving Vertical Fluidized Systems: V. Cocurrent Cogravity Flow," AIChE J., 7, 260 (1961).

5. Struve, D. L., L. Lapidus, and J. C. Elgin, "The Mechanics of Moving Vertical Fluidized Systems: III. Application to Cocurrent Countergravity Flow," Can. J. Chem. Eng., 36, 141 (1958).

Operating Characteristics and Flooding in Countercurrent Packed Columns

1. Bain, W. A., Jr., and O. A. Hougen, "Flooding Velocities in Packed Columns," Trans. AIChE, 40, 29 (1944).

2. Baker, T., T. H. Chilton, and H. C. Vernon, "The Course of Liquor Flow in Packed Towers," Trans. AIChE., 31, 296 (1935).

3. Bertetti, J. W., "Theoretical Flooding Velocities in Packed Columns," Trans. AIChE, 38, 1023 (1942).

4. Eduljee, H. E., "Pressure Drop, Loading and Flooding in Irrigated Packed Towers," Brit. Chem. Eng., 5, 330 (1960).

5. Elgin, J. C., and F. B. Weiss, "Liquid Holdup and Flooding in Packed Towers," Ind. Eng. Chem., 31, 435 (1939).

6. Fan, L., "Pressure Drop of Single Phase Flow Through Raschig Ring Type Tower Packings: Effect of Hole Size," Can. J. Chem. Eng., 38, 138 (1960).

7. Frantz, T. F., and K. I. Glass, "Pressure Drop and Flooding Velocities for 1/4 Inch Berl Saddles," J. Chem. Eng. Data, 7, 147 (1962).

8. Furnas, C. C., and F. Bellinger, "Operating Characteristics of Packed Columns," Trans. AIChE, 34, 251 (1938).

9. Gardner, G. C., "Holdup and Pressure Drop for Water Irrigating 'Non-Wettable' Coke," Chem. Eng. Sci., 5, 101 (1956).

10. Hill, S., "Channelling in Packed Columns," Chem. Eng. Sci., 1, 247 (1952).

11. Hwa, C. S., and R. B. Beckman, "Radiological Study of Liquid Holdup and Flow Distribution in Packed Gas-Absorption Columns," AIChE J., 6, 359 (1960).

12. Lerner, B. J., and C. S. Grove, Jr., "Critical Conditions of Two-Phase Flow in Packed Columns," Ind. Eng. Chem., 43, 216 (1951).

13. Lobo, W. E., L. Friend, F. Hashmall, and F. Zenz, "Limiting Capacity of Dumped Tower Packings," Trans. AIChE, 41, 693 (1945).

14. Piret, E. L., C. A. Mann, and T. Wall, Jr., "Pressure Drop and Liquid Holdup in a Packed Tower," Ind. Eng. Chem., 32, 861 (1940).

15. Sakiadis, B. C., and A. I. Johnson, "Generalized Correlation of Flooding Rates," Ind. Eng. Chem., 46, 1229 (1954).

16. Schoenborn, E. M., and W. J. Dougherty, "Pressure Drop and Flooding Velocity in Packed Towers with Viscous Liquids," Trans. AIChE, 40, 51 (1944).

17. Turner, G. A., and G. F. Hewitt, "The Amount of Liquid Held at the Point of Contact of Spheres and the Static Liquid Holdup in Packed Beds," Trans. Instn. Chem. Eng. (London), 37, 329 (1959).

18. Venkataraman, G., and G. S. Laddha, "Limiting Velocities, Holdup, and Pressure Drop at Flooding in Packed Extraction Columns," AIChE J., 6, 355 (1960).

19. Whitt, F. R., "Countercurrent Gas and Liquor Flow Through Beds of Random Packed Raschig Rings," Brit. Chem. Eng., 5, 179 (1960).

Gas-Liquid Two Phase Flow in Open Pipes

1. Alves, G. E., "Cocurrent Liquid-Gas Flow in a Pipe-Line Contactor," Chem. Eng. Prog., 50, 449 (1954).

2. Aziz, K., and G. W. Govier, "Horizontal Annular-Mist Flow of Natural Gas-Water Mixtures," Can. J. Chem. Eng., 40, 51 (1962).

3. Carter, C. O., and R. L. Huntington, "Cocurrent Two-Phase Upward Flow of Air and Water Through an Open Vertical Tube and Through an Annulus," Can. J. Chem. Eng., 39, 248 (1961).

4. Galegar, W. C., W. B. Stovall, and R. L. Huntington, "More Data on Two-Phase Vertical Flow," Petr. Ref., 33, No. 11, 208 (1954).

5. Hatch, M. R., and R. B. Jacobs, "Prediction of Pressure Drop in Two-Phase Single Component Fluid Flow," AIChE J., 8, 18 (1962).

6. Isbin, H. S., H. A. Rodriguez, H. C. Larson, and B. D. Pattie, "Void Fractions in Two-Phase Flow," AIChE J., 5, 427 (1959).

7. Isbin, H. S., N. C. Sher, and K. C. Eddy, "Void Fractions in Two-Phase Steam-Water Flow," AIChE J., 3, 136 (1957).

8. Johnson, H. A., "Heat Transfer and Pressure Drop for Viscous-Turbulent Flow of Oil-Air Mixtures in a Horizontal Pipe," Trans. ASME, 77, 1257 (1955).

9. Kordyban, E. S., "A Flow Model for Two-Phase Slug Flow in Horizontal Tubes," J. Basic Eng., 83, 613 (1961).

10. Lamb, D. E., and J. L. White, "Use of Momentum and Energy Equations in Two-Phase Flow," AIChE J., 8, 281 (1962).

11. Levy, S., "Prediction of Two Phase Pressure Drop and Density Distribution from Mixing Length Theory," ASME Preprint No. 62-HT-6 (1962).

12. Marchaterre, J. F., "Two-Phase Frictional Pressure Drop Prediction from Levy's Momentum Model," J. Heat Trans., 83, 503 (1961).

13. Nemet, A. G., "Flow of Gas-Liquid Mixtures in Vertical Tubes," Ind. Eng. Chem., 53, 151 (1961).

14. Nicklin, D. J., J. O. Wilkes, and J. F. Davidson, "Two-Phase Flow in Vertical Tubes," Trans. Instn. Chem. Eng. (London), 40, 61 (1962).

15. Reid, R. C., A. B. Reynolds, A. J. Diglio, I. Spiewak, and D. H. Kliptein, "Two-Phase Pressure Drops in Large-Diameter Pipes," AIChE J., 3, 321 (1957).

16. Sobocinski, D. P., and R. L. Huntington, "Cocurrent Flow of Air, Gas-Oil, and Water in a Horizontal Pipe," Trans. ASME, 80, 252 (1958).

17. Vohr, J., "The Energy Equation for Two-Phase Flow," AIChE J., 8, 280 (1962).

18. White, P. D., and R. L. Huntington, "Horizontal Co-Current Two-Phase Flow of Fluids in Pipe Lines," Petr. Eng., 27, No. 9, D-40 (1955).

19. Wicks, Moye, III, and A. E. Dukler, "Entrainment and Pressure Drop in Cocurrent Gas-Liquid Flow: I. Air-Water in Horizontal Flow," AIChE J., 6, 463 (1960).

20. Zuber, N., "On the Variable-Density Single Fluid Model for Two-Phase Flow," J. Heat Trans., 82, 255 (1960).